

More on the Brownian force model: avalanche shapes, tip driven, higher d

Pierre Le Doussal

Laboratoire de Physique de l'École Normale Supérieure, ENS, Université PSL,
CNRS, Sorbonne Université, Université de Paris, 75005 Paris, France

(Dated: March 23, 2022)

The Brownian force model (BFM) is the mean-field model for the avalanches of an elastic interface slowly driven in a random medium. It describes the spatio-temporal statistics of the velocity field, and, to some extent is analytically tractable. We extend our previous studies to obtain several observables for the BFM with short range elasticity, related to the local jump sizes $S(x)$ and to the avalanche spatial extension in $d = 1$, or the avalanche span in $d > 1$. In $d = 1$ we consider both driving (i) by an imposed force (ii) by an imposed displacement "at the tip" and obtain in each case the mean spatial shape $\langle S(x) \rangle$ at fixed extension, or at fixed seed to edge distance. We find that near an edge x_e , $S(x) \simeq \sigma |x - x_e|^3$ where σ has a universal distribution that we obtain. We also obtain the spatiotemporal shape near the edge. In $d > 1$ we obtain (i) the mean shape $\langle S(x_1, x_\perp) \rangle$ for a fixed span, which exhibits a non-trivial dependence in the transverse distance to the seed x_\perp (ii) the mean shape around a point which has not moved, $\langle S(x) \rangle_{S(0)=0}$, which vanishes at the center as $|x|^{b_d}$ with non trivial exponents, $b_1 = 4$, $b_2 = 2\sqrt{2}$ and $b_3 = \frac{1}{2}(\sqrt{17} - 1)$. We obtain the probability distributions in any d for the maximal radius of an avalanche and the minimal distance of approach to a given point, as well as the probability of not hitting a cone in $d = 2$. These results equivalently apply to the continuum limit of some branching diffusions, as detailed in a companion paper.

PACS numbers:

Contents

I. Introduction	3
A. Definition of the model	3
B. Avalanche observables and driving protocols	4
1. Finite kick driving, avalanche size distribution, massive and massless units	4
2. Infinitesimal kick driving, avalanche seed, quasi-static avalanche densities	5
3. Avalanche spatial support and extension: recall of previous results	5
C. Avalanches upon driving by the tip	7
II. Aim of the present paper, and summary of main results	7
A. Density of local jump $S(x)$, versus the distance to the seed at $x = x_s$	8
B. Spatial shape: mean shape and fluctuations	8
1. Mean spatial shape $\langle S(x) \rangle_{\ell_2}$ for fixed edge-to-seed distance ℓ_2	9
2. Universal fluctuations of the shape near the edge	9
3. Mean spatial shape $\langle S(x) \rangle_\ell$ for fixed total extension ℓ	10
4. Mean spatial shape $\langle S(x) \rangle_{\ell,p}$ for fixed total extension ℓ and aspect ratio p	11
C. Spatiotemporal shape near the edge of the avalanche	12
D. Higher dimension	13
1. Probability that a given point has not moved and mean shape around it	13
2. Maximal distance reached by an avalanche and minimal distance of its support to a point	14
3. Probability of not hitting a cone in two dimension	15
4. Avalanche span and shape in $d > 1$	15
E. Tip driving PDF of local and total sizes, extension distribution and spatial shape	16
1. Distribution of local jumps at the tip	16
2. Distribution of total sizes	17
3. Joint distribution of total size and of local jump at the tip	17
4. Distributions of extensions for tip-driven avalanches	18
5. Mean shape of a tip-driven avalanche and its fluctuations near the edge	18

III. Method: generating function and instanton equation	20
IV. Bulk driving: density of local size versus the distance to the seed	20
A. Massless case	21
B. Massive case	23
V. Bulk driving: spatial shape conditioned to one boundary	24
A. Massless case	24
1. PDF of seed-to-edge distance ℓ_2	24
2. Mean shape conditioned on the seed-to-edge distance ℓ_2	25
3. joint PDF of total size S and ℓ_2	27
4. Higher moments of the shape	28
B. spatiotemporal shape near a boundary	31
C. Massive case	33
1. PDF of seed-to-edge distance ℓ_2	33
2. Mean shape conditioned to the seed-to-edge distance ℓ_2	33
3. Joint PDF of total size S and ℓ_2	35
VI. Bulk driving: spatial shape conditioned to two boundaries	36
A. PDF and density of ℓ_1, ℓ_2 and of ℓ, p	36
B. Mean shape conditioned to total extension and aspect ratio	37
C. Joint density of size and extension	41
D. Mean shape conditioned to total extension	43
VII. Avalanches upon driving by a point ("driving by the tip")	43
A. Model	43
B. Joint distribution of the local jump at the tip and of the total size	43
1. Moments and joint moments	44
2. Distribution of total size $P_w(S)$: crossover between two limit forms	45
3. Calculation of the PDF of the local jump $P_w(S_0)$	45
4. Calculation of the joint PDF of the total and local size $P_w(S, S_0)$	47
C. Distribution of the extension for avalanches driven by the tip: crossover as m_0 is varied	48
D. Mean avalanche shape in the limit $m_0 = +\infty$	49
1. Limit $m_0 = +\infty$ and CDF of ℓ_2	50
2. The shape	51
3. The second shape	53
4. Direct calculation of the conditional moments of the total avalanche size	54
VIII. Avalanches in the BFM in higher dimension $d > 1$	55
A. Probability that an avalanche does not contain the neighborhood of a given point	55
B. Probability distribution of $\Sigma = \int d^d x \frac{S(x)}{(x-x_0)^4}$ conditioned to $S(x_0) = 0$	55
C. Mean avalanche shape around a point such that $S(x_0) = 0$	56
D. Probability that an avalanche does not reach a distance R from the seed	59
E. Span and shape in $d > 1$	61
F. Probability that an avalanche does not hit a cone in two dimension	64
Acknowledgments	66
A. Weierstrass and Elliptic functions	67
B. Levy stable laws and some inverse Laplace transforms	68
C. Density of local sizes, details for the massive case	70
D. Expansion in λ, more details	71
E. Expectation values conditioned to avalanche extensions	71
F. expansion around λ^*	72

G. Bessel functions	73
H. Shape with two boundaries, expansions in powers of λ	73
I. Higher conditional moments of the total size	73
J. Driving at the tip, local jumps $P_w(S_0)$, massive case.	74
K. Mean shape $d > 1$ in the massive case and the Green function of the $1/r^2$ potential	74
References	74

I. INTRODUCTION

A. Definition of the model

The Brownian force model (BFM) has emerged as the mean-field theory for the space-time statistics of the instantaneous velocity field in an avalanche, for elastic interfaces driven in a disordered medium¹⁻³. It is expected to be an accurate description of this statistics for random media with short range correlations, in the case of interfaces of internal dimension d above or at the upper critical dimension, i.e. $d \geq d_{uc}$. It is also a starting point to describe models with short range disorder in a dimensional expansions around d_{uc} ³⁻⁷. Furthermore, since it is analytically tractable, with non trivial physics, it is also an interesting model of avalanche motion per se, to study in any dimension d ⁸⁻¹¹. It is the natural extension to an elastic manifold of internal dimension d , of the celebrated ABBM toy model, which describes the motion of a point driven in a Brownian force landscape, i.e. the $d = 0$ limit^{8,12-16}.

Consider the overdamped equation of motion (with friction coefficient η) for an elastic interface, with internal coordinate $x \in \mathbb{R}^d$, parameterized by a position field (i.e. height or displacement field) $u(x, t)$ in a quenched random force field $F(u, x)$

$$\eta \partial_t u(x, t) = \nabla_x^2 u(x, t) + F(u(x, t), x) + m^2(w(x, t) - u(x, t)) \quad , \quad f(x, t) = m^2 w(x, t) \quad (1)$$

where we focus in this paper on short-ranged elastic forces, modeled by the d -dimensional Laplacian ∇_x^2 . We have added a confining quadratic potential of curvature m , centered at $w(x, t)$, acting as a driving (here and below we use interchangeably $\partial_t u$ or \dot{u} to denote time derivatives). Eq. (1) describes the "massive" problem, for which the driving force is $f(x, t) = m^2 w(x, t)$, and below we will also study the related massless problem where one sets $m \rightarrow 0$ keeping $f(x, t)$ fixed. Equations of motion such as (1) obey the Middleton property¹⁷⁻¹⁹, which ensures that under monotonous forward driving the interface always moves forward, and, e.g. for a uniform driving $w(x, t) = vt$, converges to a unique attractor in configuration space (called the Middleton attractor), independent of the initial condition.

In the BFM model, the random force field is chosen as a collection of independent one-sided Brownian motions in the u direction with correlator

$$\overline{F(u, x)F(u', x')} = 2\sigma\delta^d(x - x') \min(u, u') \quad . \quad (2)$$

This choice makes the BFM more tractable analytically than the case of short-range correlated random force field.

Indeed, taking the temporal derivative ∂_t of Eq. (1), and choosing the driving velocity always positive, $\dot{w}(x, t) \geq 0$, which implies from the Middleton property that $\dot{u}(x, t) \geq 0$ at all $t \geq 0$ if $\dot{u}(x, t = 0) \geq 0$, one can show^{2,3} that (1) implies, for the time evolution of the velocity variable $\partial_t u(x, t) \equiv \dot{u}(x, t)$, the following stochastic equation (in the Ito sense):

$$\eta \partial_t \dot{u}(x, t) = \nabla_x^2 \dot{u}(x, t) + \sqrt{2\sigma \dot{u}(x, t)} \xi(x, t) + m^2(\dot{w}(x, t) - \dot{u}(x, t)) \quad , \quad \dot{f}(x, t) = m^2 \dot{w}(x, t) \quad (3)$$

where $\overline{\xi(x, t)\xi(x', t')} = \delta^d(x - x')\delta(t - t')$ is a space time white noise. The equation (3) can equally well be taken as the definition of the Brownian Force Model (BFM) in space dimension d . The fact that the time evolution of the velocity is Markovian, even in a quenched random medium, is remarkable and results from the properties of the Brownian motion, combined with the Middleton property. The details of the correspondence are given in^{3,8} where subtle aspects of the position theory, and its links to the mean-field theory of realistic models of interfaces in short-ranged disorder via the Functional Renormalisation Group (FRG), are discussed.

Here we will study the BFM mainly in dimension $d = 1$, with some additional results in dimension $d = 2$ and some for any $d < 4$. In fact, even from the solution in $d = 1$ one can already obtain some (integrated) information for

$d > 1$. Indeed, the BFM (3) in space dimension d has the property that the velocity field integrated over $d - d_c$ space dimensions, also satisfies the BFM equation in dimension d_c . For instance, consider Euclidean d -dimensional space, and $\nabla_x^2 = \sum_{i=1}^d \partial_{x_i}^2$. Then $\dot{u}(x_1, t) := \int dx_2 \dots dx_d u(x_1, \dots, x_d, t)$ satisfies exactly the BFM equation (3) in dimension $d = d_c = 1$, in the variable $x = x_1$. Note that there are many possible variants of the BFM (discrete versions, long range elasticity, non-local in time) but here we study the simplest one (3).

B. Avalanche observables and driving protocols

1. Finite kick driving, avalanche size distribution, massive and massless units

Kick driving. Let us define what we want to study. We are interested in the solutions of Eq. (3) with an initial condition with zero velocity, $\dot{u}(x, t = 0^-) = 0$, in response to a driving function $\dot{f}(x, t)$ which is a kick at time $t = 0$, i.e. of the form

$$\dot{f}(x, t) = f(x) \delta(t) \quad , \quad f(x) = m^2 \delta w(x) \geq 0 \quad (4)$$

equivalent to a step $\delta w(x)$ in the driving function $w(x, t)$. This kick, which may be space-dependent, produces an avalanche with $\dot{u}(x, t \geq 0) \geq 0$, which starts at time $t = 0$ and terminates at a time $t = T$, when all velocities vanish, i.e. $\dot{u}(x, t) = 0$ for all x . It can be shown that such a duration time T exists for the BFM (3) with no need to introduce any ad-hoc additional cutoff. If $f(x) = f$ it is called a uniform (or homogeneous) kick.

Avalanche size distributions. For this avalanche one defines the size $S(x)$ of the local jump (local avalanche size) and the total size S

$$S(x) = \int_0^\infty dt \dot{u}(x, t) \quad , \quad S = \int d^d x S(x) \quad (5)$$

We denote symbolically $P_{\{f(x)\}}[\{S(x)\}] \prod_x dS(x)$ the probability measure for the field $S(x)$ observed after the kick (4). There is an *exact* formula for that probability measure for the BFM, Eq. (49) of Ref.⁹, not reproduced here, as not so useful for our purpose. Let us recall instead the probability distribution function (PDF) of the total size S

$$P_{\{f(x)\}}(S) = \frac{\int d^d x f(x)}{2\sqrt{\pi} m^2 S_m^{1/2} S^{3/2}} e^{-\frac{(S - \frac{1}{m^2} \int d^d x f(x))^2}{4 S S_m}} \quad (6)$$

Units, massive case. Here in Eq. (6) and below, except when explicitly mentioned, we use the natural units for the massive problem, i.e. we express lengths in units of $x_m = 1/m$, total size S in units of S_m , and time in units of τ_m with

$$S_m = \frac{\sigma}{m^4} \quad , \quad \tau_m = \frac{\eta}{m^2} \quad (7)$$

and $w(x) \sim u(x, t) \sim S(x)$ in units $\sigma m^{-\zeta}$ with $\zeta = 4 - d$, which is equivalent to setting $m = \sigma = \eta = 1$. We can see from (6) that S_m is the large-size cutoff for avalanches. In the BFM the disorder is scale invariant, hence the only small scale cutoff is the size of the driving, i.e. from (6) as $S \rightarrow 0$ we see that the smallest avalanches are of typical size $S_{\min} \simeq (\int d^d x f(x))^2 / \sigma$. In these units Eq. (6) reads $P_{\{f(x)\}}(S) = \frac{\int d^d x f(x)}{2\sqrt{\pi} S^{3/2}} e^{-\frac{(S - \int d^d x f(x))^2}{4 S}}$.

Units, massless limit. In the massless limit $m \rightarrow 0$ the driving force $f(x, t)$ is kept fixed. Hence the equations of motion (1) and (3) are valid with

$$\begin{aligned} m^2(w(x, t) - u(x, t)) &\rightarrow f(x, t) \\ m^2(\dot{w}(x, t) - \dot{u}(x, t)) &\rightarrow \dot{f}(x, t) \end{aligned} \quad (8)$$

In that limit we see that Eq. (6) becomes

$$P_{\{f(x)\}}(S) = \frac{\int d^d x f(x)}{2\sqrt{\pi} \sigma^{1/2} S^{3/2}} e^{-\frac{(\int d^d x f(x))^2}{4 \sigma S}} \quad (9)$$

We can define time in units of η and $u \sim w$ in units of σ , which is equivalent to setting $\eta = \sigma = 1$. The results still have an unfixed dimension of length. There is no more large scale cutoff size, or cutoff length for the avalanches. In some cases one can introduce a finite system size L to act as a cutoff and to construct dimensionless quantities.

2. Infinitesimal kick driving, avalanche seed, quasi-static avalanche densities

The limit of a small kick amplitude $f(x)$ is of special importance to define (i) the seed of an avalanche (ii) quasi-static avalanches (iii) avalanche densities. As can be seen on (6), in that limit one has, for any fixed $S > 0$ (in the massive case)

$$P_{\{f(x)\}}(S) = \int d^d x f(x) \rho_x(S) + O(f^2) \quad , \quad \rho_x(S) = \frac{1}{2\sqrt{\pi} S^{3/2}} e^{-S/4} \quad , \quad \rho_x(S) = \left. \frac{\delta P_{\{f(x)\}}(S)}{\delta f(x)} \right|_{f=0} \quad (10)$$

where $\rho_x(S)$ is the so-called local density associated to S (it has unit $1/(wS_m)$, i.e. it is a density per unit length - along u). Note that as $f(x) \rightarrow 0$ the weight of the PDF in (6) concentrates on very small avalanches, $S \sim [\int d^d x f(x)]^2$, so that (10) represents the rare larger, i.e. $S = O(1)$, avalanches. Densities $\rho_x[\mathcal{O}]$ for many other avalanche observables \mathcal{O} , e.g. $\mathcal{O} = S(x_0)$, or the avalanche spatial extension (see below), can be similarly defined (by the derivative of the probability as in (10)). We see from (10) that $\rho_{x_s}(S)$ is the density corresponding to performing a local driving kick $f(x) = f\delta^d(x - x_s)$. It turns out that $\rho_x[\mathcal{O}]$ is also a *density associated to avalanches which have their seed at x* . The *seed of an avalanche* is the location of the first point which starts moving. If the driving kick is local, i.e. $f(x) = f\delta^d(x - x_s)$, then the seed is at x_s , and the avalanche spreads from there. Formula (10) says that for an *extended kick of very small amplitude $f(x)$* , the avalanche will start from $x = x_s$ with a probability proportional to $f(x_s)$. In particular, consider a uniform driving $f(x) = f$. In the limit $f \rightarrow 0^+$, at fixed interface size L , one can reach a "single avalanche regime" for avalanches of size $O(1)$ ³⁵. The distribution of location of the seed x_s for this avalanche is uniform in space x . By contrast, for larger kicks $f(x)$, the terms of order f^2 and higher in (10) cannot be neglected, and can be interpreted as "several successive avalanches". One can ask about the correlations of such avalanches. As described in details in^{9,20}, the avalanches in the BFM are uncorrelated and form a Levy-type process (see also¹ for a static version, and^{20,21} for correlations in short range models).

Another protocol, a priori different from (4), is to drive the interface with a fixed uniform driving velocity v , $w(x, t) = vt$, in presence of a mass $m^2 > 0$. Considering the unique (Middleton) steady state, and taking the limit $v \rightarrow 0^+$ leads to the standard quasi-static avalanches. One can show that these have the same statistics (the same densities) as the ones produced by the infinitesimal uniform kick $f(x) = f$ in the limit $f \rightarrow 0^+$.

None of the above made any reference to the position field $u(x, t)$ of the interface, which could thus equally well be defined as $u(x, t) - u(x, t = 0) = \int_0^t dt' \dot{u}(x, t')$. There is however an interpretation^{3,8,9} in the position theory, described by Eqs. (1)-(2), of the avalanches following a kick (4) with the initial condition $\dot{u}(x, t = 0^-) = 0$. At $t < 0$, the interface is driven forward for a sufficient amount of time, with a driving which stops and converges to $w(x, t = 0^-) = w_0(x)$, in such a way that at $t = 0^-$ the interface is at rest, in the (unique) Middleton metastable state³⁶ corresponding to $w_0(x)$, denoted $u(x, t = 0^-) = u(x; w_0(x))$. At $t = 0$, the center of the confining potential is increased abruptly from $w_0(x)$ to $w(x, t = 0^+) = w_0(x) + \delta w(x)$, with $\delta w(x) = f(x)/m^2$, and remains constant for all $t > 0$. As a consequence, the interface moves forward (since $\delta w(x) \geq 0$) up to a new metastable state of the Middleton attractor, specifically $\lim_{t \rightarrow +\infty} u(x, t) = u(x; w_0(x) + \delta w(x))$.

Note that the mass $m^2 > 0$ is important to guarantee a steady state, and well defined statistics for all avalanches (small and large). On the other hand, one can verify that the statistics of small avalanches $S \ll S_m$, is well described by the massless limit, and universal. This is why we often focus on this limit, where calculations are simpler.

3. Avalanche spatial support and extension: recall of previous results

For the BFM with short range elasticity, as in (3), it is possible to define the *support of the avalanche* (with no need for any ad-hoc additional cutoff) as the (connected) set of points which have moved during the avalanche

$$\Omega = \{x \in \mathbb{R}^d \quad \text{s.t.} \quad S(x) > 0\} \quad (11)$$

In the complementary set, one has $S(x) = 0$. It is easy to show that following a kick $\dot{f}(x, t) = f(x)\delta(t)$, all points where $f(x) > 0$ will move, hence Ω contains the support of $f(x)$.

Consider now a local kick at $x = x_s$, $f(x) = f\delta(x - x_s)$. In $d = 1$, for the model (3), we have shown^{9,10} (see also below) that Ω is an interval containing the seed x_s , i.e. there are two edges beyond which $S(x) = 0$ strictly. Hence we can further define the *avalanche spatial extension* (also called length) ℓ as the length of that interval. It is also interesting to define the distances ℓ_1, ℓ_2 of each edge to the seed of the avalanche, see Fig. 1. That is, for

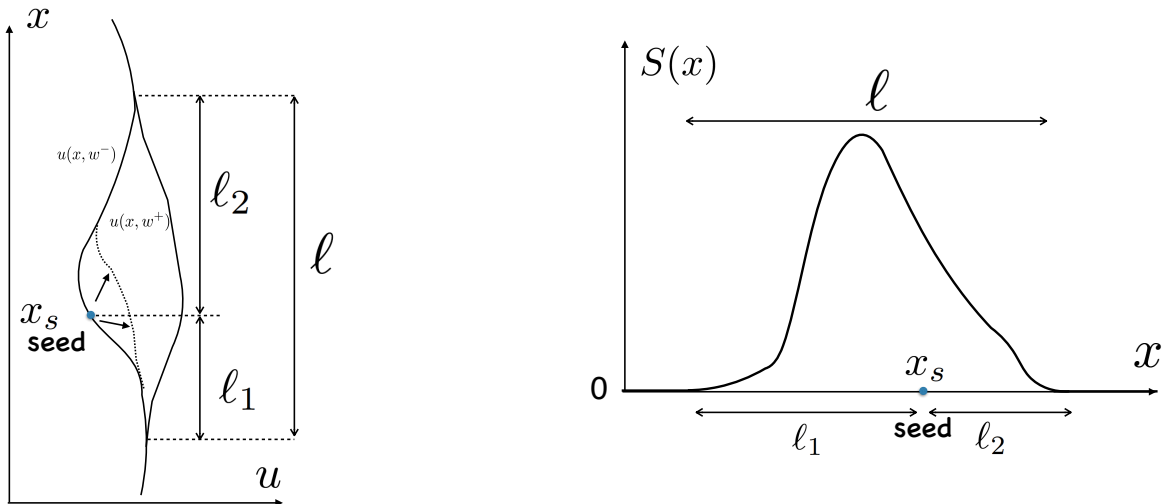


FIG. 1: Left: schematic representation of an avalanche for a 1 dimensional interface ($d = 1$), between metastable configurations $u(x; w^-) = u(x, t = 0)$ and $u(x; w^+) = u(x, t = +\infty)$. The avalanche starts at the seed point x_s (the dotted curve represents an intermediate time configuration). The set of points which move during the avalanche has a finite extension ℓ . The distance of the seed from either edges of the avalanche are respectively ℓ_2 (upper) and ℓ_1 (lower) with $\ell_2 + \ell_1 = \ell$. Such an avalanche has aspect ratio $p = \ell_2/(\ell_1 + \ell_2)$. Right: resulting total jump size $S(x) = \int_0^{+\infty} dt \dot{u}(x, t)$ of point x during the avalanche. Beyond the edges it vanishes strictly.

an avalanche with its seed at x_s , the lower (respectively upper) extension ℓ_1 (respectively ℓ_2) is defined such that $\Omega = [x_s - \ell_1, x_s + \ell_2]$, and the total extension is then $\ell = \ell_1 + \ell_2$. Finally one also defines the *aspect ratio*

$$p = \frac{\ell_2}{\ell_1 + \ell_2} \quad (12)$$

which measures the location of the seed relative to the total length, i.e. $p \in [0, 1]$. The natural units for ℓ is $1/m$ in the massive case. In a previous work¹⁰ we have calculated in $d = 1$ the joint cumulative distribution function (CDF) of ℓ_1, ℓ_2 and obtained

$$\text{Prob}(\ell_1 < l_1, \ell_2 < l_2) = e^{-6f\mathcal{P}_0(p)/l^2} \quad , \quad p = \frac{\ell_2}{\ell_1 + \ell_2} \quad , \quad l = \ell_1 + \ell_2 \quad (13)$$

where $\mathcal{P}_0(z)$ is an elliptic Weierstrass function whose definition is as follows

$$\mathcal{P}_0(z) := \mathcal{P}(z; g_2 = 0, g_3 = g_3^0 := \frac{\Gamma(1/3)^{18}}{(2\pi)^6}) \quad (14)$$

where $\mathcal{P}(z; g_2, g_3)$ is the standard elliptic Weierstrass function, doubly periodic in the complex plane, with invariants g_2, g_3 , see Appendix A for definitions. Here the value of g_3 is such that the real period is unity, i.e. $2\Omega(g_2 = 0, g_3^0) = 1$, see (A10). Its most important properties for us are, in addition to periodicity $\mathcal{P}_0(z + 1) = \mathcal{P}_0(z)$,

$$\mathcal{P}_0(1 - z) = \mathcal{P}_0(z) \quad , \quad \mathcal{P}_0(z) \simeq_{z \rightarrow 0} \frac{1}{z^2} \quad (15)$$

Taking the limit of small f , we obtained from (13) the avalanche densities for the couple (p, ℓ) , and, by integration over the aspect ratio p , for the total length ℓ , as

$$\rho(\ell, p) = \frac{8\pi\sqrt{3}\tilde{P}(p)}{\ell^3} \quad , \quad \rho(\ell) = \frac{8\pi\sqrt{3}}{\ell^3} \quad (16)$$

where $\tilde{P}(p)$ is given below, see (38), and is the PDF of the aspect ratio, i.e. it is normalized to unity $\int_0^1 dp \tilde{P}(p) = 1$. Here, for the massless case, we see that it is independent of the total length (note that in¹⁰ we defined the aspect

ratio as $k = (\ell_1 - \ell_2)/(2(\ell_1 + \ell_2))$ and the function $R(k) = 8\pi\sqrt{3}\tilde{P}(p)$. The above results were obtained for the massless model (see units above in section IB1). This corresponds to the limit $\ell \ll 1$, that is $\ell \ll \ell_m = 1/m$, in the massive model. Note that we have assumed that $\ell \ll L$, where L is the system size (or $L \gg \ell_m$ in the massive case), so that translational invariance in x holds. Finally let us recall that the obtained power law, $\rho(\ell) \sim \ell^{-\kappa}$, with $\kappa = 3$ for the extension exponent, is consistent with the general scaling relation $\kappa = d + \zeta - 1$, with $d + \zeta = 4$ for the BFM.

The above results for a local kick, $f(x) = f\delta(x - x_s)$, can be extended to any kick $f(x)$ with bounded support, see section VA. It is important to note that for a *uniform kick* $f(x) = f$, and more generally for uniform driving, one cannot strictly define the avalanche extension since all points move. However, in the limit of a small $f \rightarrow 0^+$, one can access the "single avalanche regime" discussed above, and distinguish points which move by $O(1)$, and points which move by $O(f^2)$. In that sense one can still define the extension of a single avalanche. The position of the seed x_s is then a random variable, equiprobable along the interface (for $f(x) = f$), and once it is chosen, the above results apply w.r.t. x_s . From the above discussion, this will also hold for quasi-static avalanches obtained by driving at fixed velocity in the limit $v \rightarrow 0^+$.

Studying the $d = 1$ problem gives some information about the "span" of the avalanches in the d -dimensional BFM. Indeed, in any dimension d , the event "the support is contained in the band $[x_s - \ell_1, x_s + \ell_2] \times \mathbb{R}^{d-1}$ " has the same probability as for $d = 1$. Indeed it is easy to see that the statistics of the field $S(x_1)$ defined as $S(x_1) := \int dx_2 \dots dx_d S(x_1, \dots, x_d)$, under the driving $f(x_1) = \int dx_2 \dots dx_d f(x_1, \dots, x_d)$ in the d -dimensional BFM, is the same as the one of the field $S(x_1)$ under driving $f(x_1)$ in the $d = 1$ BFM. Now clearly if $S(x_1) = 0$ is some interval, then all $S(x_1, \dots, x_d) = 0$ for all x_2, \dots, x_d and x_1 in that interval. We will return to this below.

C. Avalanches upon driving by the tip

Above we mentioned the case of a local kick when the driving is applied only at a point $f(x) = f\delta(x)$. This is driving with an *imposed force*. It is also interesting to study, what happens in the case where the displacement of one point of the interface (or one region) is imposed, i.e. *imposed displacement*. This case was studied numerically in Ref.²². This can be achieved in the following variant of the equation of motion

$$\eta \partial_t u(x, t) = \nabla_x^2 u(x, t) - m^2 u(x, t) + F(u(x, t), x) + m_0^2 \delta(x)(w(t) - u(x, t)) \quad (17)$$

with $x \in \mathbb{R}$, where $F(u, x)$ is again a Brownian force landscape, leading to

$$\eta \partial_t \dot{u}(x, t) = \nabla_x^2 \dot{u}(x, t) - m^2 \dot{u}(x, t) + \sqrt{2\sigma \dot{u}(x, t)} \xi(x, t) + m_0^2 \delta(x)(\dot{w}(t) - \dot{u}(0, t)) \quad (18)$$

Here we have written the model in $d = 1$ and we drive by a point at $x = 0$. Then $1/m_0^2$ has dimension of length. We can either study this massive model (i.e. with $m^2 > 0$) and use the massive units (7), or study the massless model setting $m^2 = 0$. In the limit $m_0^2 \rightarrow +\infty$ the position of the point $x = 0$ is imposed.

Finally, one can generalize the model to any dimension d , and drive the interface by a subspace of dimension $d_w < d$, i.e. replace $\delta(x) \rightarrow \prod_{i=1}^{d-d_w} \delta(x_i)$ in (17). Again, if we look at a d -dimensional interface, driven by the $d_w = d - 1$ dimensional subspace $x_1 = 0$, then the avalanche sizes integrated over the coordinates x_2, \dots, x_d will be described by the $d = 1$ model.

II. AIM OF THE PRESENT PAPER, AND SUMMARY OF MAIN RESULTS

The aim of the present paper is to pursue the investigations started in^{9,10}, and also in⁵ where we calculated the mean shape centered on the seed, and study many more more observables, not calculated there. A large part of the results are for $d = 1$, but there are also results for $d > 1$.

Remark: relations to branching processes and to the super-Brownian motion. As detailed in a companion paper²³, the BFM is equivalent to a scaled limit of the branching Brownian motion which is a measure-valued process called the super-Brownian motion (SBM), studied in the probability community. There is a one to one correspondence between the observables in each system, for instance the velocity field of the BFM, $\dot{u}(x, t)$, maps onto the density of the SBM measure $\rho(x, t)$ (the limiting density of a large number of branching random walks). Although the two fields have developed separately, and the interest is a bit different in each field, there is some overlap reviewed in²³. The many new results in this paper can thus be easily translated in terms of branching diffusions. Some of that

translation is discussed in²³.

Note added. This work was started around 2015 and most results were obtained around that time. It is independent, and in part complementary, of Ref.²⁴ which appeared while this work was almost completed. That paper also addresses the mean shape at fixed extension, $\langle S(x) \rangle_\ell$, by a slightly different method, but not the many other observables obtained here.

We now present our main results.

A. Density of local jump $S(x)$, versus the distance to the seed at $x = x_s$

Let us first describe our results in $d = 1$ in the massless case, obtained in section IV. For a point x at a distance $|x - x_s|$ from the seed, there is a finite probability $p_f = e^{-6f/(x-x_s)^2}$ that no motion occurred. There is thus a probability $1 - e^{-6f/(x-x_s)^2} \simeq 6f/(x-x_s)^2$ (at small f), that some motion occurred at x . It is possible to calculate the density of the local jump size $S_0 \equiv S(x)$, as a function of the distance $|x - x_s|$ to the seed. We obtain the density (and its normalization)

$$\rho_{x_s}(S_0) = \frac{1}{S_0^{5/3}} \phi\left(\frac{S_0}{|x - x_s|^3}\right) \quad , \quad \int_{S_0 > 0} dS_0 \rho_{x_s}(S_0) = \frac{6}{(x - x_s)^2} \quad (19)$$

in terms of the scaling function

$$\phi(s) := -12 \times 3^{2/3} s \int_0^{+\infty} dt t^2 e^{-2 \times 3^{2/3} t s^{1/3}} \text{Ai}'(t) \quad (20)$$

which also admits the explicit expression (115) in terms of exponential-integral functions. It vanishes linearly as $\phi(s) \simeq \frac{12\sqrt{3} \times 3^{1/3} \Gamma(2/3)}{\pi} s$ at small s , and goes to a constant $\phi(+\infty) = \frac{1}{3^{2/3} \Gamma(\frac{1}{3})}$ at large s . It matches previously known results, i.e. the density at the seed¹⁰, and the total density³ (with no conditioning to the seed) $\rho(S_0) = \int dx_s \rho_{x_s}(S_0)$

$$\rho_{x_s}(S_0 = S(x_s)) = \frac{1}{3^{2/3} \Gamma(\frac{1}{3}) S_0^{5/3}} \quad , \quad \rho(S_0) = \frac{2}{3^{1/3} \Gamma(\frac{2}{3}) S_0^{4/3}} \quad (21)$$

The result (19) describes the crossover which occurs for $S_0 \sim |x - x_s|^3$, consistent with the scaling $S_0 \sim \ell^3$ between typical local jump and typical avalanche extension. As the distance to the seed increases (equivalently as S_0 decreases), the behavior of the jump density changes from $\rho_{x_s}(S_0) \sim S_0^{-5/3}$ for $S_0 \gg |x - x_s|^3$, valid within the typical avalanche extension, to $\rho_{x_s}(S_0) \sim S_0^{-2/3} |x - x_s|^{-3}$ for $S_0 \ll |x - x_s|^3$ valid outside the typical avalanche extension.

We have also calculated the effect of a mass in section IV B. In that case, setting $x_s = 0$ for notational simplicity, we obtain, in the massive units (we recall that here and above $S_0 = S(x)$)

$$\rho_{x_s=0}(S_0) = \frac{1}{S_0^{5/3}} \frac{4e^{-|x|}}{(1 + e^{-|x|})^2} \phi\left(\frac{S_0}{\left(\frac{2(1-e^{-|x|})}{1+e^{-|x|}}\right)^3}, 3^{1/3} S_0^{2/3}\right) \quad (22)$$

where the scaling function $\phi(s, s_0)$ is given in (126). Spatial dependence controlled by the mass is now exponential at large distance instead of power law.

B. Spatial shape: mean shape and fluctuations

The spatial shape of an avalanche is encoded in the random function $S(x)$ as a function of x , and represents a fluctuating profile. To define the "mean shape", and study its fluctuations, one first needs to center it. There are several ways to do it, some being easier to handle for calculations. One, easy to extract from experimental data, amounts to center it on its center of mass. An easier one from the point of view of theory is to center it on its seed x_s . In numerics, and sometimes in experiments, it is possible to determine the seed of each avalanche. In Ref.⁵ we calculated the mean shape centered on the seed, and conditioned to its total size S (i.e. at fixed fixed total size), that is $\langle S(x_s + x) \rangle_S$ as a function of x , in the BFM for any d .

We restrict here to $d = 1$. Our first set of results concern the mean shape conditioned on the distance, ℓ_2 , from the seed x_s to one of the edges of the avalanche, see Fig. 1. For a uniform kick we can then average over the position of the seed and obtain the absolute mean shape centered on one of the edges. Second, we obtain the mean shape of the avalanche conditioned on its total extension ℓ . Finally we can also condition on the aspect ratio of the avalanche, i.e. the parameter $p = \ell_2/(\ell_1 + \ell_2)$ defined in (13). We also show that the fluctuations of the shape are universal near the edge and we calculate the associated probability distribution. Our results are for the massless case, unless stated otherwise.

1. Mean spatial shape $\langle S(x) \rangle_{\ell_2}$ for fixed edge-to-seed distance ℓ_2

The PDF of the distance ℓ_2 from the seed to one of the edges of the avalanche, see Fig. 1, is given by

$$P(\ell_2) = \frac{12f}{\ell_2^3} e^{-6f/\ell_2^2} \quad (23)$$

In practice, it can be read in two ways: either one knows the position of the seed and one predicts the statistics of the position of one of the two edges, or, for a uniform driving, one measures the position of one edge and one predicts the statistics of the position of the seed (in the single avalanche regime, as discussed above).

We can first ask for the mean shape $\langle S(x) \rangle_{\ell_2}$ conditioned on ℓ_2 , i.e. at fixed ℓ_2 . With no loss of generality, let us denote $x_s = 0$ the position of the seed, the edge being at $x = \ell_2 > 0$. The calculation is elementary and amounts to solve a 1D Schrodinger problem in a $1/x^2$ potential. It is performed in Section V A 2. We find that if x is between the seed and the edge, the mean shape depends only on the distance to the edge $\ell_2 - x$

$$\langle S(x) \rangle_{\ell_2} = \frac{1}{21}(\ell_2 - x)^3 - \frac{1}{28} \frac{(\ell_2 - x)^4}{\ell_2} + \frac{f}{7} \frac{(\ell_2 - x)^4}{\ell_2^3} \quad , \quad x_s = 0 < x < \ell_2 \quad (24)$$

hence at fixed f it vanishes with a cubic law near the edge, $\langle S(x) \rangle_{\ell_2} \simeq \frac{1}{21}(\ell_2 - x)^3$, while in the large f limit the apparent exponent is 4. If x is on the other side of the seed the mean shape has a slow, power law decay with exponent -3 , due to the contribution of large avalanches

$$\langle S(x) \rangle_{\ell_2} = \frac{1}{21} \frac{(\ell_2)^6}{(\ell_2 - x)^3} - \frac{1}{28} \frac{(\ell_2)^7}{(\ell_2 - x)^4} + \frac{f}{7} \frac{\ell_2^4}{(\ell_2 - x)^3} \quad , \quad x < x_s = 0 < \ell_2 \quad (25)$$

Note that this mean shape is continuous but has a derivative jump $-f$ at the position of the seed $x = x_s$. For $f \rightarrow 0^+$ it remains only a jump in the third derivative, as a signature of the seed.

It is interesting to display the cumulative conditioned version, i.e. the mean shape conditioned on the event $\ell_2 < l_2$, for which it is easier to obtain good statistics in numerics, and which has a rather compact expression (with $x < l_2$, $l_2 > 0$)

$$\langle S(x) \rangle_{\ell_2 < l_2} = \frac{f}{7} \frac{(\ell_2 - x)^4}{\ell_2^3} \theta(x > x_s = 0) + \frac{f}{7} \frac{l_2^4}{(l_2 - x)^3} \theta(x < x_s = 0) \quad (26)$$

One can also ask about the mean shape, denoted $\bar{S}(y)$, obtained by centering the avalanche on the edge (defined as $y = 0$), and averaging uniformly over the position of the seed. This amounts to average $\langle S(x = \ell_2 - y) \rangle_{\ell_2}$ over $P(\ell_2)$. The result is that $\bar{S}(y) = f^{3/2} g(y/f^{1/2})$ where $g(z)$ is obtained in (151). It has the universal cubic behavior $g(z) \simeq \frac{z^3}{21}$ for small z and a linear one $g(z) \simeq \frac{z}{5}$ for large z . This is understood as follows. To produce motion at y , the avalanche must have an extension larger than y . For small f , typical avalanches are small, of extensions $\sim f^{1/2}$, the small scale cutoff. The cubic behavior is then visible only for distance to the edge smaller than the extension of these typical avalanches $y \ll f^{1/2}$. For larger distances $y \gg f^{1/2}$, only a fraction of order $1/y^2$ of the avalanche have extension larger than y , which upon averaging transforms the cubic into linear behavior.

Other results are obtained in Section V A 3, such as the distribution of the total avalanche size S conditioned on ℓ_2 , which is found to decay as $P(S|\ell_2) \sim S^{-5/2}$ for large $S \gg \ell_2^4$.

2. Universal fluctuations of the shape near the edge

Since $S(x)$ is a random profile, we can ask how the higher moments of $S(x)$ (here conditioned to a fixed edge to seed distance ℓ_2) vanish near the edge as a function of $\ell_2 - x$. We have also obtained these *fluctuations* of the shape

near the edge in Section V A 4. To leading order in the distance to the edge, we show that one can write

$$S(x) \simeq (\ell_2 - x)^3 \sigma \quad (27)$$

where σ is a random variable of $O(1)$, a form which accounts for the leading asymptotics for all the moments near the edge. We find that the PDF, $p(\sigma)$, of the random variable σ is given by its Laplace transform as

$$\int_0^{+\infty} d\sigma p(\sigma) e^{\lambda\sigma} = \frac{1}{A(\lambda)} - \frac{3\lambda A'(\lambda)}{A(\lambda)^2} \quad (28)$$

where the function $A(\lambda)$ is solution of the self-consistent equation

$$A^2 = \mathcal{P}(1; 0, -\frac{\lambda^2}{36} - \frac{2}{3}\lambda A^3) \quad \Leftrightarrow \quad A = A(\lambda) \quad (29)$$

From this, it is easy to obtain the moments up to a very high order. The lowest order ones are

$$\langle \sigma \rangle = \frac{1}{21} \quad , \quad \langle \sigma^2 \rangle = \frac{1}{273} \quad , \quad \langle \sigma^2 \rangle^c = \frac{8}{5733} \quad , \quad \langle \sigma^3 \rangle = \frac{265}{677768} \quad , \quad \langle \sigma^4 \rangle = \frac{1223}{22874670} \quad (30)$$

Hence we find that the amplitude of the cubic behavior fluctuates from avalanche to avalanche, the factor $\frac{1}{21}$ obtained above in (24) is only its mean value. Note for instance the dimensionless ratio for $x \rightarrow \ell_2$, i.e. x near the edge

$$\frac{\langle S(x)^2 \rangle}{\langle S(x) \rangle^2} \simeq \frac{\langle \sigma^2 \rangle}{\langle \sigma \rangle^2} = \frac{21}{13} = 1.61538 \quad (31)$$

We have also obtained the exponential tail of $p(\sigma)$ at large σ in (199).

Universality. It turns out that the form (27) at the edge of an avalanche, and the result (28)-(29) for $p(\sigma)$ are *universal* (for the BFM with SR elasticity). For instance, in Section VII D 2 and VII D 3 we calculate exactly the mean shape and "second shape" $\langle S(x)^2 \rangle_{\ell_2}$ for a completely different type of avalanches (i.e. driven by the tip) and the result near the edge is identical (for all moments, as we show there).

The above results, near one edge, are also independent (to leading order in the distance to the edge) of whether one fixes only one edge (as here) or two edges (as below). Indeed, although fixing the edge to seed distance ℓ_2 is different from fixing the total extension $\ell = \ell_1 + \ell_2$ of the avalanche, some results do not depend on that, as we check below, such as the small distance behavior near the edge. Obtaining them here via the fixed ℓ_2 calculation, was thus much easier.

Results for the massive case. Some of the above results have been obtained also in the massive case in section V C. The PDF of the seed-to-edge distance ℓ_2 is displayed in (222). The mean shape conditioned on ℓ_2 is given in (232) and (234). One sees in (233) that it again vanishes as $\sim \frac{1}{21}(\ell_2 - x)^3$ near the edge, however the coefficient of the $O((\ell_2 - x)^4)$ term explicitly depend on the ratio $r = \ell_2/\ell_m = m\ell_2$. We have also calculated the mean size of the avalanche conditioned on ℓ_2 , $\langle S \rangle_{\ell_2}$, in (243).

3. Mean spatial shape $\langle S(x) \rangle_{\ell}$ for fixed total extension ℓ

Until now we have conditioned only to one boundary, i.e. the distance ℓ_2 between the seed and the edge. One can also condition to the total extension $\ell = \ell_1 + \ell_2$, see Fig. 1. The calculation is more involved and is performed in several steps in Sections VIB, VIC and VID. It is related to the solution of the so-called Lamé equation. The final result, obtained and discussed in Section VID reads

$$\langle S(x) \rangle_{\ell} = \ell^3 \mathfrak{s}(z) \quad , \quad z = \frac{x + \ell_1}{\ell} \quad (32)$$

where z is the distance to the lower edge normalized to the total extension (so that $z = 0, 1$ at the two edges). The scaling function has the explicit expression, from (317),

$$\mathfrak{s}(z) = \frac{1}{4\pi\sqrt{3}} (2g(z) + (1 - 2z)g'(z) + z(z - 1)g''(z)) \quad (33)$$

in terms of the function $g(z)$

$$g(z) = g(1-z) = \frac{1}{6g_3^0} (2\mathcal{P}_0(z)^2 - \frac{4\pi\mathcal{P}_0(z)}{\sqrt{3}} + \mathcal{P}'_0(z)(\zeta(z; 0, g_3^0) - \frac{2\pi z}{\sqrt{3}})) \quad (34)$$

where $\mathcal{P}_0(z)$ and g_3^0 were defined in (14) and $\zeta(z; g_2, g_3)$ is the Weirstrass Zeta function, a primitive of $\mathcal{P}_0(z)$. The mean shape function is symmetric around $z = 1/2$ and has the following expansion near the edge (at small z)

$$s(z) = \frac{z^3}{21} - \frac{z^4}{28} - \frac{3\sqrt{3}z^7\Gamma(\frac{1}{3})^{18}}{98560\pi^7} + \frac{3\sqrt{3}z^8\Gamma(\frac{1}{3})^{18}}{112640\pi^7} + O(z^9) \quad (35)$$

and near its maximum at $z = \frac{1}{2}$

$$s(z) = 0.00182091 - 0.0314909(z - \frac{1}{2})^2 + .. \quad (36)$$

Integrating the mean shape we obtain the mean total avalanche size for a fixed extension ℓ

$$\langle S \rangle_\ell = \ell^4 \int_0^1 dz s(z) = 0.00073657566 \ell^4 \quad (37)$$

which we also verify through a distinct, more direct and simpler calculation in Section VIC.

4. Mean spatial shape $\langle S(x) \rangle_{\ell, p}$ for fixed total extension ℓ and aspect ratio p

We now consider the mean shape conditioned to the couple (ℓ_1, ℓ_2) equivalently to the couple (ℓ, p) where p is the aspect ratio defined in (12). The calculation is performed in Section VIB.

First let us recall¹⁰ that the avalanche density $\rho(\ell, p)$ is given by (see also Section VIA, e.g. Eq. (260), using $\mathcal{P}_0''(p) = 6\mathcal{P}_0(p)^2$).

$$\rho(\ell, p) = \frac{\tilde{R}(p)}{\ell^3} \quad , \quad \tilde{R}(p) = 8\pi\sqrt{3}\tilde{P}(p) = -36 \left((p-1)p\mathcal{P}_0(p)^2 + (p - \frac{1}{2})\mathcal{P}'_0(p) + \mathcal{P}_0(p) \right) \quad (38)$$

and $\tilde{P}(p) \simeq_{p \ll 1} \frac{3\sqrt{3}\Gamma(\frac{1}{3})^{18}}{896\pi^7} p^3$. Hence the aspect ratio p and the total length ℓ are *independent random variables* and $\tilde{P}(p) = \tilde{P}(1-p)$ is the PDF of the aspect ratio in the limit of small applied force. Its lowest moments are $\langle p \rangle = \frac{1}{2}$ and $\langle p^2 \rangle = 0.275664$.

Let us first display the result for the cumulative conditioning, which are simpler. We find

$$\langle S(x) \rangle_{\ell_1 < l_1, \ell_2 < l_2} = \frac{fl}{3g_3^0} (\psi_1(z)\psi_1(p)\theta(z < 1-p) + \psi_1(1-z)\psi_1(1-p)\theta(z > 1-p)) \quad (39)$$

$$z = \frac{x + l_1}{l} \quad , \quad l = l_1 + l_2 \quad , \quad p = \frac{l_2}{l_1 + l_2} \quad (40)$$

where $z = p$ is the position of the seed ($x = 0$ is the seed), and $\psi_1(z)$ is a solution to the Lamé equation, see (270), given by

$$\psi_1(z) = 2\mathcal{P}_0(z) + z\mathcal{P}'_0(z) \quad (41)$$

Note that (39) is symmetric in the variables z, p . Note that the notation p is a slight abuse of notation here in (40), since the aspect ratio is really $\frac{\ell_2}{\ell_1 + \ell_2}$. One can compare with the behavior near a single edge obtained above in Section IIB1, and one finds $\langle S(x) \rangle_{\ell_1 < l_1, \ell_2 < l_2} = \frac{f}{7} \frac{(l_2 - x)^4}{r_2^3} \phi(\frac{l_2}{l_1 + l_2})$ where $\phi(z)$ is a smoothly decaying function from $\phi(0) = 1$ to $\phi(1) = 0$, given in (284). Finally, the formula for the (cumulative) conditional mean total size, $\langle S \rangle_{\ell_1 < l_1, \ell_2 < l_2}$ is given in (306).

The mean shape for fixed extension ℓ and aspect ratio p is obtained in (293)-(294) and reads

$$\langle S(x) \rangle_{\ell,p} = \ell^3 \mathbf{s}_p(z) \quad (42)$$

$$\mathbf{s}_p(z) = \frac{1}{3g_3^0 \tilde{R}(p)} (G(p, z)\theta(z < 1-p) + G(1-p, 1-z)\theta(z > 1-p)) \quad , \quad z = \frac{x + \ell_1}{\ell} \quad (43)$$

$$G(p, z) = (p-1)p\psi_1(z)\psi_1''(p) + (z-1)z\psi_1(p)\psi_1''(z) + (p(2z-1) - z + 1)\psi_1'(p)\psi_1'(z) \quad (44)$$

where $\psi_1(z)$ is given in (41) and $\tilde{R}(p)$ in (38). Since $\tilde{R}(p) = \tilde{R}(1-p)$ one has $\mathbf{s}_p(z) = \mathbf{s}_{1-p}(1-z)$ as expected from parity invariance. Note also that $G(p, z)$ is a symmetric function of its arguments which gives an expected symmetry $\tilde{R}(p)\mathbf{s}_p(z) = \tilde{R}(z)\mathbf{s}_z(p)$. Expanding (42) at small z (for fixed p) we find that the behavior of $\mathbf{s}_p(z)$ near the edge $z = 0$ ($x = -\ell_1$) is

$$\mathbf{s}_p(z) = \frac{z^3}{21} + c_4(p)z^4 + \dots \quad , \quad c_4(p) = -\frac{1}{12} + \frac{p}{48} + O(p^2) \quad , \quad c_4(p) = \frac{1}{28(1-p)} - \frac{5}{48} - \frac{1-p}{64} + O((1-p)^2) \quad (45)$$

with the same behavior near the other edge $z = 1$ ($x = \ell_2$) with $p \rightarrow 1-p$. We have indicated the behavior of the coefficient of the subleading term $c_4(p)$ for p near $p = 0$ (i.e. $\ell_2 \ll \ell_1$) and near $p = 1$ (i.e. $\ell_2 \gg \ell_1$). One can check that the expectation of $c_4(p)$ over p is $\int_0^1 \tilde{P}(p)c_4(p) = -\frac{1}{28}$ consistent with the subleading term in (35). Remarkably, the leading term is again cubic with the coefficient $\frac{1}{21}$ independently of the value of the fixed aspect ratio, the same coefficient as in (35). This confirms, once again, the universality of the leading behavior near the edge, as discussed above in Section II B 2.

Finally by integration over x we obtain the result (322) for the mean total size at fixed extension and aspect ratio, which reads

$$\langle S \rangle_{\ell,p} = \frac{\mathbf{s}(p)}{\tilde{P}(p)} \ell^4 \quad (46)$$

C. Spatiotemporal shape near the edge of the avalanche

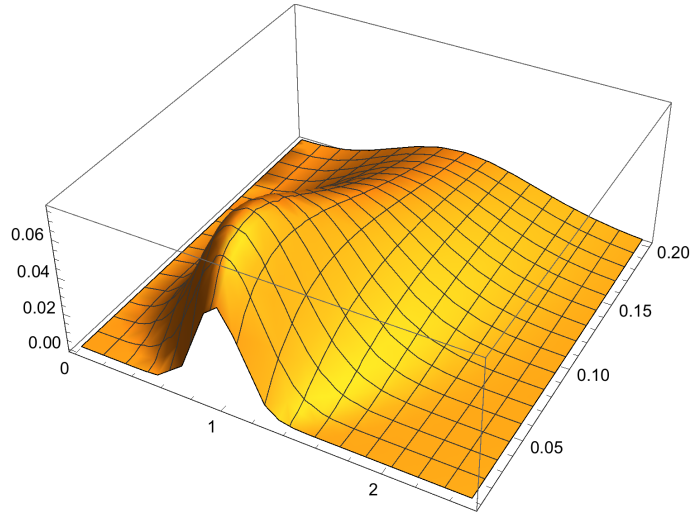


FIG. 2: Plot of the spatio-temporal shape: mean local instantaneous velocity $v(z, t) = t^{-1}F(z, 1/\sqrt{t})$, i.e. Eq. (212) for $z = \frac{\ell_2 - x_0}{\ell_2} \in [0, 2.5]$, and $t \in [0, 0.2]$. We use units such that the seed-to-edge distance is $\ell_2 = 1$. The mean velocity is larger near the seed at $x_0 = x_s = 0$, i.e. $z = 1$. It vanishes exactly for all times on the edge of the avalanche, i.e. the line $z = 0$, as given in (217).

The spatio-temporal shape is defined by the instantaneous velocity, $\dot{u}(x, t)$, for an avalanche started at time $t = 0$ with its seed at $x = 0$. We study the mean spatio-temporal shape near an edge of the avalanche in Section V B. To calculate the mean we will condition on a single edge, since it is an easier calculation. We first compute the (cumulative)

mean $\langle \dot{u}(x, t) \rangle_{\ell_2 < l_2}$ conditioned to the upper extension ℓ_2 being smaller than l_2 . It amounts to compute the euclidean Green function of a quantum particle in a $1/x^2$ potential, a well known textbook problem. We find

$$\langle \dot{u}(x, t) \rangle_{\ell_2 < l_2} = \frac{\sqrt{l_2(l_2 - x)}}{2t} I_{\frac{7}{2}}\left(\frac{l_2(l_2 - x)}{2t}\right) e^{-\frac{l_2^2 + (l_2 - x)^2}{4t}} \quad (47)$$

in terms of a modified Bessel function. Similarly we find that the mean spatiotemporal shape at fixed avalanche upper extension ℓ_2 is given by the scaling form

$$\langle \dot{u}(x, t) \rangle_{\ell_2} = \frac{\ell_2^3}{t} F\left(\frac{\ell_2 - x}{\ell_2}, \frac{\ell_2}{\sqrt{t}}\right) \quad (48)$$

where the spatiotemporal shape scaling function $F(z, r)$ is given in terms of Bessel functions in (213), and is plotted in Fig. 2. We find that the mean instantaneous local velocity vanishes with the distance to the edge of the avalanche, with the same exponent 3, as does the mean static shape. The associated amplitude \mathcal{A}_t now depends on time, and we obtain its exact time dependence

$$\langle \dot{u}(x, t) \rangle_{\ell_2} \simeq \mathcal{A}_t (l_2 - x)^3 \quad , \quad \mathcal{A}_t = \frac{1}{t} C\left(\frac{t}{\ell_2^2}\right) \quad , \quad C(\tau) = \frac{e^{-\frac{1}{4\tau}}}{5040\sqrt{\pi}\tau^{7/2}} \quad (49)$$

As time increases, the amplitude \mathcal{A}_t reaches a maximum and then decays. One can check that by integration over time $\int_0^{+\infty} dt \mathcal{A}_t = \int_0^{+\infty} \frac{d\tau}{\tau} C(\tau) = \frac{1}{21}$ one recovers the universal static amplitude.

D. Higher dimension

The BFM in higher spatial dimension $d > 1$ is more complicated to analyze since the instanton equation admits fewer analytical solutions. However one can still obtain results about some properties of the support of the avalanche. We denote this support $\Omega(x_s)$, where x_s is the position of the seed, and it consists in the set of points x which have moved during the avalanche, i.e. with $S(x) > 0$. For the SR BFM that we are studying we can surmise that the avalanche is connected, but for $d > 1$ it can contain "holes". Our study is limited to the BFM in dimension $d < 4$. The observables that we study are illustrated in the Figure 3.

1. Probability that a given point has not moved and mean shape around it

In Section VIII A we obtain the probability that a given point x_0 does not belong to the support of the avalanche. It reads, for any $d < 4$

$$\text{Prob}(S(x_0) = 0) = \text{Prob}(x_0 \notin \Omega(x_s)) = e^{-f \frac{2(4-d)}{(x_0 - x_s)^2}} \quad (50)$$

Note that it means that either the avalanche maximal radius (studied below) is smaller than $|x_s - x_0|$, or (for $d > 1$) it is larger, and the point x_0 belongs to a "hole" inside the avalanche.

Now we can compute some observables conditioned to the event that $S(x_0) = 0$. The first one is the PDF of the variable $\Sigma = \int d^d x \frac{S(x)}{(x - x_0)^4}$. It turns out that this variable is finite and its PDF is obtained in (456). It exhibits a $\Sigma^{-3/2}$ power law regime, reminiscent of the one for the total size S , with some cutoffs (see discussion there).

The second observable is the mean shape $\langle S(x) \rangle_{S(x_0)=0}$ conditioned to $S(x_0) = 0$. It amounts to solve for the Green function of a Schrodinger problem in a $1/r^2$ potential in dimension d . The complete result in any d is given in (480), and in $d = 2$ (which is simpler) it is given in (473). Note that in $d = 1$ this observable corresponds to the cumulative conditional shape with a single boundary, see (471). The most interesting property is that the shape vanishes near the point x_0 as a power law of the distance with a quite non-trivial exponent b_d^+ (we have chosen $x_0 = 0$ and denote the radial coordinates around that point as $r = |x|$ and $r_s = |x_s|$)

$$\langle S(x) \rangle_{S(x_0)=0} \simeq_{r \rightarrow 0} f C_d r_s^{b_d^-} r^{b_d^+} \quad , \quad b_d^\pm = \frac{1}{2} \left(2 - d \pm \sqrt{d^2 - 20d + 68} \right) \quad (51)$$

where C_d is a dimension dependent constant and with $b_2^+ = 2\sqrt{2}$, $b_3^+ = \frac{1}{2}(\sqrt{17} - 1)$ and $b_d^+ \rightarrow 0$ as $d \rightarrow 4^-$ (and one recovers $b_1^+ = 4$ as found in $d = 1$).

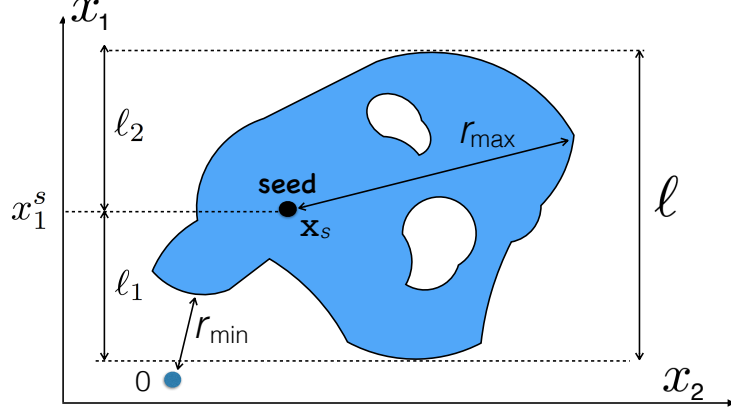


FIG. 3: Schematic representation of the support of an avalanche for a 2-dimensional interface in the internal plane $x = (x_1, x_2)$ (the direction of motion - not shown - being transverse to the plane of the figure). The region in blue is the support Ω , i.e. it contains all points that have moved ($S(x) > 0$). The region in white is the complementary, and contains all points that have not moved ($S(x) = 0$). The picture is a cartoon, as one rather expects a fractal structure. Here x_s is the position of the seed (the first point which moves). One studies here the following observables shown in the Figure: (i) the *maximal distance reached by the avalanche* r_{\max} (ii) the *minimal distance of approach* of a given point 0, r_{\min} (iii) the *total span* ℓ associated to a direction x_1 as the $\ell = \max_{x \in \Omega}(x_1) - \min_{x \in \Omega}(x_1)$, as well as the *upper span* $\ell_2 = \max_{x \in \Omega}(x_1) - x_s$ and the *lower span* $\ell_1 = x_s - \min_{x \in \Omega}(x_1)$.

2. Maximal distance reached by an avalanche and minimal distance of its support to a point

Let us define the *maximal radius* of an avalanche as $r_{\max} = \max_{x \in \Omega(x_s)} |x - x_s|$ the maximal distance that it reaches counted from the seed, see Figure 3. It is a random variable and we obtain in Section VIII D its CDF and its density, which read

$$\text{Prob}(r_{\max} < R) = e^{-c_d f / R^2} \quad , \quad \rho(r_{\max}) = \frac{2c_d}{r_{\max}^3} \quad (52)$$

with $c_{d=2} \approx 12.5634$, $c_{d=3} \approx 15.7179$. In $d = 1$ this observable identifies with $\text{Prob}(\ell_1 < R, \ell_2 < R)$ and one finds $c_1 = \frac{3}{2} \mathcal{P}_0(\frac{1}{2}, \Gamma(1/3))^{18} / (64\pi^6) = 8.8475159\dots$

Another interesting observable is the *minimal distance of approach*, i.e. $r_{\min} = \min_{x \in \Omega(x_s)} |x|$, $0 < r_{\min} < r_s = |x_s|$, the minimal distance between the origin $x = 0$ and any point of the avalanche (started at x_s), see Figure 3. We denote its PDF as $P_{r_s}(r_{\min})$. Of course, we know from (50) that there is a non zero probability, equal to $p_0 = 1 - e^{-\frac{2(d-d)f}{r_s^2}}$, that $r_{\min} = 0$, i.e. that the point $x = 0$ belongs to the avalanche. So $P_{r_s}(r_{\min})$ has a delta function piece $p_0 \delta(r_s)$ at zero. We have calculated $P_{r_s}(r_{\min})$ in (506), (507). Let us indicate here only the behavior of the associated density $\rho_{r_s}(r_{\min} = R) = \partial_f P_{r_s}(r_{\min} = R)|_{f=0+}$ when $r_{\min} \ll r_s$

$$\rho_{r_s}(r_{\min} = R) \simeq \frac{B_d}{R^{3+b_d^-} r_s^{-b_d^-}} \quad , \quad 0 < r_{\min} \ll r_s \quad (53)$$

where B_d is a dimension dependent constant, and the exponent b_d^- is defined in (51). Note that $3 + b_d^- \geq 0$ and increases from 0 to 1 as d increases from $d = 1$ to $d = 4$.

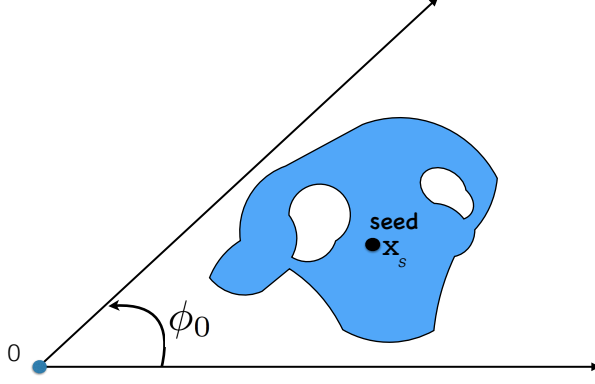


FIG. 4: Avalanche of seed x_s and support Ω (in blue) in two dimensions. We obtain the probability that it remains confined within the conical domain of apex in 0 and opening angle ϕ_0 , as represented schematically. For $\phi_0 = \pi$ it is related to the distribution of ℓ_1 defined in Fig. 3. For $\phi_0 \rightarrow 2\pi$ it becomes the probability that the avalanche does not intersect the positive half-axis.

3. Probability of not hitting a cone in two dimension

Consider the conical domain in $d = 2$, in polar coordinates $\mathcal{D} = (r, \phi) \in]0, +\infty[\times]0, \phi_0[$ with an opening angle $0 < \phi_0 \leq 2\pi$. We ask what is the probability that an avalanche $\Omega(x_s)$, with a seed inside the wedge at $x = (r_s, \phi_s)$, remains strictly confined inside the wedge (i.e. is not allowed to touch the two radial lines at $\phi = 0, \phi_0$). We find in Section VIII F that it equals

$$\text{Prob}(S(r, 0) = S(r, \phi_0) = 0, \forall r \in [0, +\infty]) = \exp\left(-\frac{6f}{r_s^2}\left(\frac{1}{3} + h_{\phi_0}(\phi_s)\right)\right) \quad (54)$$

where $h_{\phi_0}(\phi)$ is a Weierstrass function with parameter $g_3 = g_3(\phi_0)$ determined by the condition that its period, denoted $2\Omega(\frac{4}{3}, g_3)$, equals ϕ_0 , namely

$$h_{\phi_0}(\phi) = \mathcal{P}(\phi; g_2 = \frac{4}{3}, g_3(\phi_0)) \quad , \quad g_3 = g_3(\phi_0) \quad \Leftrightarrow \quad 2\Omega(\frac{4}{3}, g_3) = 2 \int_{e_1}^{+\infty} \frac{dt}{\sqrt{4t^3 - \frac{4}{3}t - g_3}} = \phi_0 \quad (55)$$

where $t = e_1$ is the largest positive root of $4t^3 - \frac{4}{3}t - g_3 = 0$, a condition equivalent to asking that $\mathcal{P}'(\phi_0/2; g_2 = \frac{4}{3}, g_3(\phi_0)) = 0$. One finds that g_3 decreases as ϕ_0 increases, with $g_3 \in [g_3^c, +\infty[$, where $g_3 \simeq g_3^0/\phi_0^6$ for a small cone opening angle $\phi_0 \ll 1$ and $g_3^c \simeq -0.295402$ corresponds to $\phi_0 = 2\pi$, i.e. the probability that the avalanche does not intersect the positive half axis.

From these results, we also obtain in Eq. (559) the joint CDF of the "angular extensions" $\varphi_2 = \max_{x=(r,\phi) \in \Omega} \phi$ and $\varphi_1 = -\min_{x=(r,\phi) \in \Omega} \phi$ (for $\phi_s = 0$), i.e. the angular analogs of ℓ_1, ℓ_2 , as well as the PDF of the total angular extension $\varphi = \varphi_1 + \varphi_2$ by differentiation.

4. Avalanche span and shape in $d > 1$

In dimension d , as we discussed above, one can define the span ℓ of the avalanche along one given axis, say x_1 , and the distances ℓ_1 and ℓ_2 from the seed to the lines (in general hyperplanes) as defined in the caption of Fig. 3.

With this definition we know that all joint statistics of ℓ_1, ℓ_2 and $S_{tot}(x_1) = \int d^{d-1}x_{\perp} S(x_1, x_{\perp})$ is *identical* to the one for the $d = 1$ BFM that we have already calculated. For instance, the mean shape integrated over the transverse space x_{\perp} , $\langle S_{tot}(x_1) \rangle_{\ell}$, is given by the same formula.

One can also ask about the local mean shape at a point, $\langle S(x_1, x_{\perp}) \rangle_{\ell}$, i.e. not integrated. It is a related but different question which contains non trivial information also in the transverse direction. This is studied in Section (VIII E),

where we obtain the following result

$$\langle S(x_1, x_\perp) \rangle_{\ell_2 < \ell_2} = f \int \frac{d^{d-1}q}{(2\pi)^{d-1}} e^{iq(x_\perp - x_\perp^s)} F_{|q|}(\ell_2 + x_1^s - x_1, \ell_2) \quad (56)$$

$$F_q(a, b) = \sqrt{ab} (I_{7/2}(qa) K_{7/2}(qb) \theta(0 < a < b) + K_{7/2}(qa) I_{7/2}(qb) \theta(0 < b < a))$$

in terms of modified Bessel functions. If one integrates this equation over x_\perp , it selects $q = 0$, in which limit one has $F_{q \rightarrow 0}(a, b) = \frac{a^4}{7b^3} \theta(0 < a < b) + \frac{b^4}{7a^3} \theta(0 < b < a)$, recovering (24) and (25) as expected (see discussion above).

One obtains similarly the mean shape at fixed upper span ℓ_2 . We display its expression in $d = 2$, choosing the origin $x_s = (x_1^s, x_\perp^s) = 0$ as the position of the seed

$$\langle S(y_1, y_\perp) \rangle_{\ell_2} = \frac{\ell_2(2\ell_2 - y_1)}{24(2\pi)(\ell_2 - y_1)^2} (y_1^2 + y_\perp^2) \Sigma \left(\frac{y_1^2 + y_\perp^2}{2\ell_2(\ell_2 - y_1)} \right) \quad (57)$$

$$\Sigma(z) = \frac{(z+1)(15z(z+2)+2)}{2z(z+2)} - \frac{3}{4}(5z(z+2)+4) \log\left(1 + \frac{2}{z}\right) \quad (58)$$

From the asymptotics of the scaling function $\Sigma(z)$, one finds again that the mean shape vanishes near the upper edge with a cubic power, but with an amplitude which decreases with $|x_\perp|$, the transverse distance to the seed, on a scale ℓ_2 , and with a high power, as $1/|x_\perp|^8$, more precisely

$$\langle S(x_1, x_\perp) \rangle_{\ell_2} = \frac{16\ell_2^7}{105\pi(\ell_2^2 + x_\perp^2)^4} (\ell_2 - x_1)^3 + O((\ell_2 - x_1)^4) \quad (59)$$

Integration of the amplitude of the cubic power over x_\perp recovers the universal coefficient $\frac{1}{21}$. So, for a given position of the seed, there is a non-trivial shape structure in the transverse direction near the edge of the avalanche.

E. Tip driving PDF of local and total sizes, extension distribution and spatial shape

We now consider driving by the tip, as described in Section IC, and focus on $d = 1$. The equation of motion is (18) contains two mass scales, a local one, m_0^2 , equal to the curvature of the local well which drives $u(x = 0, t)$ and a uniform mass m^2 which, when present, acts as a cutoff for large avalanches. We study the avalanche produced by the driving kick at $x = 0$, $f(x, t) = \delta(x)m_0^2 w \delta(t)$ in (18).

We first present the results for $m = 0$. Since $\hat{L}_{m_0} = m_0^{-2}$ has the dimension of a length scale (in the internal x direction) a crossover occurs as m_0 is varied. In the limit $m_0 \rightarrow 0$ one recovers the results for "imposed local force" driving, while for $m_0 \rightarrow +\infty$ we have "imposed local displacement". The crossover between the two was not studied in¹⁰ and is obtained here exactly. We obtain the joint PDF, $P_w(S, S_0)$, of the total size S , and of the local jump $S_0 = S(x = 0)$ at the tip $x = 0$, and its marginal distributions, as a function of m_0 . There is a crossover scale at $S = \hat{S}_{m_0}$ for avalanche sizes, such that below and above this scale the avalanche look different

$$S \ll \hat{S}_{m_0} \Leftrightarrow \text{imposed local force} \quad (60)$$

$$S \gg \hat{S}_{m_0} \Leftrightarrow \text{imposed local displacement} \quad (61)$$

with, and similarly for the crossover scale in the local size at $S_0 = \hat{S}_{m_0}^0$ (in units $\sigma = \eta = 1$)

$$\hat{S}_{m_0} = m_0^{-8} \quad , \quad \hat{S}_{m_0}^0 = m_0^{-6} \quad (62)$$

(noted with a hat to distinguish it from S_m the upper cutoff scale of avalanches in presence of a uniform mass). So large avalanches always feel the "imposed displacement". This scaling is expected, more generally one expects $\hat{S}_{m_0} \sim \hat{L}_{m_0}^{d+\zeta}$ and $S_0 \sim \hat{L}_{m_0}^\zeta$ with here $\zeta = \zeta_{\text{BFM}} = 3$ and more generally $d + \zeta_{\text{BFM}} = 4$. Note that in the limit $m_0 \rightarrow +\infty$ the local jump is exactly constrained,

1. Distribution of local jumps at the tip

Let us start with $P_w(S_0)$, we find in Section VIII B 3

$$P_w(S_0) = \frac{1}{3^{1/3} S_0^{5/3}} w m_0^2 e^{\frac{2}{3}y^3} (-y \text{Ai}(y^2) - \text{Ai}'(y^2)) \quad , \quad y = \frac{m_0^2(S_0 - w)}{2 \times 3^{1/3} S_0^{2/3}} \quad (63)$$

One can check that the first moment exists with $\langle S_0 \rangle = w$, and that in the limit $m_0 \rightarrow +\infty$, $P_w(S_0)$ converges to $\delta(S_0 - w)$ as expected, since then the displacement is fully imposed. Note that at fixed w , there is a cutoff for small avalanches $S_0^{\min} \sim m_0^3 w^{3/2}$. From (63) one obtains the density $\rho(S_0) = \partial_w P_w(S_0)|_{w=0+}$ in (350), and one finds that exhibits the single crossover scale $S_0 \sim \hat{S}_{m_0} = m_0^{-6}$. Using Airy function asymptotics (see (353)) one finds that the density crosses over between the two power laws characteristic respectively of the force imposed and the displacement imposed regimes

$$\rho(S_0) \simeq \frac{m_0^2}{3^{2/3} \Gamma(\frac{1}{3}) S_0^{5/3}} \quad , \quad S_0 \ll \hat{S}_{m_0} = m_0^{-6} \quad (64)$$

$$\rho(S_0) \simeq \sqrt{\frac{3}{2\pi}} \frac{1}{m_0^3 S_0^{5/2}} \quad , \quad S_0 \gg \hat{S}_{m_0} = m_0^{-6} \quad (65)$$

and our result (350) describes the full crossover. The first limiting case (force imposed) (64) was already obtained in¹⁰ but the behavior (65) is new. Note however that it holds only in some regime at finite m_0 , since for $m_0 = +\infty$ the displacement at the tip is fixed by the driving and equal to $S_0 = w$. This crossover is discussed in Section VII B 3.

2. Distribution of total sizes

The distribution of the total size S of the avalanche, $P_w(S)$, is obtained in Section (VII B 2) in the Laplace transform form (339). On this form one shows that it exhibits a crossover between two limits. For $S \ll \hat{S}_{m_0}$, equivalently for $m_0 \rightarrow 0$ at fixed S, w

$$P_w(S) = \frac{m_0^2 w e^{-\frac{m_0^4 w^2}{4S}}}{2\sqrt{\pi} S^{3/2}} \quad (66)$$

which is normalized to unity. It is exactly the massless limit $P_f(S) = \frac{f e^{-\frac{f^2}{4S}}}{2\sqrt{\pi} S^{3/2}}$ of the standard size distribution with driving at imposed force $f = \int dx dt m_0^2 w \delta(t) \delta(x)$. In the opposite limit $S \gg \hat{S}_{m_0}$, equivalently $m_0^2 \rightarrow +\infty$ at fixed S, w , we obtain

$$P_w(S) = L T_{p \rightarrow S}^{-1} e^{-w\sqrt{\frac{2}{3}}(4p)^{3/4}} = \frac{3^{2/3}}{(4w)^{4/3}} \mathcal{L}_{3/4}(3^{2/3} S / (4w)^{4/3}) \quad (67)$$

with $\mathcal{L}_{3/4}$ being the stable Levy law of index 3/4, see Appendix B where its explicit expression is given in terms of hypergeometric functions. The associated size density $\rho(S) = \partial_w|_{w=0+} P_w(S)$ has the explicit expression

$$\rho(S) = \frac{\sqrt{3}}{\Gamma(1/4) S^{7/4}} \quad (68)$$

which was also found in¹⁰.

3. Joint distribution of total size and of local jump at the tip

Although it is not easy to obtain directly an explicit expression for the full crossover form $P_w(S)$, we have able to obtain the explicit expression of the JPDP $P_w(S, S_0)$ for both the massive and massless cases in Section VII B 4. The result is bulky and displayed in (365). Here we show only its associated density, $\rho(S, S_0) = \partial_w|_{w=0} P_w(S, S_0)$, and for the massless case $m^2 = 0$. It takes the scaling form

$$\rho(S, S_0) = m_0^{20} \hat{\rho}(m_0^8 S, m_0^6 S_0) \quad (69)$$

where the scaling function reads

$$\hat{\rho}(S, S_0) = \frac{2 \cdot 3^{2/3} S_0^{1/3} \exp\left(-\frac{3S_0^3}{S^2} + \frac{S_0}{36} - \frac{S_0^2}{2S} - \frac{6S_0^4}{S^3}\right)}{\sqrt{\pi} S^{5/2}} (y \text{Ai}(y^2) - \text{Ai}'(y^2)) \quad , \quad y = S_0^{1/3} \frac{S + 6S_0}{2\sqrt{3}S} \quad (70)$$

Finally, note that we have also given the lowest moments of S, S_0 and joint moments in the massive case in Section VII B 1.

4. Distributions of extensions for tip-driven avalanches

In tip-driven avalanches the seed is always at $x_s = x = 0$. One is thus interested in the distribution of ℓ_2 the distance of the seed to the upper edge at $x = \ell_2$. In Section VII C we obtain its CDF as

$$\text{Prob}(\ell_2 < r) = e^{-6m_0^8 w \phi(rm_0^2)} \quad (71)$$

where the function $\phi(r)$ is defined by inversion

$$\phi = \phi(r) \quad \Leftrightarrow \quad r = \int_{\phi}^{+\infty} \frac{dy}{\sqrt{4y^3 + \phi^2 + 4\phi^{5/2}}} = {}_2F_1\left(\frac{1}{6}, \frac{1}{2}; \frac{7}{6}; -\frac{\phi^2 + 4\phi^{5/2}}{4\phi^3}\right) \frac{1}{\sqrt{\phi}} \quad (72)$$

which can also be written as $\phi = \mathcal{P}(r, 0, g_3 = -\phi^2 - 4\phi^{5/2})$. The detailed asymptotics of $\phi(r)$ and of the CDF are given in (378), (379) and (380). From the CDF one obtains the PDF $P(\ell_2)$ and the corresponding density, which reads

$$\rho(\ell_2) = \partial_w|_{w=0^+} P(\ell_2) = -6m_0^8 \phi'(m_0^2 \ell_2) \quad (73)$$

Its asymptotics are obtained in Section VII C as

$$\rho(\ell_2) \simeq \frac{12m_0^2}{\ell_2^3} \quad , \quad \ell_2 \ll m_0^{-2} \quad (74)$$

$$\rho(\ell_2) \simeq \frac{36\Gamma(\frac{1}{3})^3 \Gamma(\frac{7}{6})^3}{\pi^{3/2} \ell_2^4} = \frac{99.2466..}{\ell_2^4} \quad , \quad \ell_2 \gg m_0^{-2} \quad (75)$$

The first regime of small ℓ_2 also corresponds to the limit of small m_0 , i.e. $m_0 \rightarrow 0$, and one recover $\rho_f(\ell_2) = \partial_f|_{f=0^+} P(\ell_2) \simeq \frac{12}{\ell_2^3}$, i.e. (23), the result (for a single boundary) in the regime of "imposed local force" $f = m_0^2 w$. The second regime, of large extension ℓ_2 , also corresponds to the limit of large m_0 , i.e. $m_0 \rightarrow +\infty$: it is the regime of "imposed local position" and leads to a new result, with a different decay exponent, $\rho(\ell_2) \sim 1/\ell_2^4$.

Now, for finite m_0 the upper extension ℓ_2 and the lower one ℓ_1 will be correlated non-trivially. In the limit $m_0 \rightarrow +\infty$ of strict imposed displacement, however, they become two independent random variables. We now study the avalanche shape in this limit.

5. Mean shape of a tip-driven avalanche and its fluctuations near the edge

We have obtained in Section VII D 2 the mean shape of an avalanche of a given extension ℓ_2 , in the limit $m_0 \rightarrow +\infty$ of strict imposed displacement, for $0 \leq x \leq r$

$$\langle S(x) \rangle_{\ell_2 < r} = w \mathfrak{s}_>\left(\frac{x}{r}\right) \quad , \quad \mathfrak{s}_>(0) = 1 \quad , \quad \mathfrak{s}_>(1) = 0 \quad (76)$$

$$\mathfrak{s}_>(z) = \frac{1}{\mathcal{P}'(1, 0, g_3^*)} (2\mathcal{P}(1-z, 0, g_3^*) + (1-z)\mathcal{P}'(1-z, 0, g_3^*)) \quad (77)$$

where $\mathcal{P}'(1, 0, g_3^*) = -(-g_3^*)^{1/2}$ from the properties of the Weierstrass function, and $g_3^* = -\frac{4\Gamma(\frac{1}{3})^6 \Gamma(\frac{7}{6})^6}{\pi^3} = -30.400905$ is the negative root of the equation $\mathcal{P}(1, 0, g_3) = 0$. The condition $\mathfrak{s}_>(0) = 1$ is correctly recovered, as it should since for strictly imposed displacement (limit $m_0 \rightarrow +\infty$), at the tip $S(x=0) = w$ with no fluctuations. Near the edge of the avalanche

$$\mathfrak{s}_>(z) \simeq \frac{3\Gamma(\frac{1}{3})^3 \Gamma(\frac{7}{6})^3}{7\pi^{3/2}} (1-z)^4 = 1.18150748.. \times (1-z)^4 \quad (78)$$

The mean shape conditioned to the extension ℓ_2 is given by the exact formula (also compatible with $S(x=0) = w$)

$$\langle S(x) \rangle_{\ell_2} = w \mathfrak{s}_>(z) - \frac{w}{\ell_2 P(\ell_2)} z \mathfrak{s}'_>(z) \quad , \quad z = \frac{x}{\ell_2} \quad (79)$$

which, in the limit of infinitesimal driving has the finite limit, for $0 \leq x \leq \ell_2$

$$\langle S(x) \rangle_{\ell_2} = -\frac{1}{\ell_2 \rho(\ell_2)} z s'_>(z) = \ell_2^3 \tilde{s}(z) \quad , \quad z = \frac{x}{\ell_2} \quad (80)$$

$$\tilde{s}(z) = \frac{1}{6g_3^*} z(2(1-z)\mathcal{P}(1-z, 0, g_3^*)^2 + \mathcal{P}'(1-z, 0, g_3^*)) \quad (81)$$

It is plotted in Fig. 5 (note that there $s(y_0) = \tilde{s}(z = 1 - y_0)$ here). It vanishes near the tip (since $w \rightarrow 0$) as

$$\tilde{s}(z) = \frac{18\pi^{3/2}z}{\Gamma(\frac{1}{6})^3 \Gamma(\frac{1}{3})^3} + O(z^2) = 0.0302277z + O(z^2) \quad (82)$$

and near the edge $z \rightarrow 1^-$ as

$$\tilde{s}(z) = \frac{1}{21}(1-z)^3 - \frac{1}{21}(z-1)^4 + O((z-1)^9) \quad (83)$$

i.e. with the same cubic power and the same prefactor as for the force driven avalanches obtained in (35), a manifestation of the aforementioned universality of the edge behavior. More detailed series expansions are given in (420) and (421).

Integrating $\int_0^\ell dx_0$ one obtains the mean total size at fixed extension

$$\langle S \rangle_{\ell_2} = \ell_2^4 \frac{-\zeta(1; 0, g_3^*)}{18g_3^*} = 0.0022097287584 \ell_2^4 \quad (84)$$

which is also obtained by an equivalent calculation in Section VIID 4, together with the higher moments $\langle S^p \rangle_{\ell_2}$ in (445) and their generating function.

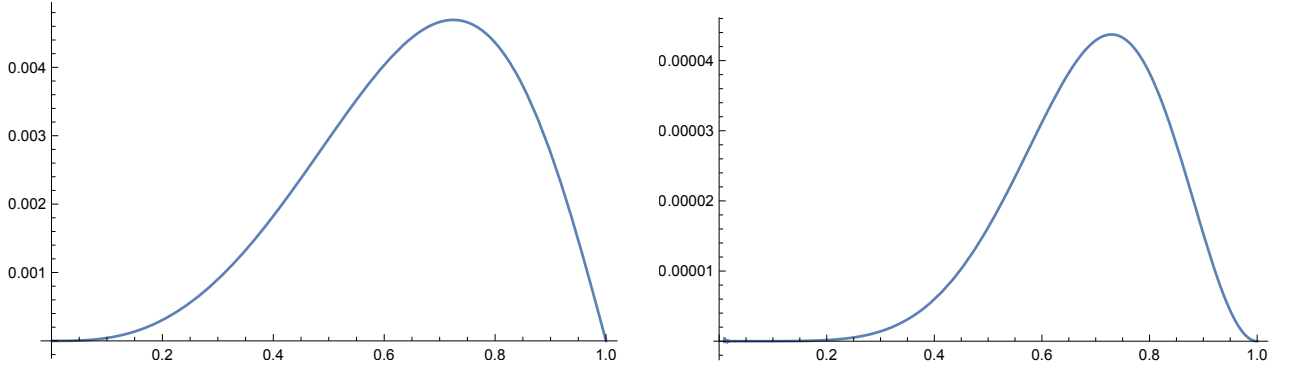


FIG. 5: Left: Plot of the scaling function describing the mean shape of an avalanche with imposed displacement at the tip ($m_0 = +\infty$). What is plotted is $s(y_0) = \tilde{s}(z = 1 - y_0)$ as a function of y_0 . The mean shape vanishes with a cubic power at the edge of the avalanche $y_0 = 0$ ($z = 1$) and linearly at the driving tip $y_0 = 1$ ($z = 0$). Right: idem for the second shape (second moment of the shape), here is a plot of $s_2(y_0)$ defined in the text. It vanishes with the sixth power at the edge, and we show that the n -th moment vanishes with power $3n$, with a prefactor that can be extracted from our general formula.

Second shape and full mean distribution near the edge. In Section VIID 3 we calculate the second shape, that is $\langle S(x)^2 \rangle_{\ell_2}$. It is given in the form $\langle S(x)^2 \rangle_{\ell_2} = \ell_2^6 s_2(1 - \frac{x}{\ell_2})$ where the scaling function $s_2(y)$, $0 \leq y \leq 1$ is given in (428) and plotted in Fig. 5. The ratio $\frac{\langle S(x)^2 \rangle_{\ell_2}}{\langle S(x) \rangle_{\ell_2}^2}$ is plotted in Fig. 6, varies between $\frac{21}{13} = 1.61538$ for x near ℓ_2 , as in (31), and 2 for x near the tip $x = 0$. One finds that near the edge of the avalanche

$$\langle S(x)^2 \rangle_{\ell_2} \simeq \frac{1}{273} (\ell_2 - x)^6 \quad (85)$$

exactly the same leading order result, up to the amplitude, as for the force imposed avalanches. We show in Section VIID 3 (see Remark about universality at the end) that for the tip driven avalanches, one can also write $S(x) \simeq \sigma \times (\ell_2 - x)^3$ near the edge, with the same probability distribution $p(\sigma)$ for the random variable σ as given in (28), (29) (with lowest order moments given in (30)), which is thus universal (and reproduces all the moments of the shape near the edge).

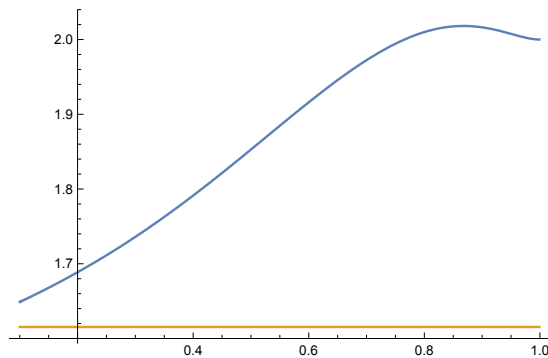


FIG. 6: Plot of the ratio $s_2(y_0)/s(y_0)^2$ for $y_0 \in [0, 1]$, with the same notations as in Fig. 5.

III. METHOD: GENERATING FUNCTION AND INSTANTON EQUATION

In the BFM model (3) it is possible to express averages of exponentials of linear functions of the velocity field in terms of solutions of a non-linear partial differential equation, see Refs.^{3,8} for details. Since here we mostly study observables based on avalanche sizes, we mostly need the "static" version of this property. It states that for an initial condition $\dot{u}(x, t = 0^-) = 0$ and any forward driving $\dot{f}(x, t) \geq 0$, as well as any "source" function $\lambda(x)$ so that the l.h.s exists, one has

$$G[\lambda(x)] := \overline{\exp\left(\int d^d x \lambda(x) S(x)\right)} = e^{\int d^d x f(x) \tilde{u}^\lambda(x)}. \quad (86)$$

where here $f(x) = \int_0^{+\infty} dt \dot{f}(x, t)$. In this paper $\overline{\dots}$ denotes the average over the disorder, i.e. the Brownian random force field, equivalently over $\xi(x, t)$ in (3). The function $\tilde{u}^\lambda(x)$ is the solution of the (time independent) "instanton equation"

$$\nabla_x^2 \tilde{u}(x) - A \tilde{u}(x) + \tilde{u}(x)^2 = -\lambda(x). \quad (87)$$

where $A = 1$ for the massive case and $A = 0$ for the massless case, in the units defined in Section IB1 in each case.

To calculate the total avalanche size one needs a uniform source in the instanton equation: $\lambda(x) = \lambda$, and for the local size we need a local source, i.e. in $d = 1$, $\lambda(x) = \lambda \delta(x)$. To obtain information about the extension of the avalanches, we consider a source localized at two points in space, in $d = 1$, $\lambda(x) = \lambda_1 \delta(x - r_1) + \lambda_2 \delta(x - r_2)$.

The dynamical version of (86) and (87) is recalled when we need it in Section VB below. In Sections IV to VII we specialize to $d = 1$, and consider $d > 1$ in Section VIII.

IV. BULK DRIVING: DENSITY OF LOCAL SIZE VERSUS THE DISTANCE TO THE SEED

We study here various properties of the local size of an avalanche in $d = 1$. We use the dimensionless units. The Laplace transform (LT) of the PDF, $P_{\{f(x)\}}(S_0)$, of the local avalanche size $S_0 = S(x = 0)$ following a kick (4) of amplitude $f(x)$ is given from (86) as

$$\overline{e^{\lambda S_0}} = \int dS_0 e^{\lambda S_0} P_{\{f(x)\}}(S_0) = e^{\int dx f(x) u^\lambda(x)} \quad (88)$$

where $u^\lambda(x)$ is the solution of the 1D equation (87)

$$\tilde{u}''(x) - A \tilde{u}(x) + \tilde{u}(x)^2 = -\lambda \delta(x) \quad (89)$$

which vanishes at $\pm\infty$, with $A = 0$ in the massless case and $A = 1$ in the massive case. The explicit solution reads (see e.g.¹⁰ and references therein)

$$\tilde{u}^\lambda(x) = \frac{6(1 - z_\lambda^2)e^{-|x|}}{(1 + z_\lambda + (1 - z_\lambda)e^{-|x|})^2}, \quad A = 1 \quad (90)$$

$$\tilde{u}^\lambda(x) = -\frac{6}{(|x| + x_\lambda)^2}, \quad A = 0 \quad (91)$$

where, ($A = 0$) from the discontinuity of the derivative at $x = 0$, $x_\lambda^3 = -\frac{24}{\lambda}$, and ($A = 1$), $z = z_\lambda$ is the solution of

$$\lambda = 3z(1 - z^2) \quad (92)$$

whose branch is continuously connected to $z = 1$ for $\lambda = 0$. Note that $\tilde{u}(x = 0) = \frac{3}{2}(1 - z^2)$ ($A = 1$) and $\tilde{u}(x = 0) = -6/x_\lambda^2 = \frac{3^{1/3}}{2}(-\lambda)^{2/3}$.

A. Massless case

In the massless case the general result reads, from (88) and (90)

$$P_{\{f(x)\}}(S_0) = LT_{-\lambda \rightarrow S_0}^{-1} e^{-6 \int dx f(x) \frac{\lambda^{2/3}}{(|x|(-\lambda)^{1/3} + (24)^{1/3})^2}} \quad (93)$$

where LT^{-1} denotes the Laplace inversion, which can be obtained explicitly in a few cases. The first two are known^{3,10,26}, and we recall them for completeness, the third is new.

- **Uniform kick** $f(x) = f$. Using $\int dx \tilde{u}^\lambda(x) = -12/x_\lambda$ we obtain

$$P_{\{f\}}(S_0) := P_f(S_0) = LT_{-\lambda \rightarrow S_0}^{-1} e^{-2 \times 3^{2/3} (-\lambda)^{1/3} f} \quad (94)$$

Denoting $\alpha = 2 \times 3^{2/3} f$ and introducing $z := (-\lambda)^{1/3}$, we can write

$$S_0 P_f(S_0) = \int_C \frac{d\lambda}{2i\pi} e^{-\lambda S_0} \partial_\lambda e^{-\alpha(-\lambda)^{1/3}} = \int_C \frac{dz}{2i\pi} e^{S_0 z^3} \partial_z e^{-\alpha z} \quad (95)$$

$$= -\alpha \Phi(a, b, c)|_{a=3S_0, b=0, c=-\alpha} \quad (96)$$

Following Appendix A of¹⁰ we have defined $\Phi(a, b, c)$, for $a \neq 0$, as

$$\Phi(a, b, c) := \int_C \frac{dz}{2i\pi} e^{a \frac{z^3}{3} + bz^2 + cz} = |a|^{-1/3} e^{\frac{2b^3}{3a^2} - \frac{bc}{a}} \text{Ai}\left(\frac{b^2}{|a|^{4/3}} - \frac{c \text{sgn}(a)}{|a|^{1/3}}\right), \quad (97)$$

in terms of the Airy function. Here and below C generically denotes appropriate contours in the complex plane. As in¹⁰, our use of inverse LT formula and change in variables therein are heuristic here and below, an approach validated by careful checks of the final formulae. This gives

$$P_f(S_0) = \frac{2 \times 3^{1/3} f}{S_0^{4/3}} \text{Ai}\left(\frac{2 \times 3^{1/3} f}{S_0^{1/3}}\right) \quad (98)$$

correctly normalized to unity, using $\int_0^{+\infty} dy \text{Ai}(y) = 1/3$. One has the two limiting behaviors

$$P_f(S_0) \simeq \frac{\sqrt[4]{\frac{3}{2}} f^{3/4} e^{-\frac{4\sqrt{\frac{3}{2}} f^{3/2}}{\sqrt{S_0}}}}{\sqrt{\pi} S_0^{5/4}}, \quad S_0 \ll f^3 \quad (99)$$

$$\simeq f \rho(S_0) + O(S_0^{-5/3}), \quad S_0 \gg f^3, \quad \rho(S_0) = \frac{2}{\sqrt[3]{3} \Gamma(\frac{2}{3}) S_0^{4/3}} \quad (100)$$

where $\rho(S_0)$ is the total density of local size, which exhibits the exponent 4/3.

- **Local kick and local size at the point of the kick** $f(x) = f\delta(x)$, and we recall, $S_0 = S(x = 0)$. Using that $\tilde{u}(x = 0) = -6/x_\lambda^2 = -\frac{3^{1/3}}{2}(-\lambda)^{2/3}$

$$P_{\{f\delta(x)\}}(S_0) = LT_{-\lambda \rightarrow S_0}^{-1} e^{-\frac{3^{1/3}}{2}(-\lambda)^{2/3} f} \quad (101)$$

Denoting $\alpha = \frac{3^{1/3}}{2}f$ and introducing $z := (-\lambda)^{1/3}$ we can write

$$S_0 P_{\{f\delta(x)\}}(S_0) = \int_C \frac{d\lambda}{2i\pi} e^{-\lambda S_0} \partial_\lambda e^{-\alpha(-\lambda)^{2/3}} = \int_C \frac{dz}{2i\pi} e^{S_0 z^3} \partial_z e^{-\alpha z^2} \quad (102)$$

$$= -2\alpha \partial_c \Phi(a, b, c)|_{a=3S_0, b=-\alpha, c=0} \quad (103)$$

leading to

$$P_{\{f\delta(x)\}}(S_0) = \frac{f e^{-\frac{f^3}{36S_0^2}}}{\sqrt[3]{3}S_0^{5/3}} (y \text{Ai}(y^2) - \text{Ai}'(y^2)) \quad , \quad y = \frac{f}{2 \times 3^{1/3} S_0^{2/3}} \quad (104)$$

The associated density exhibits the exponent 5/3 and reads

$$\rho_0(S_0) = \frac{1}{3^{2/3} \Gamma(\frac{1}{3}) S_0^{5/3}} \quad (105)$$

• **Local kick, and local size at the point at a distance $|x_s|$ from the kick**

The formula for the PDF of the local jump at $x = 0$, $S_0 = S(x = 0)$, for a kick at $x = x_s$, can be written as above as a contour integral by introducing $z := (-\lambda)^{1/3}$

$$S_0 P_{\{f\delta(x-x_s)\}}(S_0) = \int_C \frac{dz}{2i\pi} e^{S_0 z^3} \partial_z e^{-6f \frac{z^2}{(|x_s|z + (24)^{1/3})^2}} = 3S_0 \int_C \frac{dz}{2i\pi} e^{S_0 z^3} z^2 e^{-6f \frac{z^2}{(|x_s|z + (24)^{1/3})^2}} \quad (106)$$

A simpler expression can be obtained for the density. Note that there is now a non-zero probability that the avalanche started at x_s has not reached $x = 0$. The probability that $x = 0$ has moved is

$$p_f = 1 - e^{f\tilde{u}^{\lambda=-\infty}(x_s)} = -f\tilde{u}^{\lambda=-\infty}(x_s) + O(f^2) \quad , \quad \tilde{u}^{\lambda=-\infty}(x_s) = -6/x_s^2 \quad (107)$$

hence one can write

$$P_{f\delta(x-x_s)}(S_0) = (1 - p_f)\delta(S_0) + p_f \tilde{P}_{f\delta(x-x_s)}(S_0) \quad (108)$$

where the regular part, \tilde{P} , is also normalized to unity, $\int_{S_0 > 0} \tilde{P}_{f\delta(x-x_s)}(S_0) = 1$. We obtain the density by expanding in f for fixed $S_0 > 0$ as in (10) (which gets rid of a $\delta(S_0)$ piece which does not enter in the density). Taking a derivative w.r.t. f of (106) we have

$$\rho_{x_s}(S_0) = -18 \int_C \frac{dz}{2i\pi} e^{S_0 z^3} \frac{z^4}{(|x_s|z + (24)^{1/3})^2} = -18 \int_0^{+\infty} t dt \int_C \frac{dz}{2i\pi} z^4 e^{S_0 z^3 - t(|x_s|z + (24)^{1/3})} \quad (109)$$

$$= -18 \int_0^{+\infty} t dt e^{-t(24)^{1/3}} \partial_b^2 \Phi(a, b, c)|_{a=3S_0, b=0, c=-t|x_s|} \quad (110)$$

$$= \frac{4 \times 3^{1/3}}{S_0^{5/3}} \int_0^{+\infty} t dt e^{-2 \times 3^{1/3} t} \left(\frac{1}{2} \left(\frac{t|x_s|}{3^{1/3} S_0^{1/3}} \right)^2 \text{Ai} \left(\frac{t|x_s|}{3^{1/3} S_0^{1/3}} \right) + \text{Ai}' \left(\frac{t|x_s|}{3^{1/3} S_0^{1/3}} \right) \right) \quad (111)$$

It can be put in a scaling form

$$\rho_{x_s}(S_0) = \frac{1}{S_0^{5/3}} \phi \left(\frac{S_0}{|x_s|^3} \right) \quad (112)$$

$$\phi(s) = -12s^{2/3} \int_0^{+\infty} dt e^{-2 \times 3^{2/3} t s^{1/3}} \frac{d}{dt} \left(\frac{t^2}{2} \text{Ai}'(t) \right) \quad (113)$$

$$= -12 \times 3^{2/3} s \int_0^{+\infty} dt t^2 e^{-2 \times 3^{2/3} t s^{1/3}} \text{Ai}'(t) \quad (114)$$

This integral can be carried out exactly leading to

$$\phi(s) = \frac{3^{1/6} 6}{\pi} s e^{-24s} \left(4(18s - 1) (2s^{1/3} \Gamma(\frac{1}{3}) E_{\frac{4}{3}}(-24s) - 3^{2/3} \Gamma(\frac{5}{3}) E_{\frac{5}{3}}(-24s)) \right. \quad (115)$$

$$\left. + 3e^{24s} (2s^{1/3} \Gamma(\frac{1}{3}) - 3^{2/3} \Gamma(\frac{5}{3})) \right) \quad (116)$$

where $E_n(z) = \int_1^{+\infty} e^{-zt} dt/t^n$ is the exponential integral. Using that $\text{Ai}'(0) = -1/(3^{1/3}\Gamma(1/3))$ and $\int_0^{+\infty} dt t^2 \text{Ai}'(t) = 3^{2/3}/\Gamma(-2/3)$ one can write respectively the large and small s asymptotics

$$\phi(s) = \frac{1}{3^{2/3}\Gamma(\frac{1}{3})} - \frac{(\frac{1}{s})^{2/3}\Gamma(\frac{1}{3})}{4(3^{5/6}\pi)} + \frac{5\Gamma(\frac{2}{3})}{36\sqrt[3]{3}\pi s} + O\left(\left(\frac{1}{s}\right)^{4/3}\right) \quad (117)$$

$$\phi(s) = \frac{12\sqrt{3} \times 3^{1/3}\Gamma(2/3)}{\pi} s + O(s^{4/3}) \quad (118)$$

The first is consistent with the formula (105) for $x_s = 0$, and the second gives the leading behavior for fixed S_0 and the distance to the seed $|x_s| \rightarrow +\infty$

$$\rho_{x_s}(S_0) \simeq_{|x_s| \rightarrow +\infty} \frac{12\sqrt{3} \times 3^{1/3}\Gamma(2/3)}{\pi} \frac{1}{S_0^{2/3}|x_s|^3} \quad (119)$$

which is cutoff at $S_0 \sim |x_s|^3$. We also check that

$$\int_{S_0 > 0} dS_0 \rho_{x_s}(S_0) = \int_0^{+\infty} \frac{dS_0}{S_0^{5/3}} \phi\left(\frac{S_0}{|x_s|^3}\right) = \frac{1}{x_s^2} \int_0^{+\infty} \frac{ds}{s^{5/3}} \phi(s) = \frac{6}{x_s^2} = -\tilde{u}^{\lambda=-\infty}(x) \quad (120)$$

i.e. $\partial_f p_f|_{f=0}$, the probability density per unit force that motion has occurred at $x = 0$, in agreement with the discussion above. We also check that it agrees with the result (105) for the uniform kick, indeed

$$\int dx_f \rho_{x_f}(S_0) = \int dx_f \frac{1}{S_0^{5/3}} \phi\left(\frac{S_0}{|x_f|^3}\right) = \frac{2}{3} \frac{1}{S_0^{4/3}} \int_0^{+\infty} \frac{ds}{s^{4/3}} \phi(s) = \frac{2}{\sqrt[3]{3}\Gamma(\frac{2}{3})} \frac{1}{S_0^{4/3}} \quad (121)$$

B. Massive case

We now consider now the massive case. We only give the results in the massive dimensionless units and present the details of the derivation in Appendix C.

We first recall the known results^{3,10,26} (whose derivation is also given in the Appendix C). For a uniform kick $\dot{w}(x, t) = w\delta(t)$ one has

$$P_w(S_0) = \frac{2 \times 3^{1/3} w e^{6w}}{S_0^{4/3}} \text{Ai}\left(\frac{3^{1/3}(S_0 + 2w)}{S_0^{1/3}}\right) \quad (122)$$

Note that the joint PDF $P_w(S, S_0)$ for a uniform kick was calculated in¹⁰. For a local kick at $x = 0$, $w(x, t) = w\delta(x)\delta(t)$, the PDF of $S_0 = S(x = 0)$ at the position of the kick reads

$$P_{\{w\delta(x)\}}(S_0) = \frac{w}{3^{1/3}S_0^{5/3}} e^{w - \frac{w^3}{36S_0^2}} \left(y \text{Ai}(y^2 + 3^{1/3}S_0^{2/3}) - \text{Ai}'(y^2 + 3^{1/3}S_0^{2/3}) \right) \quad , \quad y = \frac{w}{2 \times 3^{1/3}S_0^{2/3}} \quad (123)$$

and the associated density reads

$$\rho_0(S_0) = -\frac{1}{3^{1/3}S_0^{5/3}} \text{Ai}'(3^{1/3}S_0^{2/3}) \quad (124)$$

For a local kick at x_s , we obtain the following scaling form for the density of $S_0 = S(x = 0)$

$$\rho_{x_s}(S_0) = \frac{1}{S_0^{5/3}} \frac{4e^{-|x_s|}}{(1 + e^{-|x_s|})^2} \phi\left(\frac{S_0}{\left(\frac{2(1-e^{-|x_s|})}{1+e^{-|x_s|}}\right)^3}, 3^{1/3}S_0^{2/3}\right) \quad (125)$$

with the scaling function defined by the following integral

$$\phi(s, s_0) = -12s^{2/3} \times \int_0^{+\infty} dt e^{-2 \times 3^{2/3} t s^{1/3}} [3^{2/3} s^{1/3} t^2 \text{Ai}'(t + s_0) - \frac{3}{2} s_0 t^2 \text{Ai}(t + s_0)] \quad (126)$$

One sees that the result (124) for $x_s = 0$ is correctly recovered using that $\phi(+\infty, s_0) = \frac{1}{3^{1/3}} \text{Ai}'(s_0)$ as easily shown by rescaling t in (126). The check that

$$\int dx_s \rho_{x_s}(S_0) = \frac{2 \times 3^{1/3}}{S_0^{4/3}} \text{Ai}(3^{1/3} S_0^{2/3}) \quad (127)$$

is performed in the Appendix C. Finally one can check that the total weight

$$\int dS_0 \rho_{x_s}(S_0) = -\tilde{u}^{\lambda=-\infty}(x) = \frac{6e^{-|x_s|}}{(1 - e^{-|x_s|})^2} \quad (128)$$

equals the probability density (per unit w) that $x = 0$ belongs to the avalanche. Another limit is $|x_s| \rightarrow +\infty$ then

$$\rho_{x_s}(S_0) = \frac{4}{S_0^{5/3}} e^{-|x_s|} \phi\left(\frac{S_0}{8}, 3^{1/3} S_0^{2/3}\right) \quad (129)$$

We can check that it is consistent with the moments (by a numerical integration over t)

$$\langle S_0 \rangle_{\rho_x} = \frac{1}{2} e^{-x}, \quad \langle S_0^2 \rangle_{\rho_x} = \frac{1}{3} e^{-x}, \quad \langle S_0^3 \rangle_{\rho_x} = \frac{23}{48} e^{-x} \quad \text{and} \quad \langle S_0^4 \rangle_{\rho_x} = \frac{13}{12} e^{-x} \quad (130)$$

which are predicted by the small λ expansion of $\tilde{u}^\lambda(x)$ at large x :

$$\tilde{u}^\lambda(x) \underset{x \rightarrow \infty, \lambda \rightarrow 0}{\sim} \frac{1}{2} \lambda e^{-x} + \frac{1}{6} \lambda^2 e^{-x} + \frac{23}{288} \lambda^3 e^{-x} + \frac{13}{288} \lambda^4 e^{-x} + O(\lambda^5) \quad (131)$$

V. BULK DRIVING: SPATIAL SHAPE CONDITIONED TO ONE BOUNDARY

In this Section we study the spatial shape conditioned to the position of one edge of the avalanche, more precisely on ℓ_2 the seed-to-edge distance. The calculations are much simpler than for the two boundary problem (conditioning on the total extension ℓ) but still very instructive.

A. Massless case

1. PDF of seed-to-edge distance ℓ_2

Consider the massless case in $d = 1$, and ask whether an avalanche under the applied force kick (4) of amplitude $f(x)$ reaches the point of the interface at position r . The probability that this point has not moved at all is

$$\text{Prob}(S(r) = 0) = \lim_{\lambda_1 \rightarrow -\infty} \overline{e^{\lambda_1 S(r)}} = e^{\int dx f(x) \tilde{u}_r(x)} \quad (132)$$

where $\tilde{u}_r(x)$ is the solution of

$$\tilde{u}''(x) + \tilde{u}(x)^2 = 0 \quad , \quad \tilde{u}(r) = -\infty \quad (133)$$

and vanishing at $x = \pm\infty$. Indeed the corresponding source term $-\lambda_1 \delta(x - r)$, when inserted in the r.h.s. of (205) and taking $\lambda_1 \rightarrow -\infty$ simply imposes that $\tilde{u}(r) = -\infty$. The solution of (205) with such boundary conditions is simply

$$\tilde{u}_r(x) = -\frac{6}{(r-x)^2} \quad (134)$$

hence we have

$$\text{Prob}(S(r) = 0) = e^{-\int dx \frac{6}{(x-r)^2} f(x)} = e^{-\int_{x < r} dx \frac{6}{(x-r)^2} f(x)} \times e^{-\int_{x > r} dx \frac{6}{(x-r)^2} f(x)} \quad (135)$$

We see on this formula that (i) all points inside the support of the force will move (since for r in the support, the integral diverges) (ii) if the applied kick has components on both sides of $x = r$ the probability of $S(r) = 0$ splits in two independent probabilities: the events of the (multiply seeded) avalanche not reaching r on each side are

independent. In the following we will thus restrict to driving included in the half line $x < r$. In that case, if a second condition $S(r') = 0$ is added, with $r' > r$, one finds that the solution of (205) with a second condition $\tilde{u}(r') = -\infty$ is $\tilde{u}_{r,r'}(x) = u_r(x)$ for $x < r$ hence $\text{Prob}(S(r) = 0, S(r') = 0) = \text{Prob}(S(r) = 0)$. As pointed out in¹⁰ this implies that the support of the avalanche is an interval.

Let us now consider a local kick at $x = x_s$, i.e. $f_x = f\delta(x - x_s)$, and recall that the point x_s is also called the seed, since the avalanche will start there. For notational simplicity we take the seed as the origin, i.e. we choose $x_s = 0$. From (135) we obtain the CDF of the edge-to-seed distance, ℓ_2 , defined in Section IB 3, see also Fig. 1 (the other segment ℓ_1 has the same distribution by symmetry, however ℓ_1 and ℓ_2 are correlated, see next Section)

$$\text{Prob}(S(r) = 0) = \text{Prob}(\ell_2 < r) = e^{-6f/r^2} \quad (136)$$

for any $r > 0$, which by differentiation gives the PDF of the one-sided extension ℓ_2

$$P(\ell_2) = \frac{12f}{\ell_2^3} e^{-6f/\ell_2^2} \quad (137)$$

It is interesting to see that this is obviously distinct from the distribution $P(\ell)$ for the total extension $\ell = \ell_1 + \ell_2$ (we use the same letter but the argument indicates that it is a different distribution) but it has the same exponent $P(\ell_2) \sim \ell_2^{-\kappa}$ with $\kappa = 3$ for the BFM, the mean-field value. Using that for the BFM $\zeta = 4 - d$, this value is in agreement with the general expected exponent relation is $\kappa = 1 + (\tau - 1)(\zeta + d) = d + \zeta - 1$ where the first equality comes from the scaling $S \sim \ell^{d+\zeta}$ and the second from the Narayan-Fisher conjecture^{4,15,25} $\tau = 2 - \frac{2}{d+\zeta}$.

2. Mean shape conditioned on the seed-to-edge distance ℓ_2

Let us now ask about the shape of the avalanche near its upper edge. More precisely we consider for $0, x_0 < r$ the Laplace transform of the joint PDF $P(S(r) = 0, S(x_0)) = P(\ell_2 < r, S(x_0))$ of the event that the local size at x_0 is $S(x_0)$ and that $\ell_2 < r$. It is given by

$$\int dS(x_0) e^{\lambda S(x_0)} P(\ell_2 < r, S(x_0)) = e^{f\tilde{u}_r^\lambda(x=0)} \quad (138)$$

where $\tilde{u}_r^\lambda(x)$ is the solution of the equation

$$\tilde{u}''(x) + \tilde{u}(x)^2 = -\lambda\delta(x - x_0) \quad , \quad \tilde{u}(r) = -\infty \quad (139)$$

for $x \in]-\infty, r]$, i.e. with $\tilde{u}_r^\lambda(r) = -\infty$ and vanishing at $x = -\infty$.

We give the solution for arbitrary λ below, which determines arbitrary moments of $S(x_0)$. As a starter, we first calculate the first moment of $S(x_0)$, the mean shape, which is elementary. To this aim, we solve (139) to first order in λ , i.e. we write its solution as $\tilde{u}_r(x) = \frac{-6}{(r-x)^2} + \lambda\tilde{u}_r^{(1)}(x) + O(\lambda^2)$, where $\tilde{u}_r^{(1)}(x)$ is the solution of the linear equation

$$\tilde{u}^{(1)''}(x) - \frac{12}{(r-x)^2}\tilde{u}^{(1)}(x) = -\delta(x - x_0) \quad (140)$$

It can be seen as the zero-energy Green function of a Schrodinger problem in a repulsive inverse square potential $V(x)$

$$u_r^{(1)}(x) = G(x, x_0) = \langle x | \frac{1}{H} | x_0 \rangle \quad , \quad H = -\partial_x^2 + V(x) \quad , \quad V(x) = -2\tilde{u}^{\lambda=0}(x) = \frac{12}{(r-x)^2} \quad (141)$$

It is easy to see that the general solution of the homogeneous equation is a sum of two powers $(r-x)^a$ with $a = -3, 4$. Imposing continuity at x_0 and the proper discontinuity from (140), i.e. $[u^{(1)}(x)]_{x_0^-}^{x_0^+} = -1$ we find that the proper solution is

$$u_r^{(1)}(x) = \frac{1}{7}(r-x_0)\left(\frac{r-x_0}{r-x}\right)^3\theta(x < x_0) + \frac{1}{7}(r-x_0)\left(\frac{r-x}{r-x_0}\right)^4\theta(x_0 < x < r) \quad (142)$$

which satisfies $u_r^{(1)}(r) = 0$ and $u_r^{(1)}(-\infty) = 0$. Note that $\int dx u_r^{(1)}(x) = \frac{1}{10}(r-x_0)^2$.

Expanding (138) to first order in λ , we obtain

$$\int dS(x_0)S(x_0)P(\ell_2 < r, S(x_0)) = fu_r^{(1)}(x)e^{-f\frac{6}{r^2}} \quad (143)$$

Dividing by the CDF (136), we obtain the mean avalanche local size at x_0 , $\langle S(x_0) \rangle_{\ell_2 < r}$, with its seed at $x_s = 0$ and conditioned to the avalanche not reaching r (i.e. to $\ell_2 < r$) as

$$\langle S(x_0) \rangle_{\ell_2 < r} = f\tilde{u}_r^{(1)}(x=0) = \frac{f}{7} \frac{(r-x_0)^4}{r^3} \theta(0 < x_0 < r) + \frac{f}{7} \frac{r^4}{(r-x_0)^3} \theta(x_0 < 0 < r) \quad (144)$$

Note that as a function of x_0 it is continuous at the position of the seed but has a jump derivative: one has $\frac{d}{dx_0} \langle S(x_0) \rangle_{\ell_2 < r} |_{x_0=x_s^+=0^+} = -4f/7$ while $\frac{d}{dx_0} \langle S(x_0) \rangle_{\ell_2 < r} |_{x_0=x_s^-=0^-} = 3f/7$. The total jump is thus $-f$.

Taking instead first a derivative of (143) w.r.t. r , and then dividing by $P(\ell_2)$ given in (137), we obtain the mean avalanche local size at x_0 , $\langle S(x_0) \rangle_{\ell_2}$, i.e. the mean spatial shape, conditioned to the seed-to-edge distance being $\ell_2 > 0$

$$\langle S(x_0) \rangle_{\ell_2} = \frac{\ell_2^3}{12} \partial_r |_{r=\ell_2} u_r^{(1)}(x=0) + f\tilde{u}_{r=\ell_2}^{(1)}(x=0) \quad (145)$$

$$= \frac{1}{21} (\ell_2 - x_0)^3 - \frac{1}{28} \frac{(\ell_2 - x_0)^4}{\ell_2} + \frac{f}{7} \frac{(\ell_2 - x_0)^4}{\ell_2^3} \quad , \quad 0 < x_0 < \ell_2 \quad (146)$$

$$= \frac{1}{21} \frac{(\ell_2)^6}{(\ell_2 - x_0)^3} - \frac{1}{28} \frac{(\ell_2)^7}{(\ell_2 - x_0)^4} + \frac{f}{7} \frac{\ell_2^4}{(\ell_2 - x_0)^3} \quad , \quad x_0 < 0 \quad (147)$$

where here the seed position has been chosen as $x_s = 0$. The general case is obtained by a change of coordinate $\ell_2 \rightarrow \ell_2 - x_s$, $x_0 \rightarrow x_0 - x_s$. Again it is continuous at the seed with $\langle S(x_0 = x_s = 0) \rangle_{\ell_2} = \frac{1}{84} \ell(\ell^2 + 12f)$, and has exactly the same left/right derivatives and jump in derivative as the cumulative mean above, i.e. $\frac{d}{dx_0} \langle S(x_0) \rangle_{\ell_2} |_{x_0=x_s^+=0^+} = -4f/7$ while $\frac{d}{dx_0} \langle S(x_0) \rangle_{\ell_2} |_{x_0=x_s^-=0^-} = 3f/7$, i.e. a total jump $-f$. The total derivative jump at the seed being $-f$ is always the case, since it simply comes from the $-\lambda\delta(x-x_0)$ in the instanton equation. Note that in the limit $f \rightarrow 0$ the first derivative jump vanishes and one finds that the second derivative is continuous at the seed, and the right and left third derivatives are respectively $4/7$ and $-10/7$ and represent the leading non-analyticity. These singularities are smoothed out when averaging over the seed position (see below).

Hence we find that the mean shape of the avalanche vanishes near its edge as

$$\langle S(x_0) \rangle_{\ell_2} \simeq \frac{1}{21} D^3 \quad , \quad D = \ell_2 - x_0 \quad (148)$$

Hence, expressed as a function of the distance D to the edge, the leading behavior (148) is fully independent on ℓ_2 and of the position of the seed at $x = x_s$. It turns out (see next section) that (148) is also independent of whether the shape is conditioned to a single edge, or to two edges. In all cases only the next order term $O(D^4)$ depends on ℓ_2 . More generally we see that in the limit $f \rightarrow 0^+$ the mean shape is only a scaling function of the ratio of distances

$$\langle S(x_0) \rangle_{\ell_2} = D^3 F(D/\ell_2) \quad , \quad F(0) = \frac{1}{21} \quad (149)$$

If this remains a general property beyond the BFM, then from a simple dimensional argument (since $S(x_0) \sim \ell_2^\zeta$) one then expects $\langle S(x_0) \rangle_{\ell_2} \simeq c_d D^\zeta$ where $\zeta_{BFM,d=3} = 4 - d = 3$.

It is also interesting to center the avalanche on the edge, and average over the position of the seed. This average can be calculated from (146), (147) and one obtains

$$\bar{S}(y) = \int_0^{+\infty} \langle S(\ell_2 - y) \rangle_{\ell_2} P(\ell_2) d\ell_2 = f^{3/2} g(y/f^{1/2}) \quad (150)$$

with

$$\begin{aligned} g(z) &= \frac{432\sqrt{6\pi}\text{erfc}\left(\frac{\sqrt{6}}{z}\right) + 5z^7 - e^{-\frac{6}{z^2}}(5z^6 + 9z^4 - 36z^2 + 432)z}{105z^4} = \frac{z^3}{21} - e^{-6/z^2} \left(\frac{3}{35} z + O(z^2) \right) \quad , \quad z \ll 1 \\ &= \frac{z}{5} - \frac{6}{z^3} + O(z^{-4}) \quad , \quad z \gg 1 \end{aligned} \quad (151)$$

It is also interesting to calculate the mean of the total avalanche size (i.e. the total mean area swept by the avalanche) conditioned to ℓ_2 , $\langle S \rangle_{\ell_2}$, as well as the mean of the total size below, $S_<$, and above, $S_>$, the seed. They read

$$\langle S_< \rangle_{\ell_2} = \int_{-\infty}^0 dx_0 \langle S(x_0) \rangle_{\ell_2} = \frac{1}{84} \ell_2^4 + \frac{f}{14} \ell_2^2 \quad , \quad \langle S_> \rangle_{\ell_2} = \int_0^{\ell_2} dx_0 \langle S(x_0) \rangle_{\ell_2} = \frac{1}{210} \ell_2^4 + \frac{f}{35} \ell_2^2 \quad (152)$$

$$\langle S \rangle_{\ell_2} = \int_{-\infty}^{\ell_2} dx_0 \langle S(x_0) \rangle_{\ell_2} = \langle S_< \rangle_{\ell_2} + \langle S_> \rangle_{\ell_2} = \frac{1}{60} \ell_2^4 + \frac{f}{10} \ell_2^2 \quad (153)$$

Note that the scaling $S \sim \ell_2^{d+\zeta} = \ell_2^4$ is expected for the BFM.

3. joint PDF of total size S and ℓ_2

One can also calculate directly the mean total size conditioned to ℓ_2 to recover the above results. The same calculation gives the joint PDF of the total size S and ℓ_2 .

To study the distribution of the total size S we need to add a space-uniform source and solve the instanton equation

$$\tilde{u}''(x) + \tilde{u}(x)^2 = -\mu \quad , \quad \tilde{u}(r) = -\infty \quad (154)$$

on $x \in]-\infty, r]$ which has the limit $-\sqrt{-\mu}$ at $x = -\infty$. Let us denote $\tilde{u}_r^\mu(x)$ its solution, which reads

$$\tilde{u}_r^\mu(x) = -c - \frac{3c}{\sinh^2(\sqrt{c}(r-x)/\sqrt{2})} \quad , \quad c = \sqrt{-\mu} \quad (155)$$

We consider a kick at $x = x_s = 0$ (position of the seed) and obtain

$$\int_0^{+\infty} dS e^{\mu S} P(\ell_2 < r, S) = e^{f \tilde{u}_r^\mu(x=0)} \quad (156)$$

with $c = \sqrt{-\mu}$, from which we can write the joint PDF $P(\ell_2 < r, S)$ as

$$P(\ell_2 < r, S) = LT_{p \rightarrow S}^{-1} \exp\left(-f(\sqrt{p} + \frac{3\sqrt{p}}{\sinh^2(p^{1/4}r/\sqrt{2})})\right) \quad (157)$$

as well as $P(\ell_2, S)$ by derivation w.r.t. r . Expanding to first order in p we obtain the conditional means

$$\langle S \rangle_{\ell_2 < r} = \frac{1}{10} f r^2 \quad (158)$$

$$\langle S \rangle_{\ell_2} = \frac{1}{10} f \ell_2^2 + \frac{1}{60} \ell_2^4 \quad (159)$$

which correctly recovers the result (153) of the previous section (obtained by integrating the spatial shape).

The above formula contain additional information about the fluctuations of S and ℓ_2 . Note that the LT in (157) has a non analyticity $\sim p^{3/2}$ at small p , which implies that the second moment for S diverges (which is possible since it is the massless case) and that the following conditional probabilities decay at large S as

$$P(S|\ell_2 < r) \simeq_{S \gg \ell_2^4} \frac{A}{S^{5/2}} \quad , \quad A = \frac{f \ell_2^4}{168\sqrt{\pi}} \quad (160)$$

$$P(S|\ell_2) \simeq_{S \gg \ell_2^4} \frac{A}{S^{5/2}} \quad , \quad A = \frac{f \ell_2^4}{168\sqrt{\pi}} + \frac{\ell_2^6}{504\sqrt{\pi}} \quad (161)$$

It means that the constraint to fix one seed-to-edge distance, ℓ_2 , does not provide an operational cutoff on the other seed-to-edge distance, ℓ_1 , which can still be very large. From the limit $f \rightarrow 0^+$ we also obtain the joint density as

$$\rho(S, \ell_2) = \partial_f|_{f=0} P(\ell_2, S) = \frac{1}{S^{7/4}} R(S/\ell_2^4) \quad , \quad R(s) = LT_{p \rightarrow s}^{-1} 3\sqrt{2} p^{3/4} \frac{\cosh(\frac{p^{1/4}}{\sqrt{2}})}{\sinh^3(\frac{p^{1/4}}{\sqrt{2}})} \quad (162)$$

The inverse LT can be performed and expressed as a series (we will not give its expression here). Its finite moments w.r.t. S are

$$\int dS \rho(S, \ell_2) = \rho(\ell_2) = \frac{12}{\ell_2^3} \quad , \quad \int dS S \rho(S, \ell_2) = \frac{\ell_2}{5} \quad (163)$$

consistent with $\langle S \rangle_{\ell_2} \simeq_{f \rightarrow 0^+} \frac{1}{60} \ell_2^4$ obtained as the ratio of the second to the first result in (163). Finally, the joint density also decays with the exponent $5/2$ at large S , i.e. one has $\rho(S, \ell_2) \simeq \ell_2^3 / (42\sqrt{\pi} S^{5/2})$ for $S \gg \ell_2^4$.

4. Higher moments of the shape

We now give the solution of Eq. (139) for arbitrary λ which allows to obtain the higher moments of the shape.

The general solution of (139) can be written as

$$\tilde{u}_r^\lambda(x) = -\frac{6}{(\rho-x)^2} \theta(x_0-x) - 6\mathcal{P}(r-x; 0, g_3) \theta(x-x_0) \quad (164)$$

where $\mathcal{P}(z; g_2, g_3)$ is the Weierstrass elliptic function, whose properties are recalled in the Appendix A (here the parameter $g_2 = 0$). We will denote $\mathcal{P}'(z; g_2, g_3) = \partial_z \mathcal{P}(z; g_2, g_3)$. Sometimes we use the shorthand $\mathcal{P}(z) = \mathcal{P}(z; g_2, g_3)$ (with here $g_2 = 0$ implicit, unless said otherwise). The unknown parameters ρ and g_3 (which depend on x_0 and λ) are determined by the following conditions of continuity and proper derivative jump at $x = x_0$

$$\frac{1}{(\rho-x_0)^2} = \mathcal{P}(r-x_0; 0, g_3) \quad (165)$$

$$-\frac{2}{(\rho-x_0)^3} - \mathcal{P}'(r-x_0; 0, g_3) = \frac{\lambda}{6} \quad (166)$$

where we recall that $\mathcal{P}(z)$ is an even function. We can use that, see (A5), that $\mathcal{P}'(z)^2 = 4\mathcal{P}(z)^3 - g_3$ (for $g_2 = 0$) to simplify one of the relations as

$$g_3 = -\frac{2}{3(\rho-x_0)^3} \lambda - \frac{\lambda^2}{36} \quad (167)$$

For $\lambda = 0$ one has $g_3 = 0$ and one uses that $\mathcal{P}(z, g_2 = 0, g_3 = 0) = \frac{1}{z^2}$ to obtain that $\rho = r$, recovering as required $\tilde{u}(x) = -\frac{6}{(r-x)^2}$.

We can now expand the system (165), (166) in powers of λ , for ρ near r and g_3 near 0. An efficient way to do it is as follows. One can use the expansion of the Weierstrass function in powers of g_3 , whose coefficients obey a simple recursion relation

$$\mathcal{P}(z, g_2 = 0, g_3) = \sum_{p=0}^{\infty} c_p g_3^p z^{6p-2} \quad , \quad c_p = \frac{1}{(p-1)(6p+1)} \sum_{k=1}^{p-1} c_k c_{p-k} \quad (168)$$

with initial conditions $c_0 = 1$, $c_1 = 1/28$ (some c_p are displayed in (A16)). We rewrite (165), (166), denoting $z = r - x_0$ as

$$\lambda = -12\mathcal{P}(z, g_3)^{3/2} - 6\mathcal{P}'(z, g_3) \quad (169)$$

and substitute (168) to obtain λ as a series in g_3 at fixed z . Then we invert the series and we find g_3 as a series in λ at fixed z , e.g.

$$g_3 = -\frac{2\lambda}{3z^3} - \frac{\lambda^2}{252} + O(\lambda^3) \quad (170)$$

higher orders being given in the Appendix D. We now calculate ρ , using (165), and again (168) and (170), leading to

$$\rho = r - z + 1/\sqrt{\mathcal{P}(z, g_3)} = r + \frac{\lambda z^4}{84} + \frac{\lambda^2 z^7}{3822} + O(\lambda^3) \quad (171)$$

which leads, using (164), to the expansion in power of λ of the desired solution of the instanton equation at $x = x_s = 0$ in power of λ as (we recall that $z = r - x_0$)

$$\tilde{u}_r^\lambda(0) = -\frac{6}{\rho^2} = -\frac{6}{r^2} + \frac{\lambda z^4}{7r^3} + \frac{\lambda^2 (16rz^7 - 13z^8)}{5096r^4} + O(\lambda^3) \quad , \quad 0 < x_0 < r \quad (172)$$

$$\tilde{u}_r^\lambda(0) = -6\mathcal{P}(r, 0, g_3) = -\frac{6}{r^2} + \frac{\lambda r^4}{7z^3} + \lambda^2 \left(\frac{r^4}{1176} - \frac{r^{10}}{3822z^6} \right) \quad , \quad x_0 < 0 \quad (173)$$

which is continuous at $x_0 = 0$, i.e. $z = r$. It is given up to $O(\lambda^4)$ in Appendix D.

We now obtain the conditional moments. Proceeding as in Section V A 2 above, or see also Appendix E, we can write

$$e^{f(\tilde{u}_r^\lambda(0) - \tilde{u}_r^0(0))} = \langle e^{\lambda S(x_0)} \rangle_{\ell_2 < r} = 1 + \sum_{p \geq 1} \frac{\lambda^p}{p!} \langle S(x_0)^p \rangle_{\ell_2 < r} \quad (174)$$

and expand both sides in powers of λ . For $p = 1$ we then recover (144), obtained there via a much simpler calculation. For $p = 2$ we obtain

$$\langle S(x_0)^2 \rangle_{\ell_2 < r} = \frac{4f(r-x_0)^7}{637r^3} - \frac{f(r-x_0)^8}{196r^4} + \frac{f^2(r-x_0)^8}{49r^6} \quad , \quad 0 < x_0 < r \quad (175)$$

$$\langle S(x_0)^2 \rangle_{\ell_2 < r} = \frac{fr^4}{588} - \frac{fr^{10}}{1911(r-x_0)^6} + \frac{f^2r^8}{49(r-x_0)^6} \quad , \quad x_0 < 0 \quad (176)$$

As shown in Appendix E

$$\langle e^{\lambda S(x_0)} \rangle_{\ell_2 = r} = \frac{\partial_r u_r^\lambda(0)}{\partial_r u_r^0(0)} e^{f(u_r^\lambda(0) - u_r^0(0))} \simeq_{f \rightarrow 0^+} \frac{\partial_r u_r^\lambda(0)}{\partial_r u_r^0(0)} \quad (177)$$

Expanding in λ on both sides gives the conditional moments, e.g. we give here the second moment in the limit $f \rightarrow 0^+$

$$\langle S(x_0)^2 \rangle_{\ell_2} \simeq \frac{(28\ell_2^2 - 38\ell_2(\ell_2 - x_0) + 13(\ell_2 - x_0)^2)(\ell_2 - x_0)^6}{7644\ell_2^2} + O(f) \quad , \quad 0 < x_0 < \ell_2 \quad (178)$$

$$\langle S(x_0)^2 \rangle_{\ell_2} = \frac{\ell_2^6 (6\ell_2^7 - 10\ell_2^6(\ell_2 - x_0) + 13(\ell_2 - x_0)^7)}{22932(\ell_2 - x_0)^7} + O(f) \quad , \quad x_0 < 0 \quad (179)$$

which is continuous at the seed, at $x_0 = x_s = 0$, where one finds $\langle S(x_0 = x_s = 0)^2 \rangle_{\ell_2} = \frac{\ell_2^2(156f^2 + 35f\ell_2^2 + 3\ell_2^4)}{7644}$.

Scaling of higher moments near the edge. From the above results we see that near the edge, i.e. for $\ell_2 - x_0 \rightarrow 0$, the first and second moment scale as

$$\langle S(x_0) \rangle_{\ell_2} \simeq \frac{1}{21}(\ell_2 - x_0)^3 \quad , \quad \langle S(x_0)^2 \rangle_{\ell_2} \simeq \frac{1}{273}(\ell_2 - x_0)^6 \quad (180)$$

i.e. they scale in a way consistent with the following ansatz: in any given realization of the disorder conditioned to a given value of ℓ_2

$$S(x_0) \simeq (\ell_2 - x_0)^3 \sigma \quad (181)$$

where σ is a positive random variable of $O(1)$, with $\langle \sigma \rangle = \frac{1}{21}$ and $\langle \sigma^2 \rangle = \frac{1}{273}$. One can ask if there is an efficient method to obtain the higher moments of σ .

It is indeed the case. One can surmise (and check a posteriori) that near the edge $\rho - x_0$ and $r - x_0$ vanish similarly, i.e. guess that the following scaling form holds

$$\frac{1}{\rho - x_0} \simeq \frac{A(\tilde{\lambda})}{r - x_0} \quad , \quad \tilde{\lambda} = (r - x_0)^3 \lambda \quad (182)$$

Then using (165), (167) and the homogeneity property of the Weierstrass function $a^2 \mathcal{P}(ay; a^{-4}g_2, a^{-6}g_3) = \mathcal{P}(y; g_2, g_3)$ (see (A4)) with $y = 1$, $a = r - x_0$, we obtain the condition

$$A(\tilde{\lambda})^2 = \mathcal{P}(1; 0, -\frac{\tilde{\lambda}^2}{36} - \frac{2}{3}\tilde{\lambda}A(\tilde{\lambda})^3) \quad (183)$$

which allows to determine $A(\tilde{\lambda})$ in an expansion in λ using the expansion (168). It gives for lowest order terms

$$A(\tilde{\lambda}) = 1 - \frac{\lambda}{84} - \frac{11\lambda^2}{91728} - \frac{289\lambda^3}{146397888} + O(\lambda^4) \quad (184)$$

Then we obtain

$$\langle e^{\lambda S(x_0)} \rangle_{\ell_2=r} |_{f=0^+} = \frac{r^3}{12} \partial_r u_r^\lambda(0) = f(\lambda(r-x_0)^3) \quad (185)$$

where the function $f(\tilde{\lambda})$ is given by

$$f(\tilde{\lambda}) = \frac{r^3}{12} \partial_r \tilde{u}_r^\lambda(0) = -\frac{r^3}{2} \partial_r \frac{1}{\rho^2} = -\frac{r^3}{2} \partial_r \frac{1}{(x_0 + \frac{(r-x_0)}{A((r-x_0)^3\lambda)})^2} = \frac{1}{A(\tilde{\lambda})} - \frac{3\tilde{\lambda}A'(\tilde{\lambda})}{A(\tilde{\lambda})^2} \quad (186)$$

discarding subdominant terms of order $O(r-x_0)$. From (181), this gives the generating function of the moments of σ , i.e.

$$\langle e^{\tilde{\lambda}\sigma} \rangle = f(\tilde{\lambda}) \quad (187)$$

Explicit calculation gives

$$f(x) = \frac{x}{21} + \frac{x^2}{546} + \frac{265x^3}{4066608} + \frac{1223x^4}{548992080} + \frac{3223267x^5}{43363786415040} + \frac{407163391x^6}{166863850125073920} + O(x^7) \quad (188)$$

which gives the six lowest moments as

$$\left\{ \frac{1}{21}, \frac{1}{273}, \frac{265}{677768}, \frac{1223}{22874670}, \frac{3223267}{361364886792}, \frac{407163391}{231755347395936} \right\} \quad (189)$$

while the cumulant are obtained from $\ln f(\tilde{\lambda})$ as

$$\left\{ \frac{1}{21}, \frac{8}{5733}, \frac{1531}{18299736}, \frac{2623}{346932495}, \frac{989243}{1084094660376}, \frac{7165892365}{52014590781175386} \right\} \quad (190)$$

Examination of $f(x)$ shows that the coefficients of λ^p behaves as $\approx 3.4(0.031)^p$ which suggests that $f(\tilde{\lambda})$ blows up at a finite λ^* . It is easy to see from (186) that such a λ^* corresponds to $A(\tilde{\lambda}^*) = 0$, which is also in agreement with examination of the series (184). Comparing with (183) we see that indeed such a root exists since we know that the Weierstrass function has a zero

$$\mathcal{P}(1; 0, g_3^*) = 0 \quad (191)$$

for the negative value (see also discussion below in Section VII D 1)

$$g_3^* = -\frac{256\pi^3\Gamma(\frac{1}{3})^6}{\Gamma(-\frac{1}{6})^6} = -\frac{4\Gamma(\frac{1}{3})^6\Gamma(\frac{7}{6})^6}{\pi^3} = -30.40090507702060 \quad (192)$$

Hence we see that

$$A(\tilde{\lambda}^*) = 0 \quad , \quad \lambda^* = 6\sqrt{-g_3^*} = \frac{12\Gamma(\frac{1}{3})^3\Gamma(\frac{7}{6})^3}{\pi^{3/2}} = 33.08220946 \quad (193)$$

We can further expand the equation (183) near λ^* . Using the following properties of the Weierstrass function

$$\partial_{g_3}\mathcal{P}(z; 0, g_3) = \frac{1}{6g_3}(2\mathcal{P}(z; 0, g_3) + \mathcal{P}'(z; 0, g_3)) \quad (194)$$

$$\mathcal{P}'^2 = 4\mathcal{P}^3 - g_2\mathcal{P} - g_3 \quad (195)$$

we see that at $g_3 = g_3^*$ one has $\mathcal{P}'(1, 0, -|g_3^*|) = -(-g_3^*)^{1/2}$, hence

$$\partial_{g_3}\mathcal{P}(z; 0, g_3)|_{g_3=g_3^*} = \frac{1}{6(-g_3^*)^{1/2}} = \frac{1}{\tilde{\lambda}^*} \quad (196)$$

Hence (183) implies the leading behavior near the singularity

$$A(\tilde{\lambda}) \simeq \frac{1}{3\sqrt{2}}(\tilde{\lambda}^* - \tilde{\lambda})^{1/2} \quad (197)$$

which in turn leads to

$$f(\tilde{\lambda}) \simeq \frac{9\tilde{\lambda}^*}{\sqrt{2}(\tilde{\lambda}^* - \tilde{\lambda})^{3/2}} \quad (198)$$

We have obtained in Appendix F three more orders in this expansion around λ^* . The leading order in (198) implies the following large σ behavior of the PDF of σ

$$p(\sigma) \simeq_{\sigma \rightarrow +\infty} \frac{9\sqrt{2}}{\sqrt{\pi}} \tilde{\lambda}^* \sigma^{1/2} e^{-\tilde{\lambda}^* \sigma} \quad (199)$$

Thus, although we have not obtained an explicit form for the exact PDF of σ we have been able to extract a lot of information from the implicit form (moments, tail behavior).

B. spatiotemporal shape near a boundary

Here we will study the dynamics near the edge of the avalanche. We consider an avalanche (started at time zero) which has its upper edge at r . Then we ask about the PDF of the instantaneous local velocity $\dot{u}(x_0, t_0)$ at some space time point (x_0, t_0) , for such an avalanche (i.e. conditioned to have its edge at r). To address this question we use the source

$$\lambda(x, t) = \lambda_r \delta(x - r) + \lambda \delta(x - x_0) \delta(t - t_0) \quad (200)$$

in the limit $\lambda_r \rightarrow -\infty$. Note that the source

$$\lambda(x, t) = \lambda_r \delta(x - r) \theta(t_0 - t) + \lambda \delta(x - x_0) \delta(t - t_0) \quad (201)$$

in the limit $\lambda_r \rightarrow -\infty$ would address a different question, by only imposing that the avalanche has not reached point r up to time t_0 (it could reach it afterwards). Here we impose that the avalanche will never reach point r , i.e. for all times, which turns out to be a simpler question.

The general method of^{2,3,8} implies that, for any (monotonous forward) driving $\dot{f}(x, t) \geq 0$, the LT of the following joint probability $P(S(r) = 0, \dot{u}(x_0, t_0)) = P(\ell_2 < r, \dot{u}(x_0, t_0))$ involving the instantaneous local velocity

$$\int_0^{+\infty} d\dot{u}(x_0, t_0) P(S(r) = 0, \dot{u}(x_0, t_0)) e^{\lambda \dot{u}(x_0, t_0)} = e^{\int_0^{+\infty} dt \int dx \dot{f}(x, t) \tilde{u}_r^\lambda(x, t)} \quad (202)$$

where $\tilde{u}_r^\lambda(x, t)$ is the solution of

$$\partial_t \tilde{u}(x, t) + \partial_x^2 \tilde{u}(x, t) + \tilde{u}(x, t)^2 = -\lambda \delta(x - x_0) \delta(t - t_0) \quad (203)$$

on $x \in]-\infty, r]$, with $\tilde{u}(r, t) = -\infty$, vanishing at $x = -\infty$. We will only determine the mean of $\dot{u}(x_0, t_0)$, hence we can expand in λ and look for a solution of the form

$$\tilde{u}_r^\lambda(x, t) = -\frac{6}{(r-x)^2} + \lambda \tilde{u}_r^{(1)}(x, t) + O(\lambda^2) \quad (204)$$

where $\tilde{u}_1(x, t) = 0$ for $t > t_0^+$ (a consequence of causality, see^{2,3}). Inserting in (203) we see that $\tilde{u}_r^{(1)}(x, t)$ is solution of the linear equation

$$\partial_t \tilde{u}^{(1)}(x, t) + \partial_x^2 \tilde{u}^{(1)}(x, t) - \frac{12}{(r-x)^2} \tilde{u}^{(1)}(x, t) = -\delta(x - x_0) \delta(t - t_0) \quad (205)$$

Here one recognizes the equation for the propagator $G = G(x, y; \tau) = \langle x | e^{-H\tau} | y \rangle$ of the 1D Schrodinger equation in imaginary time with inverse square potential, solution of

$$\partial_\tau G = -HG = \partial_x^2 G - \frac{\gamma^2 - 1/4}{x^2} G \quad , \quad G(x, y, \tau = 0) = \delta(x - y) \quad (206)$$

which reads

$$G(x, y, \tau) = \frac{\sqrt{xy}}{2\tau} I_\gamma\left(\frac{xy}{2\tau}\right) e^{-\frac{x^2+y^2}{4\tau}} \quad (207)$$

The correspondence takes the form

$$\tilde{u}_r^{(1)}(x, t) = G(r-x, r-x_0, t_0-t) \quad , \quad \gamma = \frac{7}{2} \quad (208)$$

Let us now consider a kick $\dot{f}(x, t) = f\delta(x)\delta(t)$, i.e. for which the seed of the avalanche occurs at $x_s = 0, t_s = 0$. Using the same method as in previous Sections (see Appendix E) we obtain the conditional mean velocity

$$\langle \dot{u}(x_0, t_0) \rangle_{\ell_2 < r} = f \tilde{u}_r^{(1)}(0, 0) = f \frac{\sqrt{r(r-x_0)}}{2t_0} I_{\frac{7}{2}}\left(\frac{r(r-x_0)}{2t_0}\right) e^{-\frac{r^2+(r-x_0)^2}{4t_0}} \quad (209)$$

There should be a sum rule that integrating over time one recovers the mean spatial shape, since $\int_0^{+\infty} dt_0 \dot{u}(x_0, t_0) = S(x_0)$. Indeed, integrating (209) over time, one can check that one recovers (144) using that

$$\int_0^{+\infty} d\tau G(x, y, \tau) = \frac{1}{2\gamma} x^{\frac{1}{2}-\gamma} y^{\frac{1}{2}+\gamma} \theta(x > y) + \frac{1}{2\gamma} x^{\frac{1}{2}+\gamma} y^{\frac{1}{2}-\gamma} \theta(x < y) \quad (210)$$

We can now calculate the mean spatio-temporal profile at fixed seed-to-edge distance ℓ_2 as (see Appendix E)

$$\langle \dot{u}(x_0, t_0) \rangle_{\ell_2} = \frac{1}{\rho(\ell_2)} \partial_r u_r^{(1)}(0, 0)|_{r=\ell_2} + \langle \dot{u}_{x_0 t_0} \rangle_{\ell_2 < r} \simeq_{f \rightarrow 0^+} \frac{\ell_2^3}{12} \partial_r u_r^{(1)}(0, 0)|_{r=\ell_2} \quad (211)$$

Performing the derivatives the final result takes the following scaling form

$$\langle \dot{u}(x_0, t_0) \rangle_{\ell_2} = \frac{\ell_2^3}{t_0} F\left(\frac{\ell_2 - x_0}{\ell_2}, \frac{\ell_2}{\sqrt{t_0}}\right) \quad (212)$$

where the spatiotemporal shape scaling function takes the two equivalent forms

$$F(z, r) = \frac{z+1}{48\sqrt{z}} e^{-\frac{1}{4}r^2(z^2+1)} \left(r^2 z I_{\frac{5}{2}}\left(\frac{r^2 z}{2}\right) - (6+r^2 z) I_{\frac{7}{2}}\left(\frac{r^2 z}{2}\right) \right) \quad (213)$$

$$= \frac{(z+1)e^{-\frac{1}{4}r^2(z+1)^2}}{24\sqrt{\pi} r^7 z^4} \left(12e^{r^2 z} (r^2 z (r^2 z - 10) + 30) - r^2 z (r^2 z (r^2 z (r^2 z + 12) + 72) + 240) - 360 \right) \quad (214)$$

using explicit forms of half-integer Bessel functions, see Appendix G. The spatiotemporal velocity profile is plotted in Fig. 2.

Near the avalanche edge the spatiotemporal shape scaling function exhibits the following behavior

$$F(z, r) = \frac{e^{-\frac{r^2}{4}} r^7 z^3}{5040\sqrt{\pi}} - \frac{\left(e^{-\frac{r^2}{4}} r^7 (r^2 - 8)\right) z^4}{40320\sqrt{\pi}} + \frac{e^{-\frac{r^2}{4}} r^9 (r^2 - 18) z^5}{241920\sqrt{\pi}} + O(z^6) \quad (215)$$

which leads to

$$\langle \dot{u}(x_0, t_0) \rangle_{\ell_2} = \frac{l_2^7 e^{-\frac{l_2^2}{4t_0}} (l_2 - x_0)^3}{5040\sqrt{\pi} t_0^{9/2}} - \frac{l_2^6 e^{-\frac{l_2^2}{4t_0}} (l_2^2 - 8t_0) (l_2 - x_0)^4}{40320\sqrt{\pi} t_0^{11/2}} + O((l_2 - x_0)^5) \quad (216)$$

Thus the mean instantaneous local velocity vanishes near the edge of the avalanche with the same exponent 3, as the mean shape. One can define the time dependent amplitude \mathcal{A}_{t_0} as

$$\langle \dot{u}(x_0, t_0) \rangle_{\ell_2} \simeq \mathcal{A}_{t_0} (l_2 - x_0)^3 \quad , \quad \mathcal{A}_{t_0} = \frac{1}{t_0} C\left(\frac{t_0}{\ell_2^2}\right) \quad , \quad C(\tau) = \frac{e^{-\frac{1}{4\tau}}}{5040\sqrt{\pi} \tau^{7/2}} \quad (217)$$

One finds that as time increases, the amplitude \mathcal{A}_{t_0} reaches a maximum and then decays, the maximum being reached at $t_0 = t_0^* = \ell_2^2/18$ with value $\frac{2187\sqrt{2}}{35e^{9/2}\ell_2^2} = 0.553854/\ell_2^2$.

One can now check that integrating over t_0 one recovers, order by order in $z = \frac{\ell_2 - x_0}{\ell_2}$, the mean spatial shape obtained above in (145)

$$\int_0^{+\infty} dt_0 \langle \dot{u}(x_0, t_0) \rangle_{\ell_2} = \langle S(x_0) \rangle_{\ell_2} \simeq \frac{1}{21}(\ell_2 - x_0)^3 - \frac{1}{28\ell_2}(\ell_2 - x_0)^4 \quad (218)$$

It contains only two terms, i.e. one checks that all coefficients in the expansion, beyond z^4 integrate to zero. The sum rule

$$\int_0^{+\infty} dt_0 \mathcal{A}_{t_0} = \int_0^{+\infty} \frac{d\tau}{\tau} C(\tau) = \frac{1}{21} \quad (219)$$

leads the static leading amplitude obtained in (148).

C. Massive case

In this section we study the effect of a finite mass, and generalize some of the previous results to the massive case. We use the massive units. We only sketch the derivations, which are very similar to the ones of the previous sections.

1. PDF of seed-to-edge distance ℓ_2

In the massive case, to condition to one boundary, i.e. to calculate $P(S(r) = 0)$, one needs to solve the instanton equation

$$\tilde{u}(x)'' - \tilde{u}(x) + \tilde{u}(x)^2 = 0 \quad , \quad \tilde{u}(r) = -\infty \quad (220)$$

with the condition that $\tilde{u}(x)$ vanishes at $x = -\infty$. The solution is

$$\tilde{u}_r(x) = -\frac{3}{2 \sinh(\frac{1}{2}(r-x))^2} \quad (221)$$

Considering a kick of amplitude f (we recall $f = m^2 w$ in massive case dimensionful units) applied at $x_s = 0$, it immediately leads to the CDF and PDF of the seed-to-edge distance ℓ_2 as for

$$\text{Prob}(\ell_2 < r) = e^{-f \frac{3}{2 \sinh(\frac{1}{2}r)^2}} \quad (222)$$

$$P(\ell_2) = \frac{3f}{4} \frac{\sinh \ell_2}{\sinh^4(\ell_2/2)} e^{-f \frac{3}{2 \sinh(\ell_2/2)^2}} \quad , \quad \rho(\ell_2) = \frac{3}{4} \frac{\sinh \ell_2}{\sinh^4(\ell_2/2)} \quad (223)$$

The behavior for small $\ell_2 \ll 1$ (that is $\ell_2 \ll 1/m$) is the same as the one of the massless case, Eq. (23), and more generally all small distance behavior is described by the massless case. The mass only provides a cutoff for the large avalanches.

2. Mean shape conditioned to the seed-to-edge distance ℓ_2

To calculate the mean spatial shape at the point x_0 , let us add the source term $-\lambda \delta(x - x_0)$ on the l.h.s of (220), and look for the solution in a small λ expansion as $\tilde{u}_r^\lambda(x) = \tilde{u}_r(x) + \lambda \tilde{u}_r^{(1)}(x) + O(\lambda^2)$. Then the first order term, $\tilde{u}_r^{(1)}(x)$, satisfies the linear equation

$$\tilde{u}^{(1)''}(x) - \left(1 + \frac{3}{\sinh^2((r-x)/2)}\right) \tilde{u}^{(1)}(x) = -\delta(x - x_0) \quad (224)$$

i.e. it is again the zero energy Green function $\tilde{u}_r^{(1)}(x) = \langle x | \frac{1}{H} | x_0 \rangle$ of the linear "Schrodinger" equation, with $H = -\partial_x^2 + V(x)$ and potential $V(x) = 1 + \frac{3}{\sinh^2((r-x)/2)}$.

It is convenient to introduce the variable $t = \tanh((r-x)/2)$, and write $\tilde{u}^{(1)}(x) = g(t)$. In these coordinates the homogenous part of the differential equation (224) becomes

$$(t^2 - 1)^2 g''(t) + 2t(t^2 - 1)g'(t) + g(t) \left(-\frac{12}{t^2} + 8 \right) = 0 \quad (225)$$

and we find two solutions of this equation. The first one blows up at $x = r$ and decays at large negative x

$$u_1(x) = g_1(t) = \frac{1-t^2}{t^3} = \frac{4e^{r-x}(e^{r-x}+1)}{(e^{r-x}-1)^3} \simeq \frac{8}{(r-x)^3} \quad (226)$$

where the last equation is the small $r-x$ behavior. The second solution vanishes at $x = r$ and blows up at large negative x

$$u_2(x) = g_2(t) = \frac{15(1-t^2)(r-x)}{8t^3} - \frac{8t^4 - 25t^2 + 15}{4t^2(1-t^2)} \simeq \frac{(r-x)^4}{56} \quad (227)$$

where the last equation is the small $r-x$ behavior. Each of these solutions match the two power laws that we found in the massless case in (142).

The solution of (224) is thus

$$\tilde{u}_r^{(1)}(x) = u_1(x)u_2(x_0)\theta(x < x_0) + u_2(x)u_1(x_0)\theta(x_0 < x < r) \quad (228)$$

which is continuous, and with the required derivative discontinuity $u_1(x)u_2'(x) - u_1'(x)u_2(x) = -1$, at $x = x_0$.

We give now the explicit expressions for the mean shape conditioned to the seed-to-edge distance ℓ_2 in the massive case. One finds, for a seed at $x_s = 0$

$$\langle S(x_0) \rangle_{\ell_2 < r} = f \tilde{u}_r^{(1)}(0) \quad (229)$$

$$= \frac{f}{32} \frac{\sinh(r-x_0)}{\sinh^2\left(\frac{r}{2}\right) \sinh^4\left(\frac{r-x_0}{2}\right)} \left(-14 \cosh(r) + \cosh(2r) + 30r \coth\left(\frac{r}{2}\right) - 47 \right), \quad x_0 < 0 \quad (230)$$

$$= \frac{f}{16} \frac{\coth\left(\frac{r}{2}\right)}{\sinh^2\left(\frac{r}{2}\right) \sinh^2\left(\frac{r-x_0}{2}\right)} \left(-14 \cosh(r-x_0) + \cosh(2(r-x_0)) + 30(r-x_0) \coth\left(\frac{r-x_0}{2}\right) - 47 \right), \quad x_0 > 0$$

One also can write, in the limit $f \rightarrow 0^+$

$$\langle S(x_0) \rangle_{\ell_2=r} = \frac{1}{\rho(\ell_2=r)} \partial_r \tilde{u}_r^{(1)}(0) = \frac{4}{3} \frac{\sinh^4(r/2)}{\sinh r} \partial_r \tilde{u}_r^{(1)}(0) \quad (231)$$

using (222). This leads to, the mean shape in the massive case, for $x_s = 0 < x_0 < \ell_2$

$$\langle S(x_0) \rangle_{\ell_2} = -\frac{1}{96 \sinh(\ell_2) \sinh^4\left(\frac{\ell_2-x_0}{2}\right)} \left(\cosh(2\ell_2 - 3x_0) - 10 \cosh(\ell_2 - 2x_0) - 6 \cosh(3\ell_2 - 2x_0) \right. \\ \left. - 130 \cosh(\ell_2 - x_0) - 32 \cosh(2(\ell_2 - x_0)) + 2 \cosh(3(\ell_2 - x_0)) + 80 \cosh(\ell_2) \right. \\ \left. + 5(4(3(\ell_2 - x_0)(2(\sinh(\ell_2 - x_0) + \sinh(\ell_2)) + \sinh(2\ell_2 - x_0)) + 3 \cosh(x_0) + 8) - 25 \cosh(2\ell_2 - x_0)) \right) \quad (232)$$

$$= \frac{1}{21} (\ell_2 - x_0)^3 - \frac{(4e^{\ell_2} + e^{2\ell_2} + 1)(\ell_2 - x_0)^4}{84(e^{2\ell_2} - 1)} + \frac{(\ell_2 - x_0)^7}{9240} + O((\ell_2 - x_0)^8) \quad (233)$$

One can check that for small $r, x_0 \ll 1$ (in the massive units) one recovers exactly (146). Comparing with (146) one also sees that the leading behavior of the mean shape near the edge for $\ell_2 - x_0 \rightarrow 0$ is the same as in the massless case, however the coefficient of the next order term now depends on ℓ_2 in a different way: it crosses over from $-\frac{1}{28\ell_2}$ for small ℓ_2 to $-\frac{1}{84}$ for $\ell_2 \rightarrow +\infty$. Note also the term $O((\ell_2 - x_0)^7)$ which, although its amplitude is ℓ_2 independent, does not exist in the massless case. In fact all terms of order higher than 4 disappear in this limit. One finds, for the

mean shape for $x_0 < 0$

$$\begin{aligned}
\langle S(x_0) \rangle_{\ell_2} &= \frac{1}{96 \sinh(\ell_2) \sinh^4\left(\frac{\ell_2 - x_0}{2}\right)} (-20(3\ell_2(2(\sinh(\ell_2 - x_0) + \sinh(\ell_2)) + \sinh(2\ell_2 - x_0)) + 8) \\
&\quad - 80 \cosh(\ell_2 - x_0) + 125 \cosh(2\ell_2 - x_0) + 6 \cosh(3\ell_2 - x_0) + 10 \cosh(\ell_2 + x_0) - \cosh(2\ell_2 + x_0) \\
&\quad + 130 \cosh(\ell_2) + 32 \cosh(2\ell_2) - 2 \cosh(3\ell_2) - 60 \cosh(x_0)) = A(\ell_2) e^{x_0} + O(e^{2x_0}) \quad (234) \\
A(\ell_2) &= \frac{40(3\ell_2 + 2) + e^{-3\ell_2} - 10e^{-2\ell_2} + 60e^{-\ell_2} - 6e^{2\ell_2} + 5e^{\ell_2}(12\ell_2 - 25)}{6 - 6e^{2\ell_2}} = 1 + \left(\frac{125}{6} - 10\ell_2\right)e^{-\ell_2} + O(\ell_2 e^{-2\ell_2}) \\
&= \frac{\ell_2^6}{42} - \frac{5\ell_2^7}{168} + \frac{\ell_2^8}{56} + O(\ell_2^9)
\end{aligned}$$

Hence the mean shape $\langle S(x_0) \rangle_{\ell_2}$ now decays exponentially at large $x_0 \rightarrow -\infty$, instead as a power law for the massless case. The prefactor of this exponential decay, $A(\ell_2)$, depends on ℓ_2 : it grows as ℓ_2^6 at small ℓ_2 and converges to unity at large ℓ_2 .

3. Joint PDF of total size S and ℓ_2

Finally we can ask about the the joint PDF of the total size S and ℓ_2 in the massive case. We need to solve the massive version of (154)

$$\tilde{u}''(x) - \tilde{u}(x) + \tilde{u}(x)^2 = -\mu \quad , \quad \tilde{u}(r) = -\infty \quad (235)$$

on $x \in]-\infty, r]$. The solution $\tilde{u}(x) = \tilde{u}_r^\mu(x)$ reads

$$\tilde{u}_r^\mu(x) = \frac{1}{2}(1 - \sqrt{1 - 4\mu}) - \frac{3\sqrt{1 - 4\mu}}{2 \sinh\left(\frac{1}{2}(1 - 4\mu)^{1/4}(r - x)\right)^2} \quad (236)$$

Comparing with (156)-(157) we see that

$$P_{\text{massive}}(\ell_2 < r, S) = e^{f/2} P_{\text{massless}}(\ell_2 < r, S) e^{-S/4} \quad (237)$$

where $P_{\text{massless}}(\ell_2 < r, S)$ is given in (157). A similar relation holds for the densities, taking the first order in small f .

Hence, all moments of S now exist. Let us give here the lowest conditional moments. We use the relation (see Appendix E)

$$\langle e^{\mu S} \rangle_{\ell_2 < r} = e^{f(\tilde{u}_r^\mu(0) - \tilde{u}_r^0(0))} \quad (238)$$

Expanding in powers of μ one finds the mean conditional size, together with its small ℓ_2 and large ℓ_2 behavior

$$\langle S \rangle_{\ell_2 < r} = f \frac{\cosh(r) - 3r \coth\left(\frac{r}{2}\right) + 5}{\cosh(r) - 1} = \frac{fr^2}{10} - \frac{fr^4}{168} + O(r^5) \quad (239)$$

$$= f(1 - 6(r - 2)e^{-r} + O(e^{-2r})) \quad (240)$$

Comparing with (158) we see that the leading small r term is the same as the massless case, but the next order is different. Similarly for the conditional second cumulant we find

$$\begin{aligned}
\langle S^2 \rangle_{\ell_2 < r}^c &= \frac{f}{4 \sinh^4\left(\frac{r}{2}\right)} (-6r^2 + (8 - 3r^2) \cosh(r) + 3r \sinh(r) + \cosh(2r) - 9) = \frac{fr^4}{84} - \frac{fr^6}{900} + O(r^8) \quad (241) \\
&= f(2 - 6e^{-r}(r^2 - r - 4) + O(e^{-2r}))
\end{aligned}$$

Here we cannot compare with the massless case, since the second moment does not exist in that case.

Next we can use the relation (see Appendix E)

$$\langle e^{\mu S} \rangle_{\ell_2 = r} = \frac{\partial_r \tilde{u}_r^\mu(0)}{\partial_r \tilde{u}_r^0(0)} e^{f(\tilde{u}_r^\mu(0) - \tilde{u}_r^0(0))} \quad (242)$$

Expanding in powers of μ one finds the mean conditional size, together with its small ℓ_2 and large ℓ_2 behavior

$$\begin{aligned}\langle S \rangle_{\ell_2} &= \ell_2 \left(2 \coth \left(\frac{\ell_2}{2} \right) - \coth(\ell_2) \right) - 3 + f \frac{(\cosh(\ell_2) - 3\ell_2 \coth(\frac{\ell_2}{2}) + 5)}{\cosh(\ell_2) - 1} = \frac{f\ell_2^2}{10} + \left(\frac{1}{60} - \frac{f}{168} \right) \ell_2^4 + O(\ell_2^5) \\ &= \ell_2 - 3 + 4e^{-\ell_2} \ell_2 + f(1 - 6e^{-\ell_2}(\ell_2 - 2)) + O(e^{-2\ell_2})\end{aligned}\quad (243)$$

Comparing with (158) we see that the ℓ_2^4 and $f\ell_2^2$ terms are the same as the massless case, but the next orders are different. We give the second conditional moment in the limit $f \rightarrow 0$ and its asymptotics

$$\langle S^2 \rangle_{\ell_2, f \rightarrow 0^+} = \ell_2^2 + \frac{3}{2} \ell_2 \left(\tanh \left(\frac{\ell_2}{2} \right) - 3 \coth \left(\frac{\ell_2}{2} \right) + \frac{2\ell_2}{\sinh^2 \left(\frac{\ell_2}{2} \right)} \right) - 3 = \frac{\ell_2^6}{252} - \frac{\ell_2^8}{1800} + O(\ell_2^{10}) \quad (244)$$

$$= \ell_2(\ell_2 - 3) - 3 + 12\ell_2(\ell_2 - 1)e^{-\ell_2} + O(e^{-2\ell_2}) \quad (245)$$

Note that, restoring dimensions, one has $\langle S^2 \rangle_{\ell_2} \simeq \frac{\sigma^2}{252m^2} \ell_2^6$ at small $\ell_2 \ll 1/m$, with a prefactor which indeed diverges as $m \rightarrow 0$ (since the second moment does not exist in the massless case).

VI. BULK DRIVING: SPATIAL SHAPE CONDITIONED TO TWO BOUNDARIES

We now consider the problem of the joint distribution of ℓ_1, ℓ_2 , of the total extension $\ell = \ell_1 + \ell_2$ and of the shape conditioned to ℓ and to the aspect ratio, see Fig. 1. We study the massless case.

A. PDF and density of ℓ_1, ℓ_2 and of ℓ, p

Consider the driving by a kick of amplitude $f(x)$ with a bounded support and we ask about the probability that the avalanche has remained in the interval $[r_1, r_2]$ with $r_1 < r_2$ (which includes the support of $f(x)$). It is equal to

$$P(S(r_1) = 0, S(r_2) = 0) = e^{\int dx f(x) \tilde{u}_{r_1, r_2}(x)} \quad (246)$$

where $\tilde{u}_{r_1, r_2}(x)$ is the solution of the massless instanton equation

$$\tilde{u}''(x) + \tilde{u}(x)^2 = 0 \quad , \quad \tilde{u}(x = r_1) = \tilde{u}(x = r_2) = -\infty \quad (247)$$

on the interval $x \in [r_1, r_2]$. The solution of this problem, as discussed in¹⁰, is an elliptic Weierstrass function

$$\tilde{u}_{r_1, r_2}(x) = -\frac{6}{(r_2 - r_1)^2} \mathcal{P}_0(z) \quad , \quad z = \frac{x - r_1}{r_2 - r_1} \quad (248)$$

$$\mathcal{P}_0(z) := \mathcal{P}(z; g_2 = 0, g_3 = g_3^0) := \frac{\Gamma(1/3)^{18}}{(2\pi)^6} \quad (249)$$

Here the value of g_3 is such that the real period is unity, i.e. $2\Omega(g_2 = 0, g_3^0) = 1$, see (A10). Two important properties of \mathcal{P}_0 are

$$\mathcal{P}_0(1 - z) = \mathcal{P}_0(z) \quad , \quad \mathcal{P}_0(z) \simeq_{z \rightarrow 0} \frac{1}{z^2} + \frac{g_3^0 z^4}{28} + O(z^{10}) \quad (250)$$

Because of these properties, one immediately sees that near the edges of the interval $[r_1, r_2]$ one recovers to leading order the single edge solution

$$\tilde{u}_{r_1, r_2}(x) \simeq -\frac{6}{(r_2 - x)^2} - \frac{3g_3^0}{14} \frac{(r_2 - x)^4}{(r_2 - r_1)^6} + O((r_2 - x)^{10}) \quad (251)$$

plus subleading corrections.

If we consider now a kick of amplitude f at $x = x_s = 0$ (we define the origin as the position of the seed), we have the joint CDF of ℓ_1, ℓ_2 (as defined in Fig. 1)

$$P(\ell_1 < l_1, \ell_2 < l_2) = e^{f \tilde{u}_{r_1, r_2}(0)} = e^{-6f \frac{1}{(l_1 + l_2)^2} \mathcal{P}_0\left(\frac{l_2}{l_2 + l_1}\right)} \quad , \quad l_1 = -r_1 \quad l_2 = r_2 \quad (252)$$

and of course $r_1 < 0$ and $r_2 > 0$ since the interval must contain the seed. The joint PDF is

$$P(\ell_1, \ell_2) = \partial_{\ell_1} \partial_{\ell_2} e^{-6f \frac{1}{\ell^2} \mathcal{P}_0(p)} \quad , \quad \ell = \ell_1 + \ell_2 \quad , \quad p = \frac{\ell_2}{\ell_1 + \ell_2} \quad (253)$$

where $p \in [0, 1]$ is the aspect ratio. This expression is complicated but its small f behavior, i.e. the density, is a bit simpler. The density is

$$\rho(\ell_1, \ell_2) = \partial_f|_{f=0^+} P(\ell_1, \ell_2) = \partial_{\ell_1} \partial_{\ell_2} \tilde{u}_{r_1=-\ell_1, r_2=\ell_2}(0) = -6 \partial_{\ell_1} \partial_{\ell_2} \left[\frac{1}{\ell^2} \mathcal{P}_0(p) \right] \quad (254)$$

Clearly it is better to trade the variables (ℓ_1, ℓ_2) for the pair (ℓ, p) . The reverse transformation is $\ell_1 = (1-p)\ell$ and $\ell_2 = p\ell$. The jacobian, and the partial derivative operators are

$$d\ell_1 d\ell_2 = \ell d\ell dp \quad , \quad \partial_{\ell_1} = \partial_\ell - \frac{p}{\ell} \partial_p \quad , \quad \partial_{\ell_2} = \partial_\ell + \frac{1-p}{\ell} \partial_p \quad (255)$$

$$\partial_{\ell_1} \partial_{\ell_2} = \frac{1}{\ell^2} [(2p-1)\partial_p + p(p-1)\partial_p^2] + \frac{1-2p}{\ell} \partial_p \partial_\ell + \partial_\ell^2 \quad (256)$$

$$= \frac{1}{\ell} \partial_p [p(p-1)\frac{1}{\ell} \partial_p + (1-2p)\partial_\ell] + \frac{2}{\ell} \partial_\ell + \partial_\ell^2 \quad (257)$$

Since $\rho(\ell_1, \ell_2) d\ell_1 d\ell_2 = \rho(\ell, p) d\ell dp$, we have $\rho(\ell, p) = \ell \rho(\ell_1, \ell_2)$ (with some abuse of notation, since we denote by ρ both functions, while they are different functions of their arguments). Hence

$$\rho(\ell, p) = -6\ell \partial_{\ell_1} \partial_{\ell_2} \left[\frac{1}{\ell^2} \mathcal{P}_0(p) \right] = -6 \left(\partial_p [p(p-1)\frac{1}{\ell} \partial_p + (1-2p)\partial_\ell] + 2\partial_\ell + \ell \partial_\ell^2 \right) \left[\frac{1}{\ell^2} \mathcal{P}_0(p) \right] \quad (258)$$

$$= -\frac{6}{\ell^3} (\partial_p [(p(p-1)\mathcal{P}'_0(p) + 2(2p-1)\mathcal{P}_0(p))] + 2\mathcal{P}_0(p)) \quad (259)$$

$$= -\frac{6}{\ell^3} ((p-1)p\mathcal{P}''_0(p) + (6p-3)\mathcal{P}'_0(p) + 6\mathcal{P}_0(p)) \quad (260)$$

One can check that the differential operator in p in (260) vanishes when applied to $1/p^2$ and $1/(1-p)^2$. The reason for these "zero modes" is that near any of the two edges, as mentioned above, one recovers the one boundary problem, where nothing depends on ℓ_1 or ℓ_2 (repectively). Hence it is better to replace $\mathcal{P}_0 \rightarrow \tilde{\mathcal{P}}_0 = \mathcal{P}_0(p) - 1/p^2 - 1/(1-p)^2$ which is now a regular function (vanishing quartically at each boundary $p = 0, 1$). This allows e.g. to integrate by part in the line (259) and obtain the density of total extension alone

$$\rho(\ell) = \int_0^1 dp \rho(\ell, p) = -\frac{6}{\ell^3} (-4 + 2 \int_0^1 dp \tilde{\mathcal{P}}_0(p)) = \frac{8\sqrt{3}\pi}{\ell^3} \quad (261)$$

using that $[(p(p-1)\tilde{\mathcal{P}}'_0(p) + 2(2p-1)\tilde{\mathcal{P}}_0(p))]_0^1 = -4$.

In summary one can write the joint density of total extension ℓ and of aspect ratio as

$$\rho(\ell, p) = \frac{8\pi\sqrt{3}}{\ell^3} \tilde{P}(p) \quad , \quad \tilde{P}(p) = -\frac{\sqrt{3}}{4\pi} (\partial_p [(p(p-1)\mathcal{P}'_0(p) + 2(2p-1)\mathcal{P}_0(p))] + 2\mathcal{P}_0(p)) \quad (262)$$

where $\tilde{P}(p)$ is the PDF of the aspect ratio, i.e. it is normalized to unity $\int_0^1 dp \tilde{P}(p) = 1$.

B. Mean shape conditioned to total extension and aspect ratio

In this section we obtain the mean shape conditioned to the total extension and aspect ratio. As we show, it amounts to solve a Lamé equation.

We again restrict to a local kick of amplitude f at $x_s = 0$ (taking the seed position to be the origin). We want to study the joint PDF $P(S(r_1) = 0, S(r_2) = 0, S(x_0)) = P(\ell_1 < -r_1, \ell_2 < r_2, S(x_0))$ whose Laplace transform is given by

$$\int_0^{+\infty} dS(x_0) e^{\lambda S(x_0)} P(\ell_1 < -r_1, \ell_2 < r_2, S(x_0)) = e^{f \tilde{u}_{r_1, r_2}^{\lambda, x_0}(0)} \quad (263)$$

where we denote $\tilde{u}_{r_1, r_2}^{\lambda, x_0}(x)$ the solution of the massless instanton equation with a source localized in x_0

$$\tilde{u}''(x) + \tilde{u}(x)^2 = -\lambda\delta(x - x_0) \quad , \quad \tilde{u}(x = r_1) = \tilde{u}(x = r_2) = -\infty \quad (264)$$

on the interval $x \in [r_1, r_2]$. It is easy to see that

$$\begin{aligned} \tilde{u}_{r_1, r_2}^{\lambda, x_0}(x) &= \frac{-6}{(r_2 - r_1)^2} \mathcal{P}\left(\frac{x - r_1}{r_2 - r_1}; g_2 = 0, g_3^-\right) \quad , \quad x < x_0 \\ &= \frac{-6}{(r_2 - r_1)^2} \mathcal{P}\left(\frac{r_2 - x}{r_2 - r_1}; g_2 = 0, g_3^+\right) \quad , \quad x > x_0 \end{aligned} \quad (265)$$

The parameters g_3^\pm are determined by the conditions of continuity and of proper derivative jump at $x = x_0$. They read explicitly

$$\begin{aligned} \mathcal{P}(z_0, g_2 = 0, g_3^-) &= \mathcal{P}(1 - z_0, g_2 = 0, g_3^+) \\ \mathcal{P}'(z_0, g_2 = 0, g_3^-) + \mathcal{P}'(1 - z_0, g_2 = 0, g_3^+) &= -\hat{\lambda} \\ z_0 = \frac{x_0 - r_1}{r_2 - r_1} \quad , \quad 1 - z_0 = \frac{r_2 - x_0}{r_2 - r_1} \quad , \quad \hat{\lambda} &= \frac{\lambda}{6}(r_2 - r_1)^3 \end{aligned} \quad (266)$$

We note that for $\lambda = 0$ one has

$$\lambda = 0 \Rightarrow g_3^- = g_3^+ = g_3^0 = \frac{\Gamma(1/3)^{18}}{(2\pi)^6} \quad , \quad \tilde{u}_{r_1, r_2}^{0, x_0}(x) = \frac{-6}{(r_1 - r_2)^2} \mathcal{P}_0\left(\frac{r_2 - x}{r_2 - r_1}\right) = \frac{-6}{(r_1 - r_2)^2} \mathcal{P}_0\left(\frac{x - r_1}{r_2 - r_1}\right) \quad (267)$$

since $\mathcal{P}'_0(\frac{1}{2}) = \mathcal{P}'(\frac{1}{2}, g_2 = 0, g_3^0) = 0$.

Brute force expanding in powers of λ allows to get the mean shape as well as its higher moments. This is detailed in the Appendix. For the mean shape it is equivalent but easier to write, as we did in previous sections, a linear "Schrodinger" equation. Let us define the expansion in λ of the solution of the instanton equation

$$\tilde{u}_{r_1, r_2}^{\lambda, x_0}(0) = \tilde{u}_{r_1, r_2}(x) + \lambda \tilde{u}_{r_1, r_2}^{(1)}(x) + O(\lambda^2) \quad , \quad \tilde{u}_{r_1, r_2}(x) = -\frac{6}{(r_2 - r_1)^2} \mathcal{P}_0(z) \quad , \quad z = \frac{x - r_1}{r_2 - r_1} \quad (268)$$

Inserting into (264) we see that the $O(\lambda)$ term, $\tilde{u}_{r_1, r_2}^{(1)}(x)$ is the solution of the linear equation

$$\tilde{u}^{(1)''}(x) - \frac{12}{(r_2 - r_1)^2} \mathcal{P}_0\left(\frac{x - r_1}{r_2 - r_1}\right) \tilde{u}^{(1)}(x) = -\delta(x - x_0) \quad (269)$$

which is again the zero energy Green function $\tilde{u}_{r_1, r_2}^{(1)}(x) = \langle x | \frac{1}{H} | y \rangle$ of the "Schrodinger" equation, associated to the Hamiltonian $H = -\partial_x^2 + V(x)$ with the potential $V(x) = \frac{12}{(r_2 - r_1)^2} \mathcal{P}_0\left(\frac{x - r_1}{r_2 - r_1}\right)$.

This problem is known as the Lamé problem. Let us use the reduced coordinates $z = (x - r_1)/(r_2 - r_1)$ and $z_0 = (x_0 - r_1)/(r_2 - r_1)$ and write $\tilde{u}^{(1)}(x) = \frac{1}{(r_2 - r_1)^2} \psi(z)$, then $\psi(z)$ satisfies

$$-\psi''(z) + 12\mathcal{P}_0(z)\psi(z) = (r_2 - r_1)^3 \delta(z - z_0) \quad (270)$$

on the interval $z \in [0, 1]$. Two linearly independent solutions of the homogeneous equation are, using extensively the symmetry $\mathcal{P}_0(1 - z) = \mathcal{P}_0(z)$ and the properties of the Weierstrass function (see Appendix A)

$$\psi_1(z) = 2\mathcal{P}_0(z) + z\mathcal{P}'_0(z) \quad , \quad \psi_2(z) = \psi_1(1 - z) = 2\mathcal{P}_0(z) + (z - 1)\mathcal{P}'_0(z) \quad (271)$$

Note that near the edge at $z = 0$ (that is $x = r_1$)

$$\psi_1(z) \simeq \frac{3g_3^0 z^4}{14} + \frac{3g_3^0{}^2 z^{10}}{2548} + O(z^{16}) \quad (272)$$

$$\psi_2(z) \simeq \frac{2}{z^3} - \frac{g_3^0 z^3}{7} + O(z^4) \quad (273)$$

and thus each function neatly corresponds, near the edge, to one of the two solutions with power laws exponents $a = -3, 4$ found in the single boundary problem, in (142). Note that they exchange behaviors at the other edge $z = 1$ (that is $x = r_2$) since $\psi_2(z) = \psi_1(1 - z)$. Their Wronskien is

$$\psi_1'(z)\psi_2(z) - \psi_2'(z)\psi_1(z) = 3g_3^0 \quad (274)$$

Thus the solution of (270) (continuous and with the proper derivative discontinuity at $z = z_0$) is

$$\psi(z) = \frac{(r_2 - r_1)^3}{3g_3^0} (\psi_1(z_0)\psi_2(z)\theta(z - z_0) + \psi_2(z_0)\psi_1(z)\theta(z_0 - z)) \quad (275)$$

So finally one has

$$\tilde{u}_{r_1, r_2}^{(1)}(x) = \frac{r_2 - r_1}{3g_3^0} (\psi_1(z_0)\psi_2(z)\theta(z - z_0) + \psi_2(z_0)\psi_1(z)\theta(z_0 - z)) \quad , \quad z = \frac{x - r_1}{r_2 - r_1} \quad , \quad z_0 = \frac{x_0 - r_1}{r_2 - r_1} \quad (276)$$

Let us start with the cumulative conditional mean shape, which is easier to calculate, using (see Appendix E)

$$\langle S(x_0) \rangle_{\ell_1 < -r_1, \ell_2 < r_2} = f \tilde{u}_{r_1, r_2}^{(1)}(0) \quad (277)$$

Since $x = 0$ (position of the seed) corresponds to $z = 1 - p$ we obtain for $x_0 < 0$ (i.e. $z_0 < 1 - p$)

$$\langle S(x_0 < 0) \rangle_{\ell_1 < -r_1, \ell_2 < r_2} = \frac{f}{3g_3^0} (r_2 - r_1) \psi_1(z_0) \psi_1(p) \quad , \quad p = \frac{r_2}{r_2 - r_1} \quad , \quad z_0 = \frac{x_0 - r_1}{r_2 - r_1} \quad (278)$$

$$= \frac{f}{3g_3^0} (r_2 - r_1) (2\mathcal{P}_0(z_0) + z_0 \mathcal{P}'_0(z_0)) (2\mathcal{P}_0(p) + p \mathcal{P}'_0(p)) \quad (279)$$

and for $x_0 > 0$ (i.e. $z_0 > 1 - p$)

$$\langle S(x_0 > 0) \rangle_{\ell_1 < -r_1, \ell_2 < r_2} = \frac{f}{3g_3^0} (r_2 - r_1) \psi_2(z_0) \psi_2(p) \quad , \quad p = \frac{r_2}{r_2 - r_1} \quad , \quad z_0 = \frac{x_0 - r_1}{r_2 - r_1} \quad (280)$$

$$= \frac{f}{3g_3^0} (r_2 - r_1) (2\mathcal{P}_0(z_0) + (z_0 - 1) \mathcal{P}'_0(z_0)) (2\mathcal{P}_0(p) + (p - 1) \mathcal{P}'_0(p)) \quad (281)$$

In the limit $r_1 \rightarrow -\infty$, using the asymptotic behaviors (272) we recover the result for the single boundary at $x = r_2$, i.e. (144). Let us sketch it for $x_0 < 0$, in (279) one has $p \rightarrow 0$ and $1 - z_0 = (r_2 - x_0)/(r_2 - r_1) \rightarrow 0$, thus using (272), the first line in (279) becomes $\frac{f}{3g_3^0} (r_2 - r_1) \times \frac{2}{(1 - z_0)^3} \times \frac{3g_3^0 p^4}{14} = \frac{1}{7} f \frac{r_2^4}{(r_2 - x_0)^3}$ as all factors $r_2 - r_1$ cancel. It works similarly for $x_0 > 0$. Note that the results (278), (280) can also be obtained by a direct expansion of (265) and of the self-consistent equation (266) in powers of λ , see Appendix H.

We can now study the behavior near the edges of the avalanche. Let us look at the edge at $x = r_2$, hence at $x_0 > 0$ near r_2 and at (281). Since $z_0 = 1 - \frac{r_2 - x_0}{r_2 - r_1}$ we can rewrite

$$\langle S(x_0 > 0) \rangle_{\ell_1 < -r_1, \ell_2 < r_2} = \frac{f}{3g_3^0} (r_2 - r_1) \psi_1\left(\frac{r_2 - x_0}{r_2 - r_1}\right) \psi_2(p) \simeq \frac{f}{14} \frac{(r_2 - x_0)^4}{(r_2 - r_1)^3} \psi_2(p) \quad (282)$$

To compare with the single boundary result (144), we rewrite it in the form

$$\langle S(x_0) \rangle_{\ell_1 < -r_1, \ell_2 < r_2} = \frac{f}{7} \frac{(r_2 - x_0)^4}{r_2^3} \phi\left(\frac{r_2}{r_2 - r_1}\right) \quad (283)$$

$$\phi(p) = \frac{1}{2} p^3 \psi_2(p) = \frac{1}{2} p^3 (2\mathcal{P}_0(p) + (p - 1) \mathcal{P}'_0(p)) \quad (284)$$

where $\phi(p)$ is a smoothly decaying function from $\phi(0) = 1$ to $\phi(1) = 0$

$$\phi(p) = 1 - \frac{p^6 \Gamma\left(\frac{1}{3}\right)^{18}}{896\pi^6} + \frac{3p^7 \Gamma\left(\frac{1}{3}\right)^{18}}{1792\pi^6} - \frac{5p^{12} \Gamma\left(\frac{1}{3}\right)^{36}}{41746432\pi^{12}} + O(p^{13}) \quad (285)$$

$$= \frac{3(1 - p)^4 p^3 \Gamma\left(\frac{1}{3}\right)^{18}}{1792\pi^6} + O((1 - p)^5) \quad (286)$$

For $r_1 \rightarrow -\infty$, the aspect ratio $p \rightarrow 0$, and using $\phi(0) = 1$ one recovers (144). We see that for all values of p the mean shape vanishes at the edge with the same power 4. However the coefficient depends on the aspect ratio p as described by $\phi(p)$. Hence conditioning on $\ell_1 < -r_1$ changes the coefficient of the power $(r_2 - x_0)^4$ of the mean (cumulative) conditioned shape near the edge, with respect to no conditioning to the other edge $r_1 = -\infty$.

Let us now calculate the mean shape. Let us start again from (263). Taking $\partial_{r_1} \partial_{r_2}$ on both sides we obtain the same equation for the joint PDF $P(\ell_1, \ell_2, S(x_0))$, and keeping only the term linear in f in the limit $f = 0^+$ we obtain the following equation for the joint density $\rho(\ell_1, \ell_2, S(x_0)) = \partial_f|_{f=0} P(\ell_1, \ell_2, S(x_0))$

$$\int dS(x_0) e^{\lambda S(x_0)} \rho(\ell_1, \ell_2, S(x_0)) = \partial_{\ell_1} \partial_{\ell_2} \tilde{u}_{-\ell_1, \ell_2}^{\lambda, x_0}(0) \quad (287)$$

For more details on these and the manipulation below see Appendix E. It is more convenient to use the variables ℓ, p , and using $\rho(\ell, p) = \ell \rho(\ell_1, \ell_2)$ (see remark above Eq. (260)), rewrite the above for the joint density $\rho(\ell, p, S(x_0))$ as

$$\int dS(x_0) e^{\lambda S(x_0)} \rho(\ell, p, S(x_0)) = \ell \partial_{\ell_1} \partial_{\ell_2} \tilde{u}_{-\ell_1, \ell_2}^{\lambda, x_0}(0) \quad (288)$$

Expanding to first order in λ and using (268) we find that the mean shape conditioned to the couple ℓ, p is given by, in the limit $f = 0^+$ (we recall that the seed is in position $x_s = 0$)

$$\langle S(x_0) \rangle_{\ell, p} = \frac{1}{\rho(\ell, p)} \ell \partial_{\ell_1} \partial_{\ell_2} \tilde{u}_{-\ell_1, \ell_2}^{(1)}(0) \quad (289)$$

Similarly to obtain the mean shape conditioned only on ℓ , we can integrate over p both sides of (288) and then divide by $\rho(\ell)$. This leads to

$$\langle S(x_0) \rangle_{\ell} = \frac{1}{\rho(\ell)} \int_0^1 dp \ell \partial_{\ell_1} \partial_{\ell_2} \tilde{u}_{-\ell_1, \ell_2}^{(1)}(0) \quad (290)$$

To continue the calculation from (289), (290) we need to calculate the second derivative of the solution to the instanton equation. Let us start with $x_0 < 0$, i.e. for $z_0 < 1 - p$, using (277) and (278). We obtain

$$\ell \partial_{\ell_1} \partial_{\ell_2} u_{-\ell_1, \ell_2}^1(0) = \frac{1}{3g_3^0} G(p, z_0) \quad , \quad x_0 < 0 \quad , \quad z_0 < 1 - p \quad (291)$$

$$G(p, z_0) = (p - 1)p\psi_1(z_0)\psi_1''(p) + (z_0 - 1)z_0\psi_1(p)\psi_1''(z_0) + (p(2z_0 - 1) - z_0 + 1)\psi_1'(p)\psi_1'(z_0)$$

Note that the derivative is at fixed x_0 . Note that $G(p, z_0) = G(z_0, p)$ is a symmetric function of its arguments. The calculation for $x_0 > 0$, i.e. for $z_0 > 1 - p$ using (280) gives exactly the same result replacing ψ_1 by ψ_2 hence using that $\psi_2(z) = \psi_1(1 - z)$ it gives

$$\ell \partial_{\ell_1} \partial_{\ell_2} u_{-\ell_1, \ell_2}^1(0) = \frac{1}{3g_3^0} G(1 - p, 1 - z_0) \quad , \quad x_0 > 0 \quad , \quad z_0 > 1 - p \quad (292)$$

Hence we obtain from (289) the mean shape conditioned to both the total extension and the aspect ratio

$$\langle S(x_0) \rangle_{\ell, p} = \frac{1}{\rho(\ell, p)} \hat{G}(p, z_0) \quad , \quad p = \frac{\ell_2}{\ell_2 + \ell_1} \quad , \quad z_0 = \frac{x_0 + \ell_1}{\ell_2 + \ell_1} \quad (293)$$

$$\hat{G}(p, z_0) = \frac{1}{3g_3^0} (G(p, z_0)\theta(z_0 < 1 - p) + G(1 - p, 1 - z_0)\theta(z_0 > 1 - p)) \quad (294)$$

where we recall that $G(p, z_0)$ is defined in (291), $\psi_{1,2}$ are defined in (271) and $\rho(\ell, p)$ was obtained in (262).

To obtain $\langle S(x_0) \rangle_{\ell}$ from (290) one needs to integrate over p in (291) and (292), more precisely one has

$$\langle S(x_0) \rangle_{\ell} = \frac{f(z_0)}{\rho(\ell)} \quad , \quad f(z_0) = \int_0^1 dp \hat{G}(p, z_0) \quad , \quad z_0 = \frac{x_0 + \ell_1}{\ell} \quad (295)$$

It turns out that this integral can be performed explicitly. Since it is not trivial however, we will use a trick. We note that, using the symmetry between p and z_0 in the definitions of G and \hat{G} we have that the following marginals define the same function f

$$\int_0^1 dp \hat{G}(p, z_0) = f(z_0) \Leftrightarrow \int_0^1 dz_0 \hat{G}(p, z_0) = f(p) \quad (296)$$

Hence the function $f(p)$ can be equivalently determined from the knowledge of the following conditional mean total size

$$\langle S \rangle_{\ell,p} = \int dx_0 \langle S(x_0) \rangle_{\ell,p} = \frac{\ell}{\rho(\ell,p)} \int_0^1 dz_0 \hat{G}(p, z_0) = \frac{\ell}{\rho(\ell,p)} f(p) \quad (297)$$

We now turn to the direct calculation of $\langle S \rangle_{\ell,p}$ from which we will obtain the function $f(p)$, hence the desired result for the mean shape at fixed extension from (295).

It is useful for the following to introduce the primitive of $\psi_1(z) = 2\mathcal{P}_0(z) + z\mathcal{P}'_0(z)$ which has an explicit form

$$\Psi_1(z) = \int_0^z \psi_1(z') dz' = z\mathcal{P}_0(z) - \zeta_0(z) \quad (298)$$

where $\zeta_0(z) = \zeta(z; 0, g_3^0)$ is the zeta-Weierstrass function which satisfies

$$\zeta'_0(z) = -\mathcal{P}_0(z) \quad , \quad \zeta_0(z) + \zeta_0(1-z) = \frac{2\pi}{\sqrt{3}} \quad (299)$$

The fact that $\zeta_0(z) + \zeta_0(1-z)$ is constant is a consequence of $\mathcal{P}_0(z) = \mathcal{P}_0(1-z)$ (by differentiation w.r.t. z). The constant is known since $\zeta_0(\frac{1}{2}) = \frac{\pi}{\sqrt{3}}$.

C. Joint density of size and extension

Let us now determine directly the joint density of size and extension which allows to obtain $\langle S \rangle_{\ell,p}$ and the function $f(z_0)$ in (295). The Laplace transform of the conditional distribution of the total avalanche size S (with a seed at $x=0$) can be obtained as

$$\int dS e^{\mu S} P(\ell_1 < -r_1, \ell_2 < r_2, S) = e^{f\tilde{u}_{r_1, r_2}^{\mu}(0)} \quad (300)$$

where $\tilde{u}_{r_1, r_2}^{\mu}(x)$ is the solution of

$$\tilde{u}''(x) + \tilde{u}(x)^2 = -\mu \quad , \quad \tilde{u}(r_1) = -\infty \quad , \quad \tilde{u}(r_2) = -\infty \quad (301)$$

on the interval $x \in [r_1, r_2]$. The solution is

$$\tilde{u}_{r_1, r_2}(x) = -\frac{6}{(r_2 - r_1)^2} \mathcal{P}\left(\frac{x - r_1}{r_2 - r_1}; g_2 = -\frac{1}{3}\mu(r_2 - r_1)^4, g_3\right) \quad (302)$$

where $g_3 = g_3(\mu)$ is determined by the condition that the period is unity, i.e. $2\Omega(g_2, g_3) = 1$ equivalently

$$\mathcal{P}'\left(\frac{1}{2}; g_2 = -\frac{1}{3}\mu(r_2 - r_1)^4, g_3\right) = 0 \quad (303)$$

Expanding this equation in powers of g_2 and g_3 near $g_2 = 0$ and $g_3 = g_3^0$ and matching the powers one obtains the following expansion of $g_3(\mu)$ in powers of g_2

$$g_3 = g_3(\mu) = g_3^0 - 2Xg_2 - \frac{X^2}{g_3^0}g_2^2 + \left(\frac{7}{432g_3^0} - \frac{56}{27}\frac{X^3}{(g_3^0)^2}\right)g_2^3 + O(g_2^4) \quad , \quad X := \zeta\left(\frac{1}{2}; 0, g_3^0\right) = \frac{\pi}{\sqrt{3}} \quad (304)$$

where we have used that $\mathcal{P}'_0(\frac{1}{2}) = 0$ and $\mathcal{P}_0(\frac{1}{2}) = (g_3^0/4)^{1/3}$. Here ζ is the ζ Weierstrass function mentioned in the previous subsection and $\zeta_0(z) = \zeta(z; 0, g_3^0)$ satisfies the properties (299) with $\zeta_0(\frac{1}{2}) = \frac{\pi}{\sqrt{3}}$ as mentioned there.

From (300), the formula for the conditional average of $e^{\mu S}$ is

$$\langle e^{\mu S} \rangle_{\ell_1 < -r_1, \ell_2 < r_2} = e^{f(\tilde{u}_{r_1, r_2}^{\mu}(0) - \tilde{u}_{r_1, r_2}^{\mu=0}(0))} \quad (305)$$

Expanding first to linear order in μ , and then using the solution (302) together with the first term $O(g_2)$ in the expansion (304), we obtain the cumulative conditional mean total size as

$$\langle S \rangle_{\ell_1 < -r_1, \ell_2 < r_2} = f \partial_\mu |_{\mu=0} \tilde{u}_{r_1, r_2}^\mu(0) = 2f(r_2 - r_1)^2 g(p) \quad (306)$$

$$g(p) = g(1-p) = \frac{1}{6g_3^0} (2\mathcal{P}_0(p)^2 - \frac{4\pi\mathcal{P}_0(p)}{\sqrt{3}} + \mathcal{P}'_0(p)(\zeta_0(p) - \frac{2\pi p}{\sqrt{3}})) \quad , \quad p = \frac{r_2}{r_2 - r_1} \quad (307)$$

$$= \frac{p^2}{20} - \frac{\pi p^4}{14\sqrt{3}} + \frac{3p^8 \Gamma(\frac{1}{3})^{18}}{394240\pi^6} + O(p^9) \quad (308)$$

where p is the aspect ratio of the avalanche. In the limit $r_1 \rightarrow -\infty$, i.e. $p \rightarrow 0$, and using the above asymptotics, we recover nicely the result (158) for a single boundary. The higher moments can be similarly calculated and the second moment is displayed in the Appendix I.

Let us compare with the result (279), (281), which can be written as (with $z_0 = \frac{x_0 - r_1}{r_2 - r_1}$)

$$\langle S(x_0) \rangle_{\ell_1 < -r_1, \ell_2 < r_2} = \frac{f}{3g_3^0} (r_2 - r_1) [\psi_1(z_0)\psi_1(p)\theta(z_0 < 1-p) + \psi_1(1-z_0)\psi_1(1-p)\theta(z_0 > 1-p)] \quad (309)$$

By definition of the total size of the avalanche one must have

$$\langle S \rangle_{\ell_1 < -r_1, \ell_2 < r_2} = (r_2 - r_1) \int_0^1 dz_0 \langle S(x_0) \rangle_{\ell_1 < -r_1, \ell_2 < r_2} \quad (310)$$

The two results are found to be consistent, since indeed we have checked that

$$g(p) = \frac{1}{6g_3^0} (\psi_1(p) \int_0^{1-p} dz_0 \psi_1(z_0) + \psi_1(1-p) \int_{1-p}^1 dz_0 \psi_1(1-z_0)) \quad (311)$$

Let us now calculate the conditional mean total size, $\langle S \rangle_{\ell, p}$, conditioned on both ℓ and p . Through the same manipulations as in the previous subsection, one has, in the limit $f = 0^+$

$$\langle e^{\mu S} \rangle_{\ell_1, \ell_2} = \frac{1}{\rho(\ell_1, \ell_2)} \partial_{\ell_1} \partial_{\ell_2} \tilde{u}_{-\ell_1, \ell_2}^\mu(0) \quad , \quad \langle e^{\mu S} \rangle_{\ell, p} = \frac{1}{\rho(\ell, p)} \ell \partial_{\ell_1} \partial_{\ell_2} \tilde{u}_{-\ell_1, \ell_2}^\mu(0) \quad (312)$$

Expanding to first order in μ , and using (306), we obtain the mean total size conditioned to both the total extension ℓ and the aspect ratio p as

$$\begin{aligned} \langle S \rangle_{\ell, p} &= \frac{1}{\rho(\ell, p)} \ell \partial_{\ell_1} \partial_{\ell_2} \partial_\mu |_{\mu=0} \tilde{u}_{-\ell_1, \ell_2}^\mu(0) = 2 \frac{1}{\rho(\ell, p)} \ell \partial_{\ell_1} \partial_{\ell_2} [\ell^2 g(p)] \\ &= \frac{2\ell}{\rho(\ell, p)} (6g(p) + \partial_p [p(p-1)g'(p) + 2(1-2p)g(p)]) \\ &= \frac{2\ell}{\rho(\ell, p)} (2g(p) + (1-2p)g'(p) + p(p-1)g''(p)) \end{aligned} \quad (313)$$

where we have used (257), and we recall that $\rho(\ell, p)$ is given by (262).

We now obtain the mean total size conditioned to the total extension ℓ as follows

$$\langle S \rangle_\ell = \frac{2}{\rho(\ell)} \int_0^1 dp \ell \partial_{\ell_1} \partial_{\ell_2} [\ell^2 g(p)] = \frac{\ell^3}{8\sqrt{3}\pi} \times 12\ell \int_0^1 dp g(p) = \frac{\sqrt{3}}{2\pi} \ell^4 \int_0^1 dp g(p) \quad (314)$$

where we used the second line in (313), and noted that upon integration over p the total derivative term does not contribute since $g(p)$ vanishes quadratically at $p = 0, 1$. Using that $\int_0^1 dp g(p) = 0.0026720030751$ we find

$$\langle S \rangle_\ell = 0.00073657566 \times \ell^4 \quad (315)$$

D. Mean shape conditioned to total extension

We can now compare (297) and (313) to obtain the function $f(p)$ as

$$f(p) = 2(2g(p) + (1 - 2p)g'(p) + p(p - 1)g''(p)) \quad (316)$$

which using (295) gives the mean shape conditioned to total extension

$$\langle S(x_0) \rangle_\ell = \ell^3 \mathfrak{s}(z_0) \quad , \quad z_0 = \frac{x_0 + \ell_1}{\ell} \quad (317)$$

$$\mathfrak{s}(z_0) = \frac{1}{4\pi\sqrt{3}}(2g(z_0) + (1 - 2z_0)g'(z_0) + z_0(z_0 - 1)g''(z_0)) \quad (318)$$

as a function of the scaled and centered position z_0 normalized to be 0 on the lower boundary and 1 on the upper boundary. The function g is defined in (306). This leads to the result for the mean shape presented in (32), (33) and (34). Since $g(z_0) = g(1 - z_0)$ we see that $\mathfrak{s}(z_0)$ is symmetric around $z_0 = 1/2$. The shape function has the following asymptotics near the edge $z_0 = 0$ and near the central point $z_0 = 1/2$

$$\mathfrak{s}(z_0) = \frac{z_0^3}{21} - \frac{z_0^4}{28} - \frac{3\sqrt{3}\Gamma(\frac{1}{3})^{18}z_0^7}{98560\pi^7} + \frac{3\sqrt{3}\Gamma(\frac{1}{3})^{18}z_0^8}{112640\pi^7} + O(z_0^9) \quad (319)$$

$$= 0.00182091 - 0.0314909(z_0 - \frac{1}{2})^2 + .. \quad (320)$$

We also see that

$$\langle S \rangle_\ell = \ell^4 \int_0^1 dz_0 \mathfrak{s}(z_0) = \frac{\sqrt{3}}{2\pi} \ell^4 \int_0^1 dp g(p) \quad (321)$$

is consistent with (315) since we have $\int_0^1 dz_0 \mathfrak{s}(z_0) = 0.00073657566$. Finally, using (297), (317) and (295) we see that the mean total size at fixed extension and aspect ratio can also be written as

$$\langle S \rangle_{\ell,p} = \frac{\mathfrak{s}(p)}{\tilde{P}(p)} \ell^4 \quad (322)$$

where $\mathfrak{s}(z)$ is the mean shape function (317) and $\tilde{P}(p)$ the PDF of the aspect ratio, given in (262).

VII. AVALANCHES UPON DRIVING BY A POINT ("DRIVING BY THE TIP")

A. Model

The model is a variant of the BFM in one dimension, where the driving is now exerted through a spring tied to a single point $x = 0$, through the driving term $m_0^2 \delta(x)(w(t) - u(x, t))$. It is described by the equations of motion (17) and (18). As the driving function $w(t)$ is increased, avalanches occur, with the special feature here that the seed is always at $x = x_s = 0$: the avalanches always start at $x = 0$ and propagate from there (on both sides of $x = 0$).

We will denote \hat{L}_{m_0} the internal cutoff length associated to m_0 , with $\hat{L}_{m_0} = 1/m_0^2$, not to be confused with $L_m = 1/m$ the internal cutoff length associated to the bulk mass m . We will focus mainly on zero bulk mass, $m^2 = 0$. In some cases we will also consider the case $m^2 > 0$ (which provides a cutoff for the avalanches), in which case we use the units S_m, η_m . For instance \hat{L}_{m_0} is then expressed in units $L_m = 1/m$ (and the natural ratio of length is $\hat{L}_{m_0}/L_m = m/m_0^2$).

We start by calculating the PDF of the local jump at the tip, of the total size, and next we study the avalanche extension and shape.

B. Joint distribution of the local jump at the tip and of the total size

Let us apply a local kick $\dot{w}(t) = w\delta(t)$ at the tip. This leads to an avalanche of total size S and with a local jump $S_0 := S(x = 0)$ at the position of the tip. We first want to calculate the joint PDF, $P_w(S_0, S)$, of S and S_0 . We start from the formula for the Laplace transform. From the general method described in Section III, it is given by

$$\overline{e^{\mu S + \lambda_0 S_0}} = e^{m_0^2 w \tilde{u}(x=0)} \quad (323)$$

where $\tilde{u}(x) = \tilde{u}^{\lambda,\mu}(x)$ is the solution of the following instanton equation:

$$\tilde{u}''(x) - A\tilde{u}(x) - m_0^2\delta(x)\tilde{u}(x) + \tilde{u}(x)^2 = -\mu - \lambda_0\delta(x) \quad (324)$$

where we use $A = 0$ for the massless case and $A = 1$ for the massive case. We can move the delta function term from the l.h.s. to the right hand side, and define a new source parameter λ as

$$\lambda = \lambda_0 - m_0^2\tilde{u}(0) \quad (325)$$

This allows to write the solution of (324) by analogy with (90) as

$$\tilde{u}^{\lambda,\mu}(x) = \frac{A - \beta^2}{2} + \frac{6\beta^2(1 - z^2)e^{-\beta|x|}}{(1 + z + (1 - z)e^{-\beta|x|})^2} \quad , \quad \beta = (A^2 - 4\mu)^{1/4} \quad (326)$$

where, from the discontinuity of the derivative at $x = 0$, z is the solution of

$$\frac{\lambda}{\beta^3} = 3z(1 - z^2) \quad (327)$$

which is continuously connected to $z = 1$ for $\lambda = 0$. Note that $\tilde{u}(x = 0) = \beta^2(1 - \frac{3}{2}z^2) + \frac{A}{2}$.

The joint PDF of S and S_0 is thus given by the inverse Laplace transform

$$P_w(S, S_0) = LT_{-\mu \rightarrow S, -\lambda_0 \rightarrow S_0}^{-1} e^{m_0^2 w \tilde{u}(0)} \quad (328)$$

where $m_0^2\tilde{u}(0)$ as a function of λ_0, μ is determined by eliminating λ and z in the system:

$$\lambda = \lambda_0 - m_0^2\tilde{u}(0) = \lambda_0 - m_0^2\beta^2(1 - \frac{3}{2}z^2) - m_0^2\frac{A}{2} \quad (329)$$

$$\frac{\lambda}{\beta^3} = 3z(1 - z^2) \quad , \quad \beta = (A - 4\mu)^{1/4} \quad (330)$$

It is equivalent, but more convenient to state it as follows

$$P_w(S, S_0) = LT_{-\mu \rightarrow S, -\lambda_0 \rightarrow S_0}^{-1} e^{\lambda_0 w - \lambda w} \quad (331)$$

where λ as a function of λ_0, μ is determined by eliminating z in the system:

$$\lambda = \lambda_0 - m_0^2\beta^2(1 - \frac{3}{2}z^2) - m_0^2\frac{A}{2} \quad (332)$$

$$\lambda = 3\beta^3 z(1 - z^2) \quad , \quad \beta = (A - 4\mu)^{1/4} \quad (333)$$

1. Moments and joint moments

This system can first be studied in presence of a bulk mass, i.e. setting $A = 1$. Since in that case the moments of S, S_0 do exist, one can perform an expansion in powers of λ_0, μ , which is then analytic (and corresponds to an expansion around $\beta = 1$ and $z = 1$). One obtains

$$\langle S_0 \rangle = \frac{m_0^2}{m_0^2 + 2} w \quad , \quad \langle S \rangle = \frac{2m_0^2}{m_0^2 + 2} w \quad , \quad \langle S_0^2 \rangle = \frac{m_0^2 w (3(m_0^2 + 2) m_0^2 w + 4)}{3(m_0^2 + 2)^3} \quad (334)$$

$$\langle S^2 \rangle = \frac{4m_0^2 w (m_0^4(3w + 1) + 6m_0^2(w + 1) + 12)}{3(m_0^2 + 2)^3} \quad , \quad \langle SS_0 \rangle = \frac{2m_0^2 w (3(m_0^2 + 2) m_0^2 w + m_0^2 + 6)}{3(m_0^2 + 2)^3} \quad (335)$$

We note that as $m_0 \rightarrow +\infty$, $\langle S_0^p \rangle \rightarrow w^p$ as $S_0 \rightarrow w$ i.e. it becomes deterministic. In the limit $w \rightarrow 0^+$ the above formulae give the moments over the density $\rho(S, S_0) = \partial_w|_{w=0^+} P_w(S, S_0)$

$$\langle S_0 \rangle_\rho = \frac{m_0^2}{m_0^2 + 2} \quad , \quad \langle S \rangle_\rho = \frac{2m_0^2}{m_0^2 + 2} \quad , \quad \langle S_0^2 \rangle_\rho = \frac{4m_0^2}{3(m_0^2 + 2)^3} \quad , \quad \langle S^2 \rangle_\rho = \frac{4}{3} \left(1 - \frac{8}{(m_0^2 + 2)^3} \right) \quad (336)$$

$$\langle SS_0 \rangle_\rho = \frac{2m_0^2 (m_0^2 + 6)}{3(m_0^2 + 2)^3} \quad (337)$$

2. *Distribution of total size $P_w(S)$: crossover between two limit forms*

Let us first study $P_w(S)$, hence we set $\lambda_0 = 0$ in (331), (332), and consider for simplicity the massless case $A = 0$. Then z is the root of:

$$f(z) := \frac{3z(1-z^2)}{1-\frac{3}{2}z^2} = \frac{-m_0^2}{\beta} \quad , \quad \beta = (-4\mu)^{1/4} \quad (338)$$

Since the function $f(z)$ is strictly increasing from $-\infty$ to $+\infty$ on the interval $]\sqrt{2/3}, +\infty[$ which contains $z = 1$ (with $f(1) = 0$), there is a unique (and physical) solution on this interval $z = f^{-1}(\frac{-m_0^2}{\beta})$. Defining the function $g(v) = 3f^{-1}(-1/v)(1 - (f^{-1}(-1/v))^2)$ one can write

$$P_w(S) = LT_{-\mu \rightarrow S}^{-1} e^{-w(-4\mu)^{3/4}g((-4\mu)^{1/4}/m_0^2)} \quad , \quad g(0) = \sqrt{2/3} \quad , \quad g(v) \simeq_{v \rightarrow +\infty} \frac{1}{2v} \quad (339)$$

which leads to the two limits:

- $m_0^2 \rightarrow 0$, equivalently $S \ll 1/m_0^8$, then

$$P_w(S) = LT_{-\mu \rightarrow S}^{-1} e^{-\frac{w}{2}m_0^2(-4\mu)^{1/2}} = \frac{m_0^2 w e^{-\frac{m_0^4 w^2}{4S}}}{2\sqrt{\pi} S^{3/2}} = \frac{1}{m_0^4 w^2} \mathcal{L}_{1/2}(S/m_0^4 w^2) \quad (340)$$

which is the standard PDF in the case of imposed force driving, i.e. Eq. (6) with $\int dx f(x) = m_0^2 w$ in the present case, taken in the massless limit. The distribution $\mathcal{L}_{1/2}$ is the stable Levy law of index $1/2$, see Appendix B.

- $m_0^2 \rightarrow +\infty$, equivalently $S \gg 1/m_0^8$, then

$$P_w(S) = LT_{-\mu \rightarrow S}^{-1} e^{-w\sqrt{\frac{2}{3}}(-4\mu)^{3/4}} = \frac{3^{2/3}}{(4w)^{4/3}} \mathcal{L}_{3/4}(3^{2/3}S/(4w)^{4/3}) \quad (341)$$

with $\mathcal{L}_{3/4}$ being the stable Levy law of index $3/4$, see Appendix B where its explicit expression is given in terms of hypergeometric functions. It is thus a non trivial (infinitely divisible) distribution, quite different from the standard law Eq. (6) for force imposed driving. The associated density, $\rho(S) = \partial_w|_{w=0+} P_w(S)$ has a simple expression

$$\rho(S) = -\frac{1}{S} LT_{-\mu \rightarrow S}^{-1} \partial_\mu \sqrt{\frac{2}{3}}(-4\mu)^{3/4} = \frac{\sqrt{3}}{\Gamma(1/4)S^{7/4}} \sim S^{-\tau_{\text{loc. driv.}}} \quad \text{with} \quad \tau_{\text{loc. driv.}} = \frac{7}{4} \quad (342)$$

as obtained in¹⁰.

3. *Calculation of the PDF of the local jump $P_w(S_0)$*

We now calculate the PDF, $P_w(S_0)$, of the local jump $S_0 = S(x=0)$ at the position of the tip $x=0$ following a kick w at the tip. We recall that the driving is "by the tip", i.e. through the driving term $\dot{f}(x,t) = m_0^2 \delta(x)(w\delta(t) - \dot{u}(x,t))$. It is thus different from the imposed force driving $\dot{f}(x,t) = f\delta(x-x_s)\delta(t)$ and $P_w(S_0)$ computed here should not be confused with $P_{\{f\delta(x)\}}(S_0)$ calculated there, e.g. for $x_s = 0$ in (104), (105). The two PDF's coincide only in the limit $m_0 \rightarrow 0$ with $f = wm_0^2$ fixed, as discussed below. For simplicity we treat here the massless case $m = 0$, the massive case being detailed in the Appendix J.

To calculate $P_w(S_0)$ we set $\mu = 0$ in (331), (332) (for $A = 0$). It is easy to see that in that limit $\beta \rightarrow 0$, and $z \sim z_0/\beta$ and we have

$$P_w(S_0) = LT_{-\lambda_0 \rightarrow S_0}^{-1} e^{(\lambda_0 + 3z_0^3)w} \quad (343)$$

$$-3z_0^3 - \frac{3}{2}m_0^2 z_0^2 = \lambda_0 \quad (344)$$

Let us write

$$S_0 P_w(S_0) = \int \frac{d\lambda_0}{2i\pi} e^{-\lambda_0 S_0} \partial_{\lambda_0} e^{w(\lambda_0 + 3z_0^3)} \quad (345)$$

We can trade the variable λ_0 for the variable z and write (we work up to a global sign)

$$S_0 P_w(S_0) = \int \frac{dz_0}{2i\pi} e^{(3z_0^3 + \frac{3}{2}m_0^2 z_0^2)S_0} \partial_{z_0} e^{-\frac{3}{2}m_0^2 z_0^2 w} \quad (346)$$

$$= 3wm_0^2 \int \frac{dz_0}{2i\pi} z_0 e^{3z_0^3 S_0 + \frac{3}{2}m_0^2 z_0^2 (S_0 - w)} \quad (347)$$

$$= 3wm_0^2 \partial_c \Phi(a, b, c)|_{a=9S_0, b=\frac{3}{2}m_0^2(S_0 - w), c=0} \quad (348)$$

This leads to the result

$$P_w(S_0) = \frac{1}{3^{1/3} S_0^{5/3}} w m_0^2 e^{\frac{2}{3}y^3} (-y \text{Ai}(y^2) - \text{Ai}'(y^2)) \quad , \quad y = \frac{m_0^2(S_0 - w)}{2 \times 3^{1/3} S_0^{2/3}} \quad (349)$$

We can compare with (104): we see that indeed for $m_0 \rightarrow 0$ at fixed $f = m_0^2 w$ the two formula coincide. However the above result describes the full crossover as m_0 is increased, which we now analyze. First one checks that $\langle S_0 \rangle = w$. Then one can also give the density $\rho(S_0) = \partial_w P_w(S_0)|_{w=0+}$

$$\rho(S_0) = \frac{1}{3^{1/3} S_0^{5/3}} m_0^2 e^{\frac{2}{3}y^3} (-y \text{Ai}(y^2) - \text{Ai}'(y^2)) \quad , \quad y = \frac{m_0^2 S_0^{1/3}}{2 \times 3^{1/3}} \quad (350)$$

which exhibits the single crossover scale $S_0 \sim m_0^{-6}$. This density crosses over from

$$\rho(S_0) \simeq \frac{m_0^2}{3^{2/3} \Gamma(\frac{1}{3}) S_0^{5/3}} \quad , \quad S_0 \ll m_0^{-6} \quad (351)$$

to

$$\rho(S_0) \simeq \sqrt{\frac{3}{2\pi}} \frac{1}{m_0^3 S_0^{5/2}} \quad , \quad S_0 \gg m_0^{-6} \quad (352)$$

One can be a bit more precise: since $P_w(S_0) \rightarrow \delta(S_0 - w)$ in the limit $m_0 \rightarrow \infty$, there are really two regions in the PDF. Using that

$$-y \text{Ai}(y^2) - \text{Ai}'(y^2) \simeq_{y \rightarrow +\infty} \frac{1}{8\sqrt{\pi} y^{5/2}} e^{-\frac{2}{3}y^3} \quad (353)$$

$$-y \text{Ai}(y^2) - \text{Ai}'(y^2) \simeq_{y \rightarrow -\infty} \frac{\sqrt{-y}}{\sqrt{\pi}} e^{\frac{2}{3}y^3} \quad (354)$$

we see that whenever $m_0^2(S_0 - w) \gg S_0^{2/3}$ one has

$$P_w(S_0) \simeq \sqrt{\frac{3}{2\pi}} \frac{w}{m_0^3 (S_0 - w)^{5/2}} \quad (355)$$

while whenever $m_0^2(w - S_0) \gg S_0^{2/3}$ one has

$$P_w(S_0) \simeq \frac{1}{\sqrt{6\pi}} \frac{m_0^3 w \sqrt{w - S_0}}{S_0^2} e^{-\frac{m_0^6 (w - S_0)^3}{18 S_0^2}} \quad (356)$$

While the first regime contains the tail leading to the density (352), the second regime describes the cutoff function at small S_0 . In the limit of large, but not infinite m_0^2 , the fluctuations scale as $S_0 - w \sim m_0^{-2}$ and more precisely if one defines

$$S_0 - w = 2 \times 3^{1/3} w^{2/3} \times \frac{s}{m_0^2} \quad (357)$$

then one sees from (349) that the random variable $s = O(1)$ has a limit probability density $p(s)$ as $m_0 w^{2/3} \rightarrow +\infty$

$$p(s) = 2e^{\frac{2}{3}s^3} (-s \text{Ai}(s^2) - \text{Ai}'(s^2)) \quad (358)$$

and one can check that $\int_{-\infty}^{+\infty} ds p(s) = 1$. This distribution describes the convergence to $P_w(S_0) \rightarrow \delta(S_0 - w)$, with the right and left tail regimes (355) and (356), respectively.

4. Calculation of the joint PDF of the total and local size $P_w(S, S_0)$

It turns out that one can calculate *explicitly* the joint PDF $P_w(S, S_0)$, to which we now turn. We consider simultaneously the massive, $A = 1$, and massless, $A = 0$, cases. From (331), (332) we can write

$$S_0 P_w(S, S_0) = \int \frac{d\mu}{2i\pi} e^{-\mu S} \int \frac{d\lambda_0}{2i\pi} e^{-\lambda_0 S_0} \partial_{\lambda_0} e^{wZ} \quad (359)$$

where $Z = m_0^2 \beta^2 (1 - \frac{3}{2} z^2) + m_0^2 \frac{A}{2}$ and $\lambda_0 - Z = 3\beta^3 z(1 - z^2)$. Next we can trade the variable λ_0 for the variable z and, upon the change $z \rightarrow z/\beta$ and rearranging, we obtain

$$S_0 P_w(S, S_0) = e^{m_0^2 \frac{A}{2}(w-S_0)} \int \frac{d\mu}{2i\pi} e^{-\mu S} \int \frac{dz}{2i\pi} e^{-\beta^2 [S_0(m_0^2+3z) - w m_0^2]} e^{S_0(m_0^2 \frac{3}{2} z^2 + 3z^3)} \partial_z e^{-\frac{3}{2} w m_0^2 z^2} \quad (360)$$

We can now use that

$$LT_{-\mu \rightarrow S}^{-1} e^{-B(\sqrt{A-4\mu}-A)} = \frac{B}{\sqrt{\pi} S^{3/2}} e^{-\frac{B^2}{S} + AB - A \frac{S}{4}} \quad (361)$$

with $\beta^2 = \sqrt{A-4\mu}$. Hence, performing the integration over μ , and the derivation over z , we obtain

$$S_0 P_w(S, S_0) = \frac{3w m_0^2}{\sqrt{\pi} S^{3/2}} e^{A(\frac{m_0^2}{2}(w-S_0) - \frac{S}{4}) - \frac{(S_0-w)^2 m_0^4}{S}} \quad (362)$$

$$\times \int \frac{dz}{2i\pi} [3z^2 S_0 + (S_0 - w) m_0^2 z] e^{-\frac{6S_0(S_0-w)m_0^2}{S} z + (-\frac{9S_0^2}{S} + \frac{3}{2} m_0^2 (S_0-w)) z^2 + 3S_0 z^3} \quad (363)$$

To evaluate this integral we rewrite it using the function $\Phi(a, b, c)$ defined in (97) (also in Appendix A of¹⁰) as

$$S_0 P_w(S, S_0) = \frac{3w m_0^2}{\sqrt{\pi} S^{3/2}} e^{A(\frac{m_0^2}{2}(w-S_0) - \frac{S}{4}) - \frac{(S_0-w)^2 m_0^4}{S}} \quad (364)$$

$$\times [3S_0 \partial_b + (S_0 - w) m_0^2 \partial_c] \Phi(a, b, c) \Big|_{a=9S_0, b=-\frac{9S_0^2}{S} + \frac{3}{2} m_0^2 (S_0-w), c=-\frac{6S_0(S_0-w)m_0^2}{S}}$$

and using again (97) we finally obtain the joint PDF

$$P_w(S, S_0) = B (y \text{Ai}(y^2) - \text{Ai}'(y^2)) \quad , \quad y = \frac{m_0^2 S (S_0 - w) + 6S_0^2}{2\sqrt[3]{3} S S_0^{2/3}} \quad (365)$$

$$B = \frac{2 \cdot 3^{2/3} m_0^2 S_0^{1/3} w}{\sqrt{\pi} S^{5/2}} \exp \left(-\frac{3m_0^2 S_0^2 (S_0 - w)}{S^2} + \frac{m_0^6 (S_0 - w)^3}{36S_0^2} - \frac{m_0^4 (S_0 - w)^2}{2S} - \frac{6S_0^4}{S^3} + \frac{A}{4} (2m_0^2 (w - S_0) - S) \right)$$

We have checked numerically that the moments (334) are recovered in the massive case. We have also checked numerically that integrating (365) over S one recovers $P_w(S_0)$ in (349) in the massless case.

Note that it takes the scaling form

$$P_w(S, S_0; A) = m_0^{14} \tilde{P}_{w m_0^6} (m_0^8 S, m_0^6 S_0; A/m_0^8) \quad (366)$$

where \tilde{P} is obtained from P setting $m_0 = 1$ in formula (365). Hence the characteristic crossover scales are $S \sim m_0^{-8}$, $S_0 \sim w \sim m_0^{-6}$ and one can define the reduced scales $\tilde{S} = m_0^8 S$ and $\tilde{S}_0 = m_0^6 S_0$.

We can now study the joint sizes density $\rho(S, S_0) = \partial_w|_{w=0} P_w(S, S_0)$ which is given by

$$\rho(S, S_0) = B (y \text{Ai}(y^2) - \text{Ai}'(y^2)) \quad , \quad y = S_0^{1/3} \frac{m_0^2 S + 6S_0}{2\sqrt[3]{3} S} \quad (367)$$

$$B = \frac{2 \cdot 3^{2/3} m_0^2 S_0^{1/3} \exp \left(-\frac{3m_0^2 S_0^3}{S^2} + \frac{m_0^8 S_0}{36} - \frac{m_0^4 S_0^2}{2S} - \frac{6S_0^4}{S^3} - A(S_0 \frac{m_0^2}{2} + \frac{S}{4}) \right)}{\sqrt{\pi} S^{5/2}}$$

and obeys the scaling form $\rho(S, S_0; A) = m_0^{20} \tilde{\rho}(m_0^8 S, m_0^6 S_0; A/m_0^8)$, where $\tilde{\rho}$ is obtained from ρ setting $m_0 = 1$ in formula (367).

Remark. In the limit $m_0 \rightarrow +\infty$, in the massless case ($A = 0$) the equations (331), (332) can be solved in an expansion in $1/m_0^2$ as

$$z = \sqrt{\frac{2}{3}} + \frac{1}{m_0^2} \left(\frac{\beta}{3} - \frac{\lambda_0}{\sqrt{6}\beta^2} \right) + \dots \quad (368)$$

$$\lambda_0 - \lambda = \lambda_0 - \sqrt{\frac{2}{3}}\beta^3 + \frac{1}{m_0^2}(\beta^4 - \sqrt{\frac{3}{2}}\beta\lambda_0) + \dots \quad (369)$$

Hence the value at zero of the instanton solution (326), i.e. $\tilde{u}(x=0) = \beta^2(1 - \frac{3}{2}z^2) \simeq (\lambda_0 - \sqrt{\frac{2}{3}}\beta^3)/m_0^2$ vanishes for $m_0^2 \rightarrow +\infty$. So in this limit the instanton equation becomes effectively equivalent to solving $\tilde{u}'(x) + \tilde{u}(x)^2 = -\mu$ with $\tilde{u}(x=0) = 0$, where the derivative discontinuity is free to adjust. This is true because $S_0 = w$ in that limit, hence λ_0 is not needed. Thus it amounts to solve the instanton equation on a half-axis with Dirichlet boundary conditions and one can check that the r.h.s. in $\exp(m_0^2 w \tilde{u}(x=0))$ in (328) remains finite when $m_0^2 \rightarrow +\infty$. It can be obtained from the discontinuity of the solution on the half-axis, i.e. one has $\lim_{m_0 \rightarrow +\infty} m_0^2 w \tilde{u}(x=0) = \tilde{u}'(x=0)$.

C. Distribution of the extension for avalanches driven by the tip: crossover as m_0 is varied

We now ask what is the probability that the avalanche reaches the distance ℓ_2 from the tip, i.e. from the seed at $x = 0$, i.e the driving point (on one side, say $x > 0$). Here we restrict on the case where the bulk mass is zero $m = 0$. The associated CDF is

$$P(\ell_2 < r) = e^{m_0^2 w \tilde{u}_r(x=0)} \quad (370)$$

where $\tilde{u}_r(x)$ is the solution of the instanton equation

$$\tilde{u}''(x) - m_0^2 \delta(x) \tilde{u}(x) + \tilde{u}(x)^2 = 0 \quad , \quad \tilde{u}(r) = -\infty \quad (371)$$

with $\tilde{u}(-\infty) = 0$. This is very similar to the problem studied in Section V, i.e. Eq. (371) (and boundary condition) is identical to (139) with $\lambda = -m_0^2 \tilde{u}(x=0)$ and $x_0 = 0$. We thus know that the solution is (164), i.e.

$$\tilde{u}_r(x) = -\frac{6}{(\rho - x)^2} \theta(-x) - 6\mathcal{P}(r - x, 0, g_3) \theta(x) \quad (372)$$

with the conditions of continuity at $x = 0$ and proper derivative jump are analogous to (165) and (166)

$$\frac{1}{\rho^2} = \mathcal{P}(r, 0, g_3) \quad , \quad -\frac{2}{\rho^3} - \mathcal{P}'(r, 0, g_3) = \frac{m_0^2}{\rho^2} \quad (373)$$

where we have replaced $\lambda/6 = -m_0^2 \tilde{u}(0)/6 = m_0^2/\rho^2$. The equations (373) determine the unknown parameters g_3, ρ as a function of r, m_0 . Using $\mathcal{P}'(z)^2 = 4\mathcal{P}(z)^3 - g_3$ we obtain

$$g_3 = -\frac{m_0^4}{\rho^4} - 4\frac{m_0^2}{\rho^5} \quad (374)$$

so in fact, there is a single unknown parameter ρ . Since $1/m_0^2$ is an (internal) length scale we can (for $m_0 \neq 0, +\infty$) absorb m_0 by defining the dimensionless variables

$$\tilde{r} = r m_0^2 \quad , \quad \tilde{\rho} = \rho m_0^2 \quad (375)$$

The relation between $\tilde{\rho}$ and \tilde{r} can then be written as

$$1 = \mathcal{P}\left(\frac{\tilde{r}}{\tilde{\rho}}, 0, -\tilde{\rho}^2 - 4\tilde{\rho}\right) \quad , \quad \tilde{r} = h(\tilde{\rho}) := \tilde{\rho} \int_1^{+\infty} \frac{dy}{\sqrt{4y^3 + \tilde{\rho}^2 + 4\tilde{\rho}}} = {}_2F_1\left(\frac{1}{6}, \frac{1}{2}; \frac{7}{6}; -\frac{\tilde{\rho}^2 + 4\tilde{\rho}}{4}\right) \tilde{\rho} \quad (376)$$

where we have used the homogeneity property of the Weierstrass function $\mathcal{P}(\lambda z; \lambda^{-4}g_2, \lambda^{-6}g_3) = \lambda^{-2}\mathcal{P}(z; g_2, g_3)$ as well as (A6). From (370), (372) the CDF of ℓ_2 reads

$$P(\ell_2 < r) = e^{-6m_0^2 w/\rho^2} = e^{-6m_0^6 w \phi(\tilde{r})} \quad , \quad \tilde{r} = m_0^2 r \quad (377)$$

The function $\phi(r)$, which is $\phi = 1/\tilde{\rho}^2$ as a function of \tilde{r} can be obtained from (376). At small \tilde{r} , it is easy to invert $\tilde{r} = h(\tilde{\rho})$ as a series at small $\tilde{\rho}, \tilde{r}$ and calculate $\phi(\tilde{r}) = 1/\tilde{\rho}^2$. At large \tilde{r} , it is more convenient to express $1/\tilde{r}^3$ in an expansion in small $\phi = 1/\tilde{\rho}^2$, which starts as $1/\tilde{r}^3 \sim \phi$ and then invert the series to obtain $\phi(r)$. This gives, respectively, the small r (divergence) and large r (vanishing) series expansions

$$\phi(r) = \frac{1}{r^2} - \frac{1}{7r} + \frac{43}{2548} - \frac{555r}{338884} + \frac{75573r^2}{616768880} - \frac{102969r^3}{19119835280} - \frac{474602517r^4}{2446306444734880} + O(r^5) \quad (378)$$

$$\phi(r) = \frac{2\Gamma(\frac{1}{3})^3 \Gamma(\frac{7}{6})^3}{\pi^{3/2}r^3} - \frac{6\Gamma(\frac{1}{3})^3 \Gamma(\frac{7}{6})^3}{\pi^{3/2}r^4} + O\left(\left(\frac{1}{r}\right)^{9/2}\right) \quad (379)$$

We thus obtain the power law decay of the CDF of the upper extension ℓ_2 at large \tilde{r} , i.e. $r \gg 1/m_0^2$, in the original variables

$$P(\ell_2 < r) = 1 - \frac{12w\Gamma(\frac{1}{3})^3 \Gamma(\frac{7}{6})^3}{\pi^{3/2}r^3} + \frac{36w\Gamma(\frac{1}{3})^3 \Gamma(\frac{7}{6})^3}{m_0^2\pi^{3/2}r^4} + O\left(\left(\frac{1}{r}\right)^{9/2}\right) \quad (380)$$

At small $\tilde{r} = m_0^2 r^2 \ll 1$, the CDF has the usual leading order essential singularity $P(\ell_2 < r) \simeq e^{-\frac{6m_0^2 w}{r^2}}$, the same as for the force driving by a kick $f = m_0^2 w$.

From the CDF one obtains the PDF $P(\ell_2) = \partial_r P(\ell_2 < r)|_{r=\ell_2}$. We will give here the density

$$\rho(\ell_2) := \partial_w|_{w=0+} P(\ell_2) = -6m_0^8 \phi'(m_0^2 \ell_2) \quad (381)$$

and we find

$$\rho(\ell_2) \simeq \frac{12m_0^2}{\ell_2^3}, \quad \ell_2 \ll m_0^{-2} \quad (382)$$

$$\rho(\ell_2) \simeq \frac{36\Gamma(\frac{1}{3})^3 \Gamma(\frac{7}{6})^3}{\pi^{3/2}\ell_2^4} = \frac{99.2466..}{\ell_2^4}, \quad \ell_2 \gg m_0^{-2} \quad (383)$$

Thus the density $\rho(\ell_2)$ exhibits a crossover between the "imposed force" result for $\ell_2 \ll m_0^{-2}$, i.e. $\partial_f|_{f=0+} P(\ell_2) = 12/\ell_2^3$ obtained in (137) (the m_0^2 factor comes from the different definition of the density - per unit force versus per unit displacement - there) and a new, "imposed displacement" regime $\ell_2 \gg m_0^{-2}$ with a different $\kappa_{\text{imp.displ.}} = 4$ exponent. Clearly the limit $m_0 \rightarrow +\infty$ is well defined: in that limit only the large ℓ_2 region remains and the density becomes a pure power law given by (383). If a small but non-zero bulk mass is added, an upper cutoff for large $\ell_2 \sim 1/m$ will appear.

For completeness let us indicate that one can equivalently write the CDF and the PDF in the parametric forms

$$P(m_0^2 \ell_2 < \frac{{}_2F_1\left(\frac{1}{6}, \frac{1}{2}; \frac{7}{6}; -\frac{\phi^2+4\phi^{5/2}}{4\phi^3}\right)}{\sqrt{\phi}}) = e^{-6m_0^6 w \phi} \quad (384)$$

$$P(\ell_2 = m_0^{-2} \frac{{}_2F_1\left(\frac{1}{6}, \frac{1}{2}; \frac{7}{6}; -\frac{\phi^2+4\phi^{5/2}}{4\phi^3}\right)}{\sqrt{\phi}}) = 6m_0^8 w \frac{3\phi(1+4\sqrt{\phi})}{1+m_0^2 \ell_2(1+5\sqrt{\phi})} e^{-6m_0^6 w \phi} \quad (385)$$

which allows easy plotting as ϕ is varied on $[0, +\infty[$. Indeed one can show directly from (72) that

$$\frac{d\phi}{dr} = -\frac{3\phi(1+4\sqrt{\phi})}{1+r(1+5\sqrt{\phi})} \quad (386)$$

Note that here we have studied only ℓ_2 , which is how far the avalanche reaches on the side $x > 0$. One can extend the calculation, once again, to the JPDF of ℓ_1 and ℓ_2 . For finite m_0 these are correlated and their JPDF is non-trivial. We now study the limit $m_0 = +\infty$ where simplifications occur.

D. Mean avalanche shape in the limit $m_0 = +\infty$

It turns out that one can solve directly the case $m_0 = +\infty$, where the driving is purely by imposing the displacement of the tip. Indeed from the previous subsection we found $\tilde{u}_r(0) = -6m_0^4 \phi(m_0^2 r)$. Since $\phi(z) \sim 1/z^3$ at large z , we see that $\tilde{u}_r(0) \sim m_0^{-2}$ as $m_0 \rightarrow +\infty$, i.e. the instanton solution vanishes at $x = 0$, however the product $m_0^2 w \tilde{u}(0)$ remains finite (hence the limit of the CDF is well defined).

1. Limit $m_0 = +\infty$ and CDF of ℓ_2

Thus to study the case $m_0 = +\infty$ we can simply look for the solution of the instanton equation with the following boundary conditions (we focus here on the case of no bulk mass, $m = 0$)

$$\tilde{u}''(x) + \tilde{u}(x)^2 = 0 \quad , \quad \tilde{u}(r) = -\infty \quad , \quad \tilde{u}(0) = 0 \quad (387)$$

on the interval $[0, r]$. The solution is

$$\tilde{u}(x) = \tilde{u}_r(x) := -6\mathcal{P}(r-x, 0, g_3) \quad (388)$$

and the additional condition which determines g_3 as a function of r

$$\mathcal{P}(r, 0, g_3) = 0 \quad \Leftrightarrow \quad \mathcal{P}(1, 0, r^6 g_3) = 0 \quad (389)$$

Let us now introduce the root ($g_3 < 0$) to the equation

$$\mathcal{P}(1, 0, g_3) = 0 \quad , \quad \int_0^{+\infty} \frac{dy}{\sqrt{4y^3 - g_3}} = 1 \quad (390)$$

Using the identity, valid for any g_3

$$\int_0^{+\infty} \frac{dy}{\sqrt{4y^3 + |g_3|}} = \frac{2^{1/3} \Gamma(\frac{1}{3}) \Gamma(\frac{7}{6})}{\sqrt{\pi} |g_3|^{1/6}} \quad (391)$$

the root of (390) is found to be

$$g_3^* = -\frac{256\pi^3 \Gamma(\frac{1}{3})^6}{\Gamma(-\frac{1}{6})^6} = -\frac{4\Gamma(\frac{1}{3})^6 \Gamma(\frac{7}{6})^6}{\pi^3} = -30.40090507702060 \quad (392)$$

as can also be inferred from e.g.²⁹. Hence g_3 determined by (389) is simply $g_3 = g_3^*/r^6$ and we finally obtain the solution of (387) as

$$\tilde{u}_r(x) = -6\mathcal{P}(r-x, 0, g_3^*/r^6) = -\frac{6}{r^2} \mathcal{P}_*(1 - \frac{x}{r}) \quad (393)$$

where from now on we define

$$\mathcal{P}_*(z) = \mathcal{P}(z, 0, g_3^*) \quad (394)$$

Which formula should now be used to obtain, e.g. the CDF of ℓ_2 . A priori one should use (370) in the limit $m_0 \rightarrow +\infty$. One would like to avoid this step to work directly at infinite m_0 . One then notes that (see Remark in the previous subsection)

$$\lim_{m_0 \rightarrow +\infty} m_0^2 \tilde{u}(x=0) = \tilde{u}'_r(x=0) \quad (395)$$

from the instanton equation (371), using that the discontinuity of the derivative $\tilde{u}'_r(x=0^+) - \tilde{u}'_r(x=0^-) = m_0^2 \tilde{u}(x=0)$, and that on the $x < 0$ side $\lim_{m_0 \rightarrow +\infty} \tilde{u}(x) = 0$ (see below for a more detailed derivation). Hence in the limit $m_0 \rightarrow +\infty$ the CDF is given by

$$P(\ell_2 < r) = e^{w \tilde{u}'_r(0)} \quad (396)$$

where here $\tilde{u}'_r(0) = \tilde{u}'_r(0^+)$. This derivative can be evaluated explicitly from (393) using that the Weierstrass function satisfies $\mathcal{P}'^2 = 4\mathcal{P}^3 - g_2\mathcal{P} - g_3$, hence $\mathcal{P}'_*(1) = -(-g_3^*)^{1/2}$ and then

$$\tilde{u}'_r(0) = \frac{6}{r^3} \mathcal{P}'_*(1) = -\frac{12}{r^3} \frac{\Gamma(\frac{1}{3})^3 \Gamma(\frac{7}{6})^3}{\pi^{3/2}} \quad (397)$$

Thus we find

$$P(\ell_2 < r) = e^{-\frac{12w}{r^3} \frac{\Gamma(\frac{1}{3})^3 \Gamma(\frac{7}{6})^3}{\pi^{3/2}}} \quad (398)$$

and

$$\rho(\ell_2) = \frac{18\sqrt{-g_3^*}}{\ell_2^4} = \frac{36}{\ell_2^4} \frac{\Gamma(\frac{1}{3})^3 \Gamma(\frac{7}{6})^3}{\pi^{3/2}} \quad (399)$$

which is exactly the result (383), thus validating the present approach.

Let us add some precisions about the $m_0 = +\infty$ limit. Consider the problem with two boundaries and denote $\tilde{u}_{r_1, r_2}^{m_0}(x)$ the solution of the instanton equation (371) which tends to $-\infty$ for $x = r_1, r_2$ (with $r_1 < 0 < r_2$). The solution studied in the previous subsection is thus $\tilde{u}_{r_1 = -\infty, r_2}^{m_0}(x)$. We surmise that in the limit $m_0 = +\infty$

$$\lim_{m_0 \rightarrow +\infty} \tilde{u}_{r_1, r_2}^{m_0}(x) = \tilde{u}_{r_2}^\infty(x)\theta(x) + \tilde{u}_{r_1}^\infty(x)\theta(-x) \quad (400)$$

where $\tilde{u}_{r > 0}^\infty(x)$ is the solution of (387), and $\tilde{u}_{r < 0}^\infty(x)$ is the solution of the same equation but defined on the negative $x < 0$ half-axis. In particular $\tilde{u}_{r_1}^\infty(0^-) = \tilde{u}_{r_2}^\infty(0^+) = 0$. Now from the condition of derivative discontinuity arising from (371) one has, in the limit

$$\lim_{m_0 \rightarrow +\infty} m_0^2 \tilde{u}_{r_1, r_2}^{m_0}(x) = \tilde{u}_{r_2}^{\infty'}(0^+) - \tilde{u}_{r_1}^{\infty'}(0^-) \quad (401)$$

Thus we have (using $x \rightarrow -x$ symmetry)

$$P(\ell_1 < -r_1, \ell_2 < r_2) = e^{w\tilde{u}_{r_2}^{\infty'}(0^+)} e^{-w\tilde{u}_{r_1}^{\infty'}(0^-)} = e^{w\tilde{u}_{r_2}^{\infty'}(0^+)} e^{w\tilde{u}_{-r_1}^{\infty'}(0^+)} = P(\ell_1 < -r_1)P(\ell_2 < r_2) \quad (402)$$

which is perfectly consistent that in this limit the two "half-space" completely decouple. The total avalanche extension $\ell = \ell_1 + \ell_2$ is just the sum of two independent random variables. In the previous section, we studied $r_1 = -\infty$ which leads to the vanishing solution $\tilde{u}_{r_1}^{\infty'}(0^-) = 0$. That justifies (396).

2. The shape

We now study the mean avalanche shape directly in the limit $m_0 = +\infty$. We focus once again on the half-space $x \geq 0$. We must now study the following instanton equation.

$$\tilde{u}''(x) + \tilde{u}(x)^2 = -\lambda\delta(x - x_0) \quad , \quad \tilde{u}(r) = -\infty \quad , \quad \tilde{u}(0) = 0 \quad (403)$$

on the interval $[0, r]$. We can call $\tilde{u}(x) = u_r^\lambda(x)$ the solution. We can use again (401) which extends in presence of the source. Since the source acts only for $x > 0$ the instanton solution again vanishes for $x < 0$. Using Appendix E one has

$$\langle e^{\lambda S(x_0)} \rangle_{\ell_2 < r} = e^{w(u_r^{\lambda'}(0) - u_r^0(0))} \quad (404)$$

Hence we need to calculate the derivative $u_r^{\lambda'}(0)$. The solution of (436) is now

$$\tilde{u}_r^\lambda(x) = -\frac{6}{\rho^2} \mathcal{P}\left(1 - \frac{x}{\rho}, 0, g_3^*\right) \quad , \quad 0 < x < x_0 \quad (405)$$

$$\tilde{u}_r^\lambda(x) = -\frac{6}{r^2} \mathcal{P}\left(1 - \frac{x}{r}, 0, g_3\right) \quad , \quad x_0 < x < r \quad (406)$$

note that it vanishes at $x = 0$ and diverges at $x = r$ as required. The matching conditions which determine the unknown parameters ρ and g_3 as a function of r, x_0, λ

$$\frac{1}{\rho^2} \mathcal{P}\left(1 - \frac{x_0}{\rho}, 0, g_3^*\right) = \frac{1}{r^2} \mathcal{P}\left(1 - \frac{x_0}{r}, 0, g_3\right) \quad (407)$$

$$\frac{6}{r^3} \mathcal{P}'\left(1 - \frac{x_0}{r}, 0, g_3\right) - \frac{6}{\rho^3} \mathcal{P}'\left(1 - \frac{x_0}{\rho}, 0, g_3^*\right) + \lambda = 0 \quad (408)$$

For $\lambda = 0$ the solution is $\rho = r$ and $g_3 = g_3^*$ and one recovers the solution of the previous section. We now expand

$$g_3 = g_3^* + g_3^{(1)}\lambda + g_3^{(2)}\lambda^2 + O(\lambda^3) \quad (409)$$

$$\rho = r + r^{(1)}\lambda + r^{(2)}\lambda^2 + O(\lambda^3) \quad (410)$$

and solve the consistency equations (407) order by order in λ . Then we insert the result in the quantity that we need to calculate

$$\tilde{u}_r^{\lambda'}(0) = \frac{6}{\rho^3} \mathcal{P}'_*(1) = -\frac{6}{\rho^3} (-g_3^*)^{1/2} = -\frac{A}{\rho^3} \quad , \quad A = 6(-g_3^*)^{1/2} = 12 \frac{\Gamma(\frac{1}{3})^3 \Gamma(\frac{7}{6})^3}{\pi^{3/2}} \quad (411)$$

The explicit calculation sketched above leads to

$$\partial_\lambda|_{\lambda=0} \tilde{u}^{\lambda'}(0) = \frac{A}{6g_3^*} (2\mathcal{P}_*(y_0) + y_0 \mathcal{P}'_*(y_0)) \quad , \quad y_0 = 1 - z_0 = 1 - \frac{x_0}{r} \quad (412)$$

where we used the identity $\mathcal{P}_*'^2 = 4\mathcal{P}_*^3 - g_3^*$. From this we obtain the cumulative conditional mean shape as

$$\langle S(x_0) \rangle_{\ell_2 < r} = w \partial_\lambda|_{\lambda=0} u_r^{\lambda'}(0) = w f(y_0 = 1 - \frac{x_0}{r}) \quad (413)$$

$$f(y_0) = \frac{-1}{(-g_3^*)^{1/2}} (2\mathcal{P}_*(y_0) + y_0 \mathcal{P}'_*(y_0)) \quad , \quad g_3^* = -\frac{4\Gamma(\frac{1}{3})^6 \Gamma(\frac{7}{6})^6}{\pi^3} \quad (414)$$

$$= \frac{3}{14} |g_3^*|^{1/2} y_0^4 - \frac{3}{2548} |g_3^*|^{3/2} y_0^{10} + O(y_0^{16}) \quad (415)$$

where in the last line we show the behavior at small y_0 . We recall that \mathcal{P}_* is given by (394). We note that the scaling function f satisfies

$$\int_0^1 dy_0 f(y_0) = \frac{1}{|g_3^*|^{1/2}} \zeta(1; 0, g_3^*) = 0.219308.. \quad (416)$$

The mean shape at fixed extension is then, e.g. from Appendix E see (E6),

$$\langle S(x_0) \rangle_{\ell_2} = w f(y_0) + \frac{1}{\ell_2 \rho(\ell_2)} (1 - y_0) f'(y_0) \quad , \quad y_0 = 1 - \frac{x_0}{\ell_2} \quad (417)$$

In the limit of small w we can neglect the first term and using the density $\rho(\ell_2) = 18|g_3^*|^{1/2}/\ell_2^4$ from (399) we obtain the mean shape at fixed extension ℓ_2 in the limit $w = 0^+$

$$\langle S(x_0) \rangle_{\ell_2} = \ell_2^3 s(y_0) \quad , \quad y_0 = 1 - \frac{x_0}{\ell_2} \quad (418)$$

$$s(y_0) = -\frac{1}{6|g_3^*|} (1 - y_0) (2y_0 \mathcal{P}_*(y_0)^2 + \mathcal{P}'_*(y_0)) \quad (419)$$

where g_3^* is given in (392) and \mathcal{P}_* in (394). The scaling function $s(y_0)$ is plotted in Fig. 5. We find that the shape vanishes at $y_0 = 0$, i.e. $x_0 = \ell_2$ and at $y_0 = 1$, i.e. $x_0 = 0$. The latter is a consequence of the exact result that $S(x=0) = w$ (it can be checked on the exact formula (417)), from the imposed displacement driving at $m_0 = +\infty$. We find that the shape vanishes near the avalanche edge at $x = r$ as

$$s(y_0) = \frac{y_0^3}{21} - \frac{y_0^4}{21} - \frac{5y_0^9 \left(\Gamma(\frac{1}{3})^6 \Gamma(\frac{7}{6})^6 \right)}{1911\pi^3} + \frac{5y_0^{10} \Gamma(\frac{1}{3})^6 \Gamma(\frac{7}{6})^6}{1911\pi^3} + O(y_0^{15}) \quad (420)$$

We note that the leading term $\langle S(x_0) \rangle_{\ell_2} \simeq \frac{1}{21} (\ell_2 - x_0)^3$ is the same as the one in (148) and in (319), hinting a universal behavior near the edge (since the present tip driven avalanches are quite different from the standard ones studied in previous sections).

The behavior near the driving tip $x = 0$ is linear (cusp)

$$s(y_0) = \frac{z_0}{6\sqrt{|g_3^*|}} - \frac{z_0^3}{3} + \frac{2z_0^4}{3} - \frac{1}{3} \sqrt{|g_3^*|} z_0^6 + \frac{1}{2} \sqrt{|g_3^*|} z_0^7 - \frac{5|g_3^*| z_0^9}{28} + \frac{5|g_3^*| z_0^{10}}{21} + O(z_0^{11}) \quad , \quad z_0 = 1 - y_0 = \frac{x}{\ell_2} \quad (421)$$

From the mean shape at fixed extension ℓ_2 we can extract the first conditional moment of the total size S of the avalanche. From (417) and (419) we see that (using also (416))

$$\int_0^1 dy_0 s(y_0) = \frac{1}{18|g_3^*|^{1/2}} \int_0^1 dy_0 f(y_0) = \frac{-\zeta(1; 0, g_3^*)}{18g_3^*} \quad (422)$$

which implies the first moment

$$\langle S \rangle_{\ell_2} = \int_0^{\ell_2} dx_0 \langle S(x_0) \rangle_{\ell_2} = \ell_2^4 \frac{-\zeta(1; 0, g_3^*)}{18g_3^*} = 0.0022097287584 \ell_2^4 \quad (423)$$

3. The second shape

We now calculate the second shape, i.e. $\langle S(x_0)^2 \rangle_{\ell_2}$. For this purpose we need to expand to next order in λ the equations (411) and insert in $\tilde{u}_r^{\lambda'}(0) = -\frac{A}{\rho^3}$ from (407). Using (404) we obtain first the cumulative second shape

$$\langle S(x_0)^2 \rangle_{\ell_2 < r} = w \partial_\lambda^2 |_{\lambda=0} u_r^{\lambda'}(0) + O(w^2) = w r^3 f_2(y_0 = 1 - \frac{x_0}{r}) + O(w^2) \quad (424)$$

with

$$f_2(y_0) = \frac{1}{9(-g_3^*)^{3/2}} \left(g_3^* (y_0 - 1) y_0 \right. \quad (425)$$

$$\left. + \mathcal{P}_*(y_0) \left((1 - 2(y_0 - 1)(3y_0^2 \mathcal{P}_*(y_0) - 1)) \mathcal{P}'_*(y_0) + 2\mathcal{P}_*(y_0) \left((5 - 8y_0) y_0 \mathcal{P}_*(y_0) + 4 \right) \right) \right) \quad (426)$$

From Appendix E, see (E3), we have

$$\langle e^{\lambda S(x_0)} \rangle_{\ell_2} = \frac{\partial_r u_r^{\lambda'}(0)}{\partial_r u_r^{0'}(0)} e^{w(u_r^{\lambda'}(0) - u_r^{0'}(0))} |_{r=\ell_2} \simeq_{w \rightarrow 0^+} \frac{1}{\rho(\ell_2)} \partial_r u_r^{\lambda'}(0) |_{r=\ell_2} \quad (427)$$

Hence we have $\langle S(x_0)^2 \rangle_{\ell_2} = \frac{1}{\rho(\ell_2)} \partial_r \partial_\lambda^2 |_{\lambda=0} u_r^{\lambda'}(0) |_{r=\ell_2}$. This leads to the second shape for $w \rightarrow 0^+$ as

$$\langle S(x_0)^2 \rangle_{\ell_2} = \ell_2^6 \mathfrak{s}_2(y_0) \quad , \quad y_0 = 1 - \frac{x_0}{\ell_2} \quad (428)$$

$$\mathfrak{s}_2(y_0) = \frac{1}{54|g_3^*|^2} \left(-|g_3^*| (y_0 - 1) y_0 + \mathcal{P}_*(y_0) \left(4|g_3^*| (y_0 - 1)^2 y_0^2 \right. \right. \quad (429)$$

$$\left. \left. + (2(y_0 - 1)(8y_0 - 7) y_0 \mathcal{P}_*(y_0) - 4y_0 + 5) \mathcal{P}'_*(y_0) + 2\mathcal{P}_*(y_0) (y_0 \mathcal{P}_*(y_0) (14y_0 (y_0 - 1)^2 \mathcal{P}_*(y_0) - 6y_0 + 3) + 4) \right) \right)$$

where the scaling function is now obtained as $\mathfrak{s}_2(y_0) = \frac{1}{\rho(\ell_2)} (3f_2(y_0) + (1 - y_0)f_2'(y_0))$. It is plotted in Fig. 5. The behavior near the edge is

$$\mathfrak{s}_2(y_0) = \frac{y_0^6}{273} - \frac{38y_0^7}{5733} + \frac{5y_0^8}{1764} - \frac{|g_3^*| y_0^{12}}{5586} + \frac{155|g_3^*| y_0^{13}}{435708} - \frac{55|g_3^*| y_0^{14}}{321048} + O(y_0^{15}) \quad (430)$$

and near the tip

$$\mathfrak{s}_2(y_0) = \frac{z_0^2}{18|g_3^*|} - \frac{7z_0^4}{36\sqrt{|g_3^*|}} + \frac{z_0^5}{9\sqrt{|g_3^*|}} + \frac{z_0^6}{2} + O(z_0^7) \quad , \quad z_0 = 1 - y_0 = \frac{x}{\ell_2} \quad (431)$$

We note that the ratio

$$\frac{\langle S(x_0)^2 \rangle_{\ell_2}}{\langle S(x_0) \rangle_{\ell_2}^2} = \frac{\mathfrak{s}_2(y_0)}{\mathfrak{s}_1(y_0)^2} \quad (432)$$

plotted in Fig. 6, varies between $\frac{21}{13} = 1.61538$ for x near ℓ_2 , and 2 for x near the tip $x = 0$.

Remark. We notice that the leading behavior for the second moment near the edge is

$$\langle S(x_0)^2 \rangle_{\ell_2} \simeq \frac{1}{273} (\ell_2 - x_0)^6 \quad (433)$$

This is exactly the same behavior as found in (189) with the same amplitude. This is not fortuitous. Indeed one can show that for the present tip driven avalanches one also has $S(x_0) \simeq (\ell_2 - x_0)^3 \sigma$ where the random variable σ has the same PDF as in (187), which thus appears to be universal (at least within the BBM with short-range elasticity). To see that, compare Eqs. (407) with Eqs. (165), (166). It is easy to see that in both systems of equations, $\rho - x_0$ and $r - x_0$ vanish similarly, and under the ansatz (182), the two systems become asymptotically equivalent. Indeed in both cases the scaling regime is such that λ hence g_3 are very large. On the l.h.s of the first equation in (407) g_3^* is fixed so as $\rho - x_0 \rightarrow 0$ the l.h.s. becomes identical to the l.h.s in (165). The r.h.s can also be made to coincide using the homogeneity property of the Weierstrass function and changing $g_3 \rightarrow g_3/r^6$. Similarly the second equation

in (407) becomes identical to the one in (166) by the same manipulation. Since g_3 is eliminated between the two equations its rescaling is immaterial. The two systems are then equivalent. One has

$$\langle e^{\lambda S(x_0)} \rangle_{\ell_2=r} = \frac{\partial_r u_r^\lambda(0)}{\partial_r u_r^0(0)} = \frac{\partial_r \rho^{-2}}{\partial_r r^{-2}} \simeq \partial_r \rho \quad (434)$$

$$\langle e^{\lambda S(x_0)} \rangle_{\ell_2} = \frac{\partial_r u_r^{\lambda'}(0)}{\partial_r u_r^{0'}(0)} = \frac{\partial_r \rho^{-3}}{\partial_r r^{-3}} \simeq \partial_r \rho \quad (435)$$

since $\rho \simeq r$ when $x_0 \rightarrow r$. Hence the generating functions are identical in this regime, and the PDF's of the random variable σ are identical.

4. Direct calculation of the conditional moments of the total avalanche size

We can also calculate the conditional moments of the total avalanche size S . We need to solve now

$$\tilde{u}''(x) + \tilde{u}(x)^2 = -\mu\theta(x) \quad , \quad \tilde{u}(r) = -\infty \quad , \quad \tilde{u}(0) = 0 \quad (436)$$

on the interval $[0, r]$. We can call $\tilde{u}(x) = u_r^\mu(x)$ the solution. The solution reads

$$\tilde{u}_r^\mu(x) = -\frac{6}{r^2} \mathcal{P}\left(\frac{r-x}{r}; g_2 = -\frac{1}{3}\mu r^4, g_3(\mu)\right) \quad (437)$$

where $g_3(\mu)$ is such that, where in the second equation we use (A6)

$$\mathcal{P}(1; g_2 = -\frac{1}{3}\mu r^4, g_3(\mu)) = 0 \quad \Leftrightarrow \quad \int_0^{+\infty} \frac{dy}{\sqrt{4y^3 + \frac{1}{3}\mu r^4 y - g_3(\mu)}} = 1 \quad (438)$$

with $g_3(0) = g_3^*$. Using mathematica and $\mathcal{P}_*(1) = 0$, $\mathcal{P}'(1) = -(-g_3^*)^{1/2}$ one easily finds

$$g_3(\mu) = -|g_3^*| + \frac{1}{3}\mu r^4 X - \frac{\mu^2 r^8 (\sqrt{|g_3^*|} - 2X^2)}{72|g_3^*|} + \frac{7\mu^3 r^{12} (-9\sqrt{|g_3^*|}X + |g_3^*| + 16X^3)}{11664|g_3^*|^2} + O(\mu^4), \quad X = \zeta(1; 0, g_3^*) \quad (439)$$

We aim to calculate

$$\tilde{u}_r^{\mu\mu}(0) = \frac{6}{r^3} \mathcal{P}'(1, g_2 = -\frac{1}{3}\mu r^4, g_3(\mu)) \quad (440)$$

$$= -\frac{6\sqrt{|g_3^*|}}{r^3} + \frac{\mu r X}{\sqrt{|g_3^*|}} - \frac{\mu^2 (r^5 (\sqrt{|g_3^*|} - 4X^2))}{24|g_3^*|^{3/2}} + \frac{\mu^3 r^9 (-90\sqrt{|g_3^*|}X + 7|g_3^*| + 220X^3)}{3888|g_3^*|^{5/2}} + O(\mu^4) \quad (441)$$

from which we obtain the conditional generating functions, see Appendix E

$$\langle e^{\mu S} \rangle_{\ell_2 < r} = e^{w(u_r^{\mu\mu}(0) - u_r^{0\mu}(0))} = 1 + w(u_r^{\mu\mu}(0) - u_r^{0\mu}(0)) + O(w^2) \quad , \quad \langle e^{\mu S} \rangle_{\ell_2} |_{w=0^+} = \frac{1}{\rho(\ell_2)} \partial_r u_r^{\mu\mu}(0) |_{r=\ell_2} \quad (442)$$

where $\rho(\ell_2)$ is given in (399). This leads to the lowest moments

$$\{ \langle S \rangle_{\ell_2 < r}, \langle S^2 \rangle_{\ell_2 < r}, \langle S^3 \rangle_{\ell_2 < r} \} = w \left\{ \frac{rX}{\sqrt{|g_3^*|}}, -\frac{r^5 (\sqrt{|g_3^*|} - 4X^2)}{12|g_3^*|^{3/2}}, \frac{r^9 (-90\sqrt{|g_3^*|}X + 7|g_3^*| + 220X^3)}{648|g_3^*|^{5/2}} \right\} \quad (443)$$

$$= w \{ 0.2193081289r, 0.0001665224164r^5, 5.244855047 * 10^{-7} r^9 \} + O(w^2) \quad (444)$$

as well as

$$\begin{aligned} \{ \langle S \rangle_{\ell_2}, \langle S^2 \rangle_{\ell_2}, \langle S^3 \rangle_{\ell_2} \} |_{w=0^+} &= \left\{ \frac{\ell_2^4 X}{18|g_3^*|}, -\frac{5\ell_2^8 (\sqrt{|g_3^*|} - 4X^2)}{216|g_3^*|^2}, \frac{\ell_2^{12} (-90\sqrt{|g_3^*|}X + 7|g_3^*| + 220X^3)}{1296|g_3^*|^3} \right\} \\ &= \{ 0.002209728758\ell_2^4, 8.389323605 \times 10^{-6} \ell_2^8, 4.756201414 \times 10^{-8} \ell_2^{12} \} \end{aligned} \quad (445)$$

We see that the result for the first conditional moment $\langle S \rangle_{\ell_2}$ is in agreement with the formula (423) obtained there by integrating the mean shape over x_0 .

VIII. AVALANCHES IN THE BFM IN HIGHER DIMENSION $d > 1$

We now study the BFM in space dimension $d > 1$, as defined by the equations of motion (1) and (3).

A. Probability that an avalanche does not contain the neighborhood of a given point

One can ask about the PDF of the local size $S_0 = S(x=0)$ in dimension d , and in particular about the probability that an avalanche does not reach the point $x = 0$, i.e. that $S_0 = 0$. We focus on the massless case. To this aim one must solve the instanton equation with the source $\lambda(x) = \lambda\delta^d(x)$

$$\nabla_x^2 \tilde{u} + \tilde{u}^2 = -\lambda\delta^d(x) \quad (446)$$

where ∇_x^2 is the d -dimensional Laplacian. By contrast with $d = 1$, there is no explicit solution for arbitrary λ . Furthermore, although (446) remains well defined in perturbation theory in λ , and can be solved iteratively as such (leading to finite moments of S_0 upon adding a mass) in $d \geq 2$ there are some UV problems with the delta source, especially if one wants to study the limit $\lambda \rightarrow -\infty$. It is safer to consider a smoothed out source, e.g. $\lambda(x) = \lambda a^{-d}\theta(a - |x|)$. One can then take $\lambda \rightarrow -\infty$ and obtain the probability that the avalanche does not enter a ball of radius a (a problem studied below). On the sphere $|x| = a$ one has $\tilde{u}(|x| = a) = -\infty$. Taking then $a \rightarrow 0^+$ the problem converges to the instanton equation

$$\nabla_x^2 \tilde{u} + \tilde{u}^2 = 0 \quad , \quad \tilde{u}(0) = -\infty \quad (447)$$

which thus describes the probability that the avalanche does not reach an infinitesimal ball $a = 0^+$ around $x = 0$.

It turns out that there is a very simple solution to (447). Indeed, looking for a rotationally invariant solution, we rewrite it in radial coordinates $r = |x|$

$$\frac{d^2}{dr^2} \tilde{u} + \frac{d-1}{r} \frac{d}{dr} \tilde{u} + \tilde{u}^2 = 0 \quad (448)$$

and a solution to this equation, valid in any $d < 4$, is

$$\tilde{u}(x) = -\frac{2(4-d)}{x^2} \quad (449)$$

Using this solution we can thus obtain the probability that an avalanche following a kick at x_s , i.e. with driving $\dot{f}(x, t) = f\delta(t)\delta^d(x - x_s)$, does not contain the point x_0 (more precisely, a small ball around it, see discussion above)

$$\text{Prob}(S(x_0) = 0) = \text{Prob}(x_0 \notin \Omega) = e^{-f \frac{2(4-d)}{(x_0 - x_s)^2}} \quad (450)$$

where Ω is the support of the avalanche. Although this is interesting exact result in any d , it does not give so much information about how far the avalanche reaches, since for $d > 1$ the boundary of the avalanche can be quite complicated, fractal and a priori not simply connected (i.e. the avalanche could exhibit "holes"). However the derivative

$$dx_0 \cdot \nabla_{x_0} \text{Prob}(S(x_0) = 0) \quad (451)$$

says something about the probability that the boundary of the avalanche crosses the interval $[x_0, x_0 + dx_0]$ at least once, and possibly more (an odd number of times). Again it decays as $1/|x_0 - x_s|^3$ as in $d = 1$.

B. Probability distribution of $\Sigma = \int d^d x \frac{S(x)}{(x - x_0)^4}$ conditioned to $S(x_0) = 0$

Another exact result can be obtained for the following observable

$$\Sigma := \int d^d x \frac{S(x)}{(x - x_0)^4} \quad (452)$$

conditioned to $S(x_0) = 0$. It is associated to the following instanton equation with a source

$$\nabla_x^2 \tilde{u} + \tilde{u}^2 = -\frac{\mu}{(x - x_0)^4} \quad , \quad \tilde{u}(x_0) = -\infty \quad (453)$$

which has the simple solution

$$\tilde{u}(x) = -\frac{4-d+\sqrt{(4-d)^2-\mu}}{(x-x_0)^2} \quad (454)$$

For $\mu = 0$ it reduces to the previous calculation. Hence the LT of the joint PDF that $S(x_0) = 0$ and Σ following a kick at x_s , reads

$$\int d\Sigma e^{\mu\Sigma} P(S(x_0) = 0, \Sigma) = e^{-f \frac{4-d+\sqrt{(4-d)^2-\mu}}{(x_s-x_0)^2}} \quad (455)$$

From which we obtain the PDF of Σ *conditioned to* $S(x_0) = 0$ as

$$P(\Sigma|S(x_0) = 0) = LT_{-\mu \rightarrow \Sigma}^{-1} e^{f \frac{4-d+\sqrt{(4-d)^2-\mu}}{(x_s-x_0)^2}} = \frac{f}{2\sqrt{\pi}\Sigma^{3/2}(x_s-x_0)^2} e^{-\frac{(2(4-d)\Sigma - \frac{f}{(x_s-x_0)^2})^2}{4\Sigma}} \quad (456)$$

Note that conditioning to $S(x_0) = 0$ is necessary for Σ to be finite (which it is since its LT is analytic near $\mu = 0$).

Let us analyze this result. The first moment of Σ equals

$$\langle \Sigma \rangle_{S(x_0)=0} = \int d^d x \frac{\langle S(x) \rangle_{S(x_0)=0}}{(x-x_0)^4} = \frac{1}{2(4-d)} \frac{f}{(x_s-x_0)^2} \quad (457)$$

First note that Σ is dimensionless (and so is the combination $\frac{f}{(x_s-x_0)^2}$). Second, (457) is a non-trivial sum rule for the mean shape $\langle S(x) \rangle_{S(x_0)=0}$ around the point x_0 (such that $S(x_0) = 0$). The analog in $d = 1$ is (144), which we reproduce here in the (different) notations of the present section (and using r rather than x_0)

$$\langle S(x) \rangle_{S(r)=0} = \langle S(x) \rangle_{\ell_2 < r} = \frac{f}{7} \left(\frac{(r-x)^4}{(r-x_s)^3} \theta(x_s < x < r) + \frac{(r-x_s)^4}{(r-x)^3} \theta(x < x_s) \right) \quad (458)$$

and $\langle S(x) \rangle_{S(r)=0}$ vanishes for $x > r$ (a specificity of $d = 1$). One can check from this formula that indeed $\int_{-\infty}^{+\infty} \langle S(x) \rangle_{S(r)=0} = \frac{1}{6} \frac{f}{(r-x_s)^2}$, as predicted by (457). The mean shape $\langle S(x) \rangle_{S(x_0)=0}$ in higher dimension is studied in the next Section.

Let us analyze the main features of the PDF of Σ in (456). For large driving, i.e. large $\frac{f}{(x_s-x_0)^2} \gg 1$, the random variable Σ equals its average $\Sigma \simeq \langle \Sigma \rangle_{S(x_0)=0}$ up to $O(\langle \Sigma \rangle_{S(x_0)=0}^{1/2})$ Gaussian fluctuations. The PDF of Σ in (456) has some similarities with the PDF of the total size $S = \int d^d x S(x)$, given in (6). Indeed it exhibits the same 3/2 exponent $P(\Sigma|S(x_0) = 0) \sim \Sigma^{-3/2}$. This exponent is visible at small driving $\frac{f}{(x_s-x_0)^2} \ll 1$ over a large range of values of $\Sigma_0 \ll \Sigma \ll 1$, with

(i) a cutoff at small $\Sigma \ll 1$ given by $\Sigma_0 \sim \frac{f^2}{(x_s-x_0)^4} \ll 1$. Presumably this corresponds to small avalanches localized near the seed x_s with $\Sigma \simeq \frac{S}{(x_s-x_0)^4}$ with $S \sim S_0 \sim f^2$.

(ii) at larger Σ the term $\sim e^{-(4-d)^2 \Sigma}$ in (456) cuts Σ at values of $O(1)$.

Hence we see that although there is no mass here to cut the large avalanches, the conditioning on $S(x_0) = 0$ appears to be sufficient to cut the PDF of Σ at large Σ and make the moments finite, e.g. the second moment is

$$\langle \Sigma^2 \rangle_{S(x_0)=0} \simeq \frac{1}{4(4-d)^3} \frac{f}{(x_s-x_0)^2} \left(1 + \frac{(4-d)f}{(x_s-x_0)^2} \right) \quad (459)$$

which is finite for $d < 4$.

C. Mean avalanche shape around a point such that $S(x_0) = 0$

We ask now what is the mean shape $\langle S(x) \rangle_{S(x_0)=0}$ around a point such that $S(x_0) = 0$, for an avalanche with a seed at x_s . For simplicity we set $x_0 = 0$. We study the massless case, the massive case is briefly mentioned in Appendix K. Let us recall that

$$\langle e^{\int d^d x \lambda(x) S(x)} \rangle_{S(x_0)=0} = e^{f(u^\lambda(x_s) - u^0(x_s))} \quad (460)$$

where $u^\lambda(x)$ is the solution of

$$\nabla_x^2 \tilde{u} + \tilde{u}^2 = -\lambda(x) \quad , \quad \tilde{u}(0) = -\infty \quad (461)$$

Here we are interested only in the mean shape, i.e. averages like

$$\langle \int d^d x' \lambda(x') S(x') \rangle_{S(x_0)=0} = f \int dx' u_1(x_s, x') \lambda(x') \quad (462)$$

hence we only need to solve (461) to $O(\lambda)$, and we have defined

$$u^\lambda(x) = -\frac{2(4-d)}{x^2} + \int dx' u_1(x, x') \lambda(x') + O(\lambda^2) \quad (463)$$

Replacing into (461) we see that $u_1(x, x')$ satisfies

$$\nabla_x^2 \tilde{u}_1 - \frac{4(4-d)}{x^2} \tilde{u}_1 = -\delta^d(x-x') \quad (464)$$

hence it is the zero energy Green's function associated to the Schrodinger equation in the inverse square potential in any space dimension d . This Green function is known (see e.g.²⁷). One uses spherical coordinates $x = (r, \phi)$ where ϕ is a $d-1$ dimensional angular vector, and the representation of the Laplacian

$$\nabla_x^2 = r^{-\frac{d-1}{2}} \partial_r^2 r^{\frac{d-1}{2}} - \frac{L^2 + \frac{(d-1)(d-3)}{4}}{r^2} \quad (465)$$

where L^2 is the square angular momentum operator, i.e. minus the Laplace-Beltrami operator (Laplacian on the sphere). It has eigenvectors $Y_{\ell,m}(\phi)$, the spherical harmonics, and eigenvalues $\ell(\ell+d-2)$, $\ell \geq 0$, with degeneracies $g_\ell = (2\ell+d-2)(\ell+d-3)!/\ell!(d-2)!$. Hence one has

$$u_1(r, \phi, r', \phi) = (rr')^{-\frac{d-1}{2}} \sum_{\ell=0}^{\infty} \sum_{m=1}^{g_\ell} Y_{\ell,m}(\phi) Y_{\ell,m}^*(\phi') G_{\ell+\frac{d-2}{2}}(r, r') \quad (466)$$

where $G_{\ell+\frac{d-2}{2}}(r, r')$ is the Green function of the equivalent radial problem in the sector associated to angular momentum quantum number ℓ

$$\left(\frac{d^2}{dr^2} - \frac{4(4-d) + (\ell + \frac{d-2}{2})^2 - \frac{1}{4}}{r^2} \right) G_{\ell+\frac{d-2}{2}}(r, r') = -\delta(r-r') \quad (467)$$

whose solutions (with the proper continuity and derivative discontinuity conditions) are simple power laws, i.e.

$$G_{\ell+\frac{d-2}{2}}(r, r') = \frac{\sqrt{rr'}}{2a_{\ell,d}} \left(\left(\frac{r}{r'} \right)^{a_{\ell,d}} \theta(r' - r) + \left(\frac{r'}{r} \right)^{a_{\ell,d}} \theta(r - r') \right) \quad (468)$$

leading to the final expression

$$u_1(r, \phi, r', \phi) = \sum_{\ell=0}^{\infty} \sum_{m=1}^{g_\ell} Y_{\ell,m}(\phi) Y_{\ell,m}^*(\phi') \frac{(rr')^{\frac{2-d}{2}}}{2a_{\ell,d}} \left(\left(\frac{r}{r'} \right)^{a_{\ell,d}} \theta(r' - r) + \left(\frac{r'}{r} \right)^{a_{\ell,d}} \theta(r - r') \right) \quad (469)$$

where the exponents are

$$a_{\ell,d} = \sqrt{4(4-d) + \left(\ell + \frac{d-2}{2} \right)^2} \quad (470)$$

These non-trivial exponents are associated to a given angular sector. They can be selected by considering observables with the same symmetry.

One easily sees that for $d=1$, only $\ell=0$ and $\ell=1$ exist, with $g_0=1$, $g_1=1$ and $g_{\ell \geq 2}=0$. The exponent is $a_{0,1}=a_{1,1}=7/2$ and one recovers

$$\langle S(x=r) \rangle_{S(0)=0} = f u_1(r_s, r) = f \left(\frac{r_s^4}{7r^3} \theta(r-r_s) + \frac{r^4}{7r_s^3} \theta(r_s-r) \right) \quad (471)$$

which is exactly our result (144) for a single boundary in $d = 1$ (in different notations). Note that at variance with (144) there can be an avalanche on the other side $x = -r$ with a similar expression (which is why both $\ell = 0$ and $\ell = 1$ contribute).

Let us now analyze the case $d = 2$. The vector ϕ is then simply the polar angle $\phi \in [0, 2\pi]$. One has $g_\ell = 2 - \delta_{\ell,0}$, with

$$Y_{\ell,1}(\phi) = \frac{1}{\sqrt{2\pi}} e^{i\ell\phi} \quad Y_{\ell,2}(\phi) = \frac{1}{\sqrt{2\pi}} e^{-i\ell\phi} \quad (472)$$

and $a_{\ell,2} = \sqrt{8 + \ell^2}$. One obtains in polar coordinate (we now use ℓ to denote the eigenvalue of the L_z operator)

$$\langle S(r, \phi) \rangle_{S(0)=0} = f u_1(r_s, \phi_s, r, \phi) = \frac{f}{2\pi} \sum_{\ell=-\infty}^{+\infty} \frac{1}{2\sqrt{8 + \ell^2}} \left(\left(\frac{r_s}{r} \right)^{\sqrt{8 + \ell^2}} \theta(r - r_s) + \left(\frac{r}{r_s} \right)^{\sqrt{8 + \ell^2}} \theta(r_s - r) \right) e^{i\ell(\phi_s - \phi)} \quad (473)$$

Several features can be pointed out. First, note the invariance by $r \rightarrow 1/r$, valid in $d = 2$. Second, one can ask how the mean shape vanishes near the point where $S(x_0 = 0) = 0$. For $r \ll r_s$ the series is dominated by the term $\ell = 0$ hence we find

$$\langle S(r, \phi) \rangle_{S(0)=0} \simeq_{r \rightarrow 0} \frac{f}{8\pi\sqrt{2}} \left(\frac{r}{r_s} \right)^{2\sqrt{2}} + O\left(\left(\frac{r}{r_s} \right)^3 \cos(\phi_s - \phi) \right) \quad (474)$$

Note that $2\sqrt{2} = 2.8284\dots$, thus the correction term is quite large (the difference between the exponents is small). Similarly for large r

$$\langle S(r, \phi) \rangle_{S(0)=0} \simeq_{r \rightarrow +\infty} \frac{f}{8\pi\sqrt{2}} \left(\frac{r_s}{r} \right)^{2\sqrt{2}} + O\left(\left(\frac{r_s}{r} \right)^3 \right) \quad (475)$$

For general r we do not know of a simple formula for the series (although a few integral representations can be obtained). However for r/r_s close to unity, one expects that one can replace a sum by an integral, i.e. for $r < r_s$, we obtain, with $\ell = 2\sqrt{2} \sinh u$

$$\langle S(r, \phi) \rangle_{S(0)=0} \simeq \frac{f}{4\pi} \int_{-\infty}^{+\infty} \frac{d\ell}{\sqrt{8 + \ell^2}} e^{-\ln(\frac{r_s}{r})\sqrt{8 + \ell^2} + i\ell(\phi_s - \phi)} \quad (476)$$

$$= \frac{f}{4\pi} \int_{-\infty}^{+\infty} du e^{-2\sqrt{2} \ln(\frac{r_s}{r}) \cosh u + i2\sqrt{2}(\phi_s - \phi) \sinh u} \quad (477)$$

For $\phi = \phi_s$ we find, using that $\int_{-\infty}^{+\infty} du \exp(-b \cosh u) = 2K_0(b)$ (GR 3.337), that for $r_s - r \rightarrow 0^+$

$$\langle S(r, \phi_s) \rangle_{S(0)=0} \simeq \frac{f}{2\pi} K_0(2\sqrt{2} \ln(\frac{r_s}{r})) \simeq_{r \rightarrow r_s^-} -\frac{f}{2\pi} \ln\left(\frac{r_s - r}{r_s} e^{\gamma_E \sqrt{2}} \right) \quad (478)$$

which shows that the mean shape diverges logarithmically near the seed as $x \rightarrow x_s^-$ (this comes from small scales, see discussion in Appendix). We recalled that in $d = 1$, i.e. in (471), it has a jump discontinuity $-f$ of the first derivative at the seed. Note that the approximation (477) is not so bad even for small r/r_s since (478) yields the correct exponent (474) in that limit (but an incorrect prefactor).

Consider now the following angular averaged mean shape

$$\left\langle \int_0^{2\pi} d\phi \cos(\phi\ell) S(r, \phi) \right\rangle_{S(0)=0} = f \frac{\cos(\ell\phi_s)}{2\sqrt{8 + \ell^2}} \left(\left(\frac{r_s}{r} \right)^{\sqrt{8 + \ell^2}} \theta(r - r_s) + \left(\frac{r}{r_s} \right)^{\sqrt{8 + \ell^2}} \theta(r_s - r) \right) \quad (479)$$

which selects a given angular momentum ℓ and corresponds to a pure power law. Hence each exponent $a_{\ell,d}$ can be observed by suitably averaging the shape around the point $x_0 = 0$ (conditioned to $S(x_0) = 0$).

This analysis can be extended to any dimension $d < 4$. Denoting ϕ a $d - 1$ dimensional unit vector, the shape is

$$\langle S(r, \phi) \rangle_{S(0)=0} = f u_1(r_s, \phi_s, r, \phi) = f \sum_{\ell=0}^{\infty} \sum_{m=1}^{g_\ell} Y_{\ell,m}(\phi_s) Y_{\ell,m}^*(\phi) \frac{(r_s r)^{\frac{2-d}{2}}}{2a_{\ell,d}} \left(\left(\frac{r_s}{r} \right)^{a_{\ell,d}} \theta(r' - r) + \left(\frac{r}{r_s} \right)^{a_{\ell,d}} \theta(r - r') \right) \quad (480)$$

For $r \ll r_s$ the series is dominated by the term $\ell = 0$ hence we find

$$\langle S(r, \phi) \rangle_{S(0)=0} \simeq_{r \rightarrow 0} f C_d r_s^{b_d^-} r^{b_d^+} \quad , \quad b_d^\pm = \frac{2-d}{2} \pm a_{0,d} = \frac{1}{2} \left(2-d \pm \sqrt{d^2 - 20d + 68} \right) \quad (481)$$

and similarly

$$\langle S(r, \phi) \rangle_{S(0)=0} \simeq_{r \rightarrow +\infty} f C_d r_s^{b_d^+} r^{b_d^-} \quad , \quad b_d^\pm = \frac{2-d}{2} \pm a_{0,d} = \frac{1}{2} \left(2-d \pm \sqrt{d^2 - 20d + 68} \right) \quad (482)$$

with the non-trivial exponents

$$b^+ = 4 \quad , \quad b^- = -3 \quad \text{for } d = 1 \quad (483)$$

$$b^+ = 2\sqrt{2} \quad , \quad b^- = -2\sqrt{2} \quad \text{for } d = 2 \quad (484)$$

$$b^+ = \frac{1}{2}(\sqrt{17} - 1) \quad , \quad b^- = -\frac{1}{2}(1 + \sqrt{17}) \quad \text{for } d = 2 \quad (485)$$

$$b^+ \rightarrow 0 \quad , \quad b^- \rightarrow -2 \quad \text{for } d \rightarrow 4 \quad (486)$$

Again, one can select a given angular momentum ℓ and a pure power law with exponent

$$b_{\ell,d}^\pm = \frac{2-d}{2} \pm a_{\ell,d} = \frac{2-d}{2} \pm \sqrt{4(4-d) + \left(\ell + \frac{d-2}{2}\right)^2} \quad (487)$$

by suitably averaging the shape as in around the point $x_0 = 0$ (conditioned to $S(x_0) = 0$).

D. Probability that an avalanche does not reach a distance R from the seed

Consider a simply connected domain \mathcal{D} containing the point $x = x_s$. To obtain the probability that an avalanche started at $x = x_s$ remains inside \mathcal{D} , one must solve the instanton equation with the boundary condition $\tilde{u}(x) = -\infty$ for all points x in the complementary of the domain $\mathcal{D}^c = \mathbb{R}^d - \mathcal{D}$. However, heuristically, this appears to be equivalent to solving the same equation with the boundary condition $\tilde{u}(x) = -\infty$ on the boundary of the domain, $x \in \partial\mathcal{D}$. This is a property of the local elastic kernel that we consider here, which we already used in $d = 1$. We can safely assume it to remain true in $d > 1$ (under some conditions of regularity of the domain and its frontier).

Let us now calculate the probability that an avalanche starting at $x = x_s$ does not reach the sphere $r = R$ centered at point $x = 0$ (in spherical coordinates around $x = 0$). Here the seed can be either inside the sphere $|x| = r < R$ (and then it gives the probability that the avalanche remains inside the sphere), or outside $|x| = r > R$ (and then it gives the probability that the avalanche remains outside the sphere). This requires to find the solution, for $r \in [0, R[\cup]R, +\infty[$, denoted $\tilde{u}_R(r)$, of

$$\frac{d^2}{dr^2} \tilde{u} + \frac{d-1}{r} \frac{d}{dr} \tilde{u} + \tilde{u}^2 = 0 \quad , \quad \tilde{u}(R) = -\infty \quad , \quad \tilde{u}(+\infty) = 0 \quad (488)$$

which is smooth and bounded everywhere, except on the sphere where it diverges. It is easy to see that for $d < 4$

$$\tilde{u}_R(r) \simeq_{r \rightarrow +\infty} -\frac{2(4-d)}{r^2} \quad , \quad \tilde{u}_R(r) \simeq_{r \rightarrow R^\pm} -\frac{6}{(r-R)^2} \quad (489)$$

i.e. the behavior far from the sphere is similar to setting $R = 0$, i.e. (449), while the behavior near the sphere is similar to the single boundary $d = 1$ problem (since from close distance, the sphere looks like a hyperplane). The solution $\tilde{u}_R(r)$ interpolates between these limit behaviors. Clearly it takes the scaling form

$$\tilde{u}_R(r) = \frac{1}{R^2} \tilde{u}(r/R) \quad (490)$$

where we simply denote $\tilde{u}_{R=1}(r) = \tilde{u}(r)$ the solution with $R = 1$. In $d = 1$ we know its explicit form

$$\tilde{u}(r) = -\frac{3}{2} \mathcal{P}_0\left(\frac{1-r}{2}\right) \theta(1-r) - \frac{6}{(r-1)^2} \theta(r-1) \quad (491)$$

where $\mathcal{P}_0(z)$ is defined in (14) and satisfies the properties (15), however we do not know the explicit solution for $d > 1$. Interestingly, the scaling form (490) already leads to some information. We will analyze two observables.

(i) The probability that an avalanche is confined within a ball of radius R centered on its seed, is given by choosing $x_s = 0$. Calling $r_{\max} = \max_{x \in \Omega} |x - x_s|$ the maximal distance of any point of the avalanche to the seed we have

$$\text{Prob}(r_{\max} < R) = e^{f \tilde{u}_R(x_s=0)} = e^{\frac{f}{R^2} \tilde{u}(0)} \quad (492)$$

In $d = 1$, and in the notations of the previous sections, it is $r_{\max} = \max(\ell_1, \ell_2)$. The PDF of r_{\max} , $P(r_{\max})$ for a kick of strength f , and the associated density $\rho(r_{\max})$ are thus given by (we recall that $\tilde{u}(0) < 0$)

$$P(r_{\max}) = f \frac{-2\tilde{u}(0)}{r_{\max}^3} e^{\frac{f}{r_{\max}^2} \tilde{u}(0)} \quad , \quad \rho(r_{\max}) = \frac{-2\tilde{u}(0)}{r_{\max}^3} \quad (493)$$

To obtain the constant $\tilde{u}(0)$, we expand around $r = 0$. One can write

$$\tilde{u}(r) = \tilde{u}(0) f_d(-r^2 \tilde{u}(0)) \quad (494)$$

with $f(0) = 1$ and $f(z)$ satisfies

$$-4z f''(z) - 2df'(z) + f(z)^2 = 0 \quad (495)$$

The Taylor expansion $f(z) = \sum_{n \geq 0} f_n z^n$ obeys the recursion $f_{n+1} = \frac{1}{4(n+1)(n+\frac{d}{2})} \sum_{p=0}^n f_p f_{n-p}$ with $f_0 = 1$. The lowest coefficients are $f_n^{d=1} = \{1, \frac{1}{2}, \frac{1}{12}, \frac{1}{72}, \dots\}$, $f_n^{d=2} = \{1, \frac{1}{4}, \frac{1}{32}, \frac{1}{288}, \dots\}$, $f_n^{d=3} = \{1, \frac{1}{6}, \frac{1}{60}, \frac{11}{7560}, \dots\}$. One finds that the coefficients grow as $f_n \simeq 24(n+1)a^{-(n+1)}$, leading to $f(z) \simeq 24 \frac{a}{(z-a)^2}$ near $z = a$. This matches the expected behavior (489), $\tilde{u}(r) = -6 \frac{1}{(r-1)^2}$, near $r = 1$, upon the choice $a = -\tilde{u}(0)$. Obtaining the f_n recursively we can thus determine a and we obtain

$$\tilde{u}(0)|_{d=1} \approx -8.84752 \quad , \quad \tilde{u}(0)|_{d=2} \approx -12.5634 \quad , \quad \tilde{u}(0)|_{d=3} \approx -15.7179 \quad (496)$$

A check is obtained in $d = 1$, where the exact value, from (491), is $\tilde{u}(0) = -\frac{3}{2} \mathcal{P}_0(\frac{1}{2}, \Gamma(1/3))^{18} / (64\pi^6) = -8.8475159\dots$

(ii) The probability that an avalanche with a seed at $r = r_s$ avoids the ball $B(0, R)$. To obtain this probability, we can first study the case of large r_s , and look for an expansion of $\tilde{u}(r)$ at large r , around the leading term, from (489), $\tilde{u}(r) \simeq_{r \rightarrow +\infty} -\frac{2(4-d)}{r^2}$. The equation for the first subleading term is similar to the one studied in (464) hence one finds anomalous exponents, as encountered above in Section VIII C.

It is useful instead to write $\tilde{u}(r)$, for $r > 1$, in the form

$$\tilde{u}(r) = -\frac{2(4-d)}{r^2} (1 + v(Ar^{2+b})) \quad (497)$$

where $A > 0$ is for now arbitrary. It leads to

$$(b+2)z((b+d-4)v'(z) + (b+2)zv''(z)) + 2(d-4)v(z)^2 + 2(d-4)v(z) = 0 \quad (498)$$

and we can look for a solution such that $v(z) \simeq z$ at small z . This implies $4(-4+d) + b(-2+b+d) = 0$ which leads to $b = b_d^\pm$ as given by (482). Since we want $2+b < 0$ the solution is

$$b = b_d^- = \frac{1}{2} \left(2 - d - \sqrt{(d-20)d + 68} \right) \quad (499)$$

which leads to $b = -3$ in $d = 1$, $b = -2\sqrt{2}$ in $d = 2$ and $b = -\frac{1}{2}(1 + \sqrt{17})$ in $d = 3$. For $d \rightarrow 4^-$ we find $b \rightarrow -2^-$.

It is useful to trade d for $d = -b - \frac{8}{b+4} + 6$, and call $v(z) = v_b(z)$ the solution. Then $v_b(z)$ satisfies

$$(b+2)(b+4)z^2 v_b''(z) - 2b(-zv_b'(z) + v_b(z)^2 + v_b(z)) = 0 \quad , \quad v(0) = 0 \quad v'(0) = 1 \quad (500)$$

where we can fix $v'(0) = 1$ since A is as yet undetermined. It is then easy to generate the Taylor series $v(z) = z + \sum_{n \geq 2} v_n z^n$. One finds e.g. $v_2 = \frac{b}{b^2 + 7b + 8}$ and

$$v(z)|_{d=2} = z + \frac{1}{17} \left(7 + 4\sqrt{2} \right) z^2 + \frac{1}{238} \left(59 + 41\sqrt{2} \right) z^3 + O(z^4) \quad (501)$$

$$v(z)|_{d=3} = z + \frac{1}{12} \left(5 + \sqrt{17} \right) z^2 + \frac{1}{177} \left(46 + 11\sqrt{17} \right) z^3 + O(z^4) \quad (502)$$

The undetermined constant A in (497) will be such that $v(z)$ diverges at $z = A$, so that $\tilde{u}(r) \simeq -6/(r-1)^2$ for $r \rightarrow 1^+$. Extrapolation of the radius of convergence of the series gives $A_{d=1} \approx 1.99$, $A_{d=2} \approx 1.97$, $A_{d=3} \approx 1.9$. In $d = 1$ one knows that $\tilde{u}(r) = \frac{-6}{(r-1)^2}$ exactly. This is consistent with the above with $A = 2$ and $v(z) = \frac{z(4-z)}{(2-z)^2} = z + \frac{3z^2}{4} + \frac{z^3}{2} + \frac{5z^4}{16} + O(z^5)$.

Hence, using the scaling form (490), we can summarize our results as follows. The probability that the avalanche (of support denoted Ω) with a seed at a distance $r = r_s > R$ from the point 0, avoids the ball $B(0, R)$ is

$$\text{Prob}(B(0, R) \cap \Omega = \emptyset) = e^{f\tilde{u}_R(r_s)} = e^{\frac{f}{R^2}\tilde{u}(r_s/R)} = \exp\left(-\frac{2(4-d)f}{r_s^2} \left[1 + v\left(A\left(\frac{r_s}{R}\right)^{2+b_d^-}\right)\right]\right), \quad r_s > R \quad (503)$$

$$\simeq e^{-\frac{6f}{(r_s-R)^2}}, \quad 0 < r_s - R \ll R \quad (504)$$

where the exponent b_d^- , the function $v(z)$ and the constant A depend only on the dimension d and are given by (499) and (500),(501) (with $2 + b_d^- < 0$ and $A \approx 2$ was estimated above). Note that if we consider the limit of a small ball, $R \rightarrow 0$, we recover the result of Section VIII A which is thus validated.

Let us denote $r_{\min} = \min_{x \in \Omega} |x|$, $0 < r_{\min} < r_s$, the minimal distance between the origin $x = 0$ and any point of the avalanche (started at r_s) and denote its PDF as $P_{r_s}(r_{\min})$. Then one has

$$\text{Prob}(B(0, R) \cap \Omega = \emptyset) = \text{Prob}(r_{\min} > R) \quad (505)$$

and taking a derivative w.r.t. R gives the PDF, for any $R > 0$

$$P_{r_s}(r_{\min} = R) = -\frac{d}{dR} \text{Prob}(r_{\min} > R) = f\rho_{r_s}(R) \text{Prob}(r_{\min} > R) \quad (506)$$

where $\rho_{r_s}(r_{\min} = R) = \partial_f P_{r_s}(r_{\min} = R)|_{f=0^+}$ is the density

$$\rho_{r_s}(r_{\min} = R) = \frac{2A(2+b_d^-)(d-4)}{R^{3+b_d^-} r_s^{-b_d^-}} v' \left(A \left(\frac{r_s}{R} \right)^{2+b_d^-} \right), \quad 0 < R < r_s \quad (507)$$

$$\simeq \frac{2A(2+b_d^-)(d-4)}{R^{3+b_d^-} r_s^{-b_d^-}}, \quad 0 < R \ll r_s \quad (508)$$

$$\simeq \frac{12}{(r_s - R)^3}, \quad 0 < r_s - R \ll r_s \quad (509)$$

where in $d = 1$ the last expression is exact, and agrees with (137) since there $r_{\min} = r_s - \ell_2$. Note that for $1 \leq d < 4$ the exponent $b_d^- < -2$ (it is given in (499)), but that $3 + b_d^- \geq 0$ and increases from 0 to 1 as d increases from $d = 1$ to $d = 4$. The density of r_{\min} thus diverges both for $r_{\min} = R \rightarrow 0$ (weakly and for $d > 1$) and for $r_{\min} \rightarrow r_s$. The second divergence corresponds to small avalanches. The first divergence of the density of r_{\min} with exponent $3 + b_d^-$ is presumably related to the probability that a large avalanche in $d > 1$ contains a "hole" around $x = 0$ of size r_{\min} . Finally note that the probability of the event $r_{\min} > 0$ is not unity but equals to

$$\int_{0^+}^{+\infty} dr_{\min} P_{r_s}(r_{\min}) = e^{-\frac{2(4-d)f}{r_s^2}} = \text{Prob}(S(0) = 0) \quad (510)$$

as it should, i.e. the probability $P_{r_s}(r_{\min})$ has a delta function piece at $r_{\min} = 0$ of amplitude $1 - e^{-\frac{2(4-d)f}{r_s^2}}$.

E. Span and shape in $d > 1$

Let us now study the shape in $d > 1$ dimension conditioned to the span, see Fig. 3. Let us decompose the coordinate as $x = (x_1, x_\perp)$ where $x_1 \in \mathbb{R}$ and $x_\perp \in \mathbb{R}^{d-1}$. We want to impose that the avalanche starting at the seed $x_s = (x_1^s, x_\perp^s)$ does not reach the level $x_1 = r$ (with $x_1^s < r$). Let us use the (somewhat abusive) shorthand notation $S(r)$

$$S(r) \equiv S_{\text{tot}}(r) = \int d^{d-1} x_\perp S(r, x_\perp) \quad (511)$$

for the total size along the transverse space (in Fig. 3 one has $d = 2$ and $x_\perp = x_2$). Consider a point $y = (y_1, y_\perp)$ below the level r , i.e. $y_1 < r$, and the local size of the avalanche $S(y) = S(y_1, y_\perp)$. We are interested in the PDF of $S(y)$, denoted $P(S(y), S(r) = 0)$, joint with the event $S(r) = 0$, to ensure that the level r has not been reached. Its Laplace transform is

$$\int dS(y) e^{\lambda S(y)} P(S(y), S(r) = 0) = e^{f \tilde{u}^\lambda(x_s)} \quad (512)$$

where $\tilde{u}^\lambda(x)$ is the solution of

$$\nabla_x^2 \tilde{u}(x) + \tilde{u}(x)^2 = -\lambda \delta(x_1 - y_1) \delta^{d-1}(x_\perp - y_\perp) \quad , \quad \tilde{u}(r, x_\perp) = -\infty \quad , \quad \tilde{u}(-\infty, x_\perp) = 0 \quad (513)$$

on the strip $x_1 \in]-\infty, r[$. We denote $\tilde{u}_r(x_1, x_\perp; y_1, y_\perp)$ the solution of this problem. We will calculate only the mean shape, hence we look for a solution perturbative in λ as

$$\tilde{u}_r(x_1, x_\perp; y_1, y_\perp) = -\frac{6}{(r - x_1)^2} + \lambda \tilde{u}_{1r}(x_1, x_\perp; y_1, y_\perp) + O(\lambda^2) \quad (514)$$

Hence $\tilde{u}_1(x) = \tilde{u}_{1r}(x_1, x_\perp; y_1, y_\perp)$ is the solution of

$$\nabla_x^2 \tilde{u}_1(x) - \frac{12}{(r - x_1)^2} \tilde{u}_1(x) = -\delta(x_1 - y_1) \delta^{d-1}(x_\perp - y_\perp) \quad (515)$$

Let us Fourier transform w.r.t. the transverse space and define

$$\tilde{u}_{1r}(x_1, x_\perp; y_1, y_\perp) = \int \frac{d^{d-1}q}{(2\pi)^{d-1}} e^{iq(x_\perp - y_\perp)} \tilde{u}_{1r}(x_1, y_1; q) \quad (516)$$

where $\tilde{u}_{1r}(x_1, y_1; q)$ is now solution of

$$(\partial_{x_1}^2 - q^2) \tilde{u}_{1r}(x_1, y_1; q) - \frac{12}{(r - x_1)^2} \tilde{u}_{1r}(x_1, y_1; q) = -\delta(x_1 - y_1) \quad (517)$$

The independent solutions of the homogeneous equation depend only on $|q|$ and they are

$$\sqrt{r - x_1} K_{7/2}(|q|(r - x_1)) \sim_{q \rightarrow 0} \frac{1}{|q|^{7/2} (r - x_1)^3} \quad (518)$$

$$\sqrt{r - x_1} I_{7/2}(|q|(r - x_1)) \sim_{q \rightarrow 0} |q|^{7/2} (r - x_1)^4 \quad (519)$$

Hence we obtain the solution

$$\tilde{u}_{1r}(x_1, y_1; q) = \tilde{F}_{|q|}(r - y_1, r - x_1) \theta(x_1 < y_1 < r) + \tilde{F}_{|q|}(r - x_1, r - y_1) \theta(y_1 < x_1 < r) \quad (520)$$

$$\tilde{F}_q(a, b) = \sqrt{ab} I_{7/2}(qa) K_{7/2}(qb) \quad , \quad 0 < a < b \quad (521)$$

which is a symmetric function in (x_1, y_1) , and one can check that it has the correct derivative discontinuity $[\tilde{u}_1]_{x_1=y_1^-}^{x_1=y_1^+} = -1$. The function $\tilde{F}_q(a, b)$ has the following asymptotics for small and large q

$$\tilde{F}_q(a, b) = \frac{1}{7} \frac{a^4}{b^3} \left(1 + \frac{1}{90} q^2 (5a^2 - 9b^2) + \frac{q^4 (33b^4 - 22b^2 a^2 + 5a^4)}{3960} + O(q^6) \right) \quad (522)$$

$$= e^{-ba} \left(\frac{\cosh(aq)}{q} + \frac{6}{q^2} \left(\frac{\cosh(aq)}{b} - \frac{\sinh(aq)}{a} \right) + O\left(\frac{1}{q^3}\right) \right) \quad (523)$$

Denoting $\ell_2 = \max_{x \in \Omega} x_1$ the ‘‘upper span’’ (or one sided span), see Fig. 3, we thus obtain by expanding (512) to $O(\lambda)$

$$\int dS(y) S(y) P(S(y), \ell_2 < r - x_1^s) = f e^{-\frac{6f}{(r-x_1^s)^2}} \int \frac{d^{d-1}q}{(2\pi)^{d-1}} e^{iq(x_\perp^s - y_\perp)} \tilde{u}_{1r}(x_1^s, y_1; q)$$

where $\text{Prob}(\ell_2 < r - x_1^s) = e^{-\frac{6f}{(r-x_1^s)^2}}$, and $\rho(\ell_2) = \frac{12}{\ell_2^3}$, independently of the space dimension d , a property of the BFM previously discussed. Thus we obtain the shape conditioned to the span $\ell_2 < r - x_1^s$ as

$$\langle S(y_1, y_\perp) \rangle_{\ell_2 < r - x_1^s} = f \int \frac{d^{d-1}q}{(2\pi)^{d-1}} e^{iq(x_\perp^s - y_\perp)} \tilde{u}_{1r}(x_1^s, y_1; q) \quad (524)$$

where $\tilde{u}_{1r}(x_1, y_1; q)$ is given in (520). This gives the result (56), where here $x_s = (x_1^s, x_\perp^s)$ denote the position of the seed. One can write also the result for an arbitrary kick $f(x, t) = f(x_1, x_\perp)\delta(t)$ with support in the strip $x_1 < r$ as

$$\langle S(y_1, y_\perp) \rangle_{\ell_2 < r - x_1^s} = \int dx_1 \frac{d^{d-1}q}{(2\pi)^{d-1}} f(x_1, q) \tilde{u}_{1r}(x_1, y_1; q) e^{-iqy_\perp} \quad (525)$$

which allows to select some specific Fourier components q by tuning the shape of the kick.

In two dimension, $d = 2$, one can obtain a more explicit formula. Indeed the inverse Fourier transform of $\tilde{F}_{|q|}(a, b)$ reads

$$\int_{-\infty}^{+\infty} \frac{dq}{2\pi} e^{iqc} \tilde{F}_{|q|}(a, b) = \frac{1}{2\pi} \Phi\left(\frac{(a-b)^2 + c^2}{2ab}\right) \quad , \quad 0 < a < b \quad (526)$$

with, for $z > 0$,

$$\Phi(z) = \frac{1}{6} (4 - 15(z+1)^2) + \frac{1}{4} (z+1)(5z(z+2) + 2) \log(1 + \frac{2}{z}) \quad (527)$$

This holds because of the following identity (Gradstein ET I 49 (47) pp 1113)

$$\int_0^{+\infty} dq K_\nu(aq) I_\nu(bq) \cos(cq) = \frac{1}{2\sqrt{ab}} Q_{\nu-\frac{1}{2}}\left(\frac{a^2 + b^2 + c^2}{2ab}\right) \quad (528)$$

where Q_ν is the associated Legendre function. Here we have $\Phi(z) \equiv Q_3(1+z)$ (with a proper continuation, however). The small z and large z asymptotics of $\Phi(z)$ are

$$\Phi(z) = \frac{1}{6} (-3 \log z - 11 + 3 \log 2) + O(z) \quad (529)$$

$$= \frac{2}{35z^4} - \frac{8}{35z^5} + \frac{40}{63z^6} - \frac{32}{21z^7} + \frac{112}{33z^8} + O\left(\frac{1}{z^9}\right) \quad (530)$$

Hence we find in $d = 2$ the explicit formula

$$\langle S(y_1, y_\perp) \rangle_{\ell_2 < r - x_1^s} = \frac{f}{2\pi} \Phi\left(\frac{(y_1 - x_1^s)^2 + (y_\perp - x_\perp^s)^2}{2(r - y_1)(r - x_1^s)}\right) \quad (531)$$

a symmetric function of (x_1^s, y_1) , both smaller than r , and where $\Phi(z)$ is given in (527). It exhibits a logarithmic singularity at the position of the seed (as was also found above in Section VIII C). One can check (e.g. numerically) that upon integration over y_\perp , one recovers for the total size along the transverse space, denoted somewhat abusively $S(y_1) = \int d^{d-1}x_\perp S(y_1, x_\perp)$,

$$\langle S(y_1) \rangle_{\ell_2 < r - x_1^s} = \frac{f}{7} \frac{(r - y_1)^4}{(r - x_1^s)^3} \theta(x_1^s < y_1 < r) + \frac{f}{7} \frac{(r - x_1^s)^4}{(r - y_1)^3} \theta(y_1 < x_1^s < r) \quad (532)$$

i.e. as for the BFM in $d = 1$, as expected.

Let us now apply the general procedure given in (E6) to obtain the mean shape at fixed ‘‘upper span’’ ℓ_2 . We obtain, focusing on the limit $f \rightarrow 0^+$

$$\langle S(y_1, y_\perp) \rangle_{\ell_2 = r - x_1^s} = \frac{\ell_2^3}{12} \int \frac{d^{d-1}q}{(2\pi)^{d-1}} e^{iq(x_\perp^s - y_\perp)} \partial_r u_{1r}(x_1^s, y_1; q)|_{\ell_2 = r - x_1^s} \quad (533)$$

which can be evaluated in any dimension using (520).

In $d = 2$ one obtains an explicit expression. Denoting the distance of the measurement point y to the seed as R (remembering that we must set $x_1^s + \ell_2 = r$ in (533))

$$R^2 = (y - x_s)^2 = (y_1 - x_1^s)^2 + (y_\perp - x_\perp^s)^2 = (r - y_1 - \ell_2)^2 + (y_\perp - x_\perp^s)^2 \quad (534)$$

we have

$$\langle S(y_1, y_\perp) \rangle_{\ell_2=r-x_1^s} = -\frac{\ell_2(\ell_2 + r - y_1)}{24(2\pi)(r - y_1)^2} R^2 \Phi'(z) \Big|_{z=\frac{R^2}{2\ell_2(r-y_1)}} \quad (535)$$

with the following expression and small and large z asymptotics

$$-\Phi'(z) = \frac{(z+1)(15z(z+2)+2)}{2z(z+2)} - \frac{3}{4}(5z(z+2)+4)\log\left(1+\frac{2}{z}\right) \quad (536)$$

$$= \frac{1}{2z} + 3\log z + \frac{31}{4} - 3\log 2 + O(z \log z) \quad (537)$$

$$= \frac{8}{35z^5} - \frac{8}{7z^6} + \frac{80}{21z^7} - \frac{32}{3z^8} + O\left(\frac{1}{z^9}\right) \quad (538)$$

The mean shape conditioned to the ‘‘upper span’’ ℓ_2 , $\langle S(y_1, y_\perp) \rangle_{\ell_2}$, must vanish when y_1 reaches $y_1 - x_1^s = \ell_2$ since there can be no motion for $y_1 - x_1^s > \ell_2$. We now study how it vanishes. Expanding (535) for $y_1 = x_1^s + \ell_2 - D$, where D is the distance to the edge we find

$$\langle S(y_1, y_\perp) \rangle_{\ell_2} \Big|_{y_1=x_1^s+\ell_2-D} = \frac{16\ell_2^7}{105\pi(\ell_2^2 + (y_\perp - x_\perp^s)^2)^4} D^3 - \frac{16\ell_2^6(\ell_2^2 - (y_\perp - x_\perp^s)^2)}{105\pi(\ell_2^2 + (y_\perp - x_\perp^s)^2)^5} D^4 + O(D^5) \quad (539)$$

and one can check that integrating over y_\perp produces exactly the result (145) for the $d = 1$ BFM, i.e. $\frac{D^3}{21} - \frac{D^4}{28\ell_2} + O(D^5)$, as it should. Hence the mean shape still vanishes along any point of the ‘‘boundary’’ $y_1 = x_1^s + \ell_2$ with the cubic power, however the amplitude depends on the ratio of the transverse to longitudinal distance to the seed. Note that of course this is a mean effect, for each avalanche the point where the maximum span is realized is somewhere on the boundary $y_1 = x_1^s + \ell_2$ (finding the distribution of the position of this point is a more difficult problem).

Finally, note also the very simple result for the mean shape at the position of the seed, setting $R \rightarrow 0$ and $r - y_1 \rightarrow \ell_2$ one finds from (535) and (536)

$$\langle S(x_1^s, x_\perp^s) \rangle_{\ell_2=r-x_1^s} = \frac{\ell_2^2}{24\pi} \quad (540)$$

F. Probability that an avalanche does not hit a cone in two dimension

One can generalize the geometries of two of the previous sections, and ask what is the probability that an avalanche remains confined inside a conical domain of apex $x = 0$. Here we restrict to $d = 2$, and use polar coordinates (r, ϕ) . Consider the conical domain, or wedge, $\mathcal{D} = (r, \phi) \in]0, +\infty[\times]0, \phi_0[$ with an opening angle $0 < \phi_0 \leq 2\pi$. The probability that an avalanche Ω , with a seed inside the wedge at $x = (r_s, \phi_s)$, remains strictly confined inside the wedge (i.e. is not allowed to touch the two radial lines at $\phi = 0, \phi_0$) is

$$\text{Prob}(\Omega \cap \mathcal{D}^c = \emptyset) = \text{Prob}(S(r, 0) = S(r, \phi_0) = 0, r \in [0, +\infty[) = e^{f\tilde{u}(r_s, \phi_s)} \quad (541)$$

where $\tilde{u}(r, \phi)$ is the solution of the instanton equation

$$\left(\partial_r^2 + \frac{1}{r}\partial_r + \frac{1}{r^2}\partial_\phi^2\right)\tilde{u} + \tilde{u}^2 = 0 \quad , \quad \tilde{u}(r, 0) = \tilde{u}(r, \phi_0) = -\infty \quad , \quad r \geq 0 \quad (542)$$

which diverges on each boundary. The half plane case, $\phi_0 = \pi$, corresponds to the problem of the one-sided span considered in the previous section. Note that the opening angle of the wedge can be either smaller than for the half plane problem, $\phi_0 \leq \pi$, or larger $\pi < \phi_0 \leq 2\pi$. The case $\phi_0 = 2\pi$ is very interesting, as it requires the avalanche not to touch the positive axis, i.e. $x = (r \geq 0, \phi = 0)$. In all cases one requires that the point $x = 0$ is not visited by the avalanche, as in Section VIII A, but the restriction is always stronger as the avalanche is also required not to cross the boundaries of the wedge. Hence one has the bound

$$\text{Prob}(S(0) = 0) > \text{Prob}(S(x) = 0, x \in \mathcal{D}^c) \quad (543)$$

which will be useful below.

Given the symmetry of the problem we will search for a solution of the form (the numerical factors have been introduced for convenience)

$$\tilde{u}(r, \phi) = -\frac{6}{r^2} \left(\frac{1}{3} + h(\phi) \right) \quad (544)$$

The condition to be a solution of (542) is

$$h''(\phi) = 6h(\phi)^2 - \frac{2}{3} \quad (545)$$

whose general real solution is expressed as a Weierstrass elliptic function

$$h(\phi) = \mathcal{P}(\phi; g_2 = \frac{4}{3}, g_3) \quad (546)$$

where g_3 is for now a free real parameter. There is also an arbitrariness $\phi \rightarrow \phi + c$, which we have fixed since we must require from (542) that $h(0) = h(\phi_0) = +\infty$.

Let us recall (see Appendix) that the Weierstrass function is periodic on the real axis with half-period denoted $\Omega(g_2, g_3)$. It is smooth and bounded on its fundamental domain (one period interval) and diverges positively on both ends, i.e. at $\phi = 0^+$ as $\simeq 1/\phi^2$ and similarly at $\phi = 2\Omega(g_2, g_3)$. We thus require that

$$\phi_0 = 2\Omega(g_2 = \frac{4}{3}, g_3) \Leftrightarrow g_3 = g_3(\phi_0) \quad (547)$$

which allows to determine the parameter $g_3 = g_3(\phi_0)$ as a function of the wedge opening angle ϕ_0 . We denote

$$h_{\phi_0}(\phi) = \mathcal{P}(\phi; g_2 = \frac{4}{3}, g_3(\phi_0)) \quad (548)$$

the corresponding solution, which satisfies the required boundary conditions. Note the symmetry $h_{\phi_0}(\phi_0 - \phi) = h_{\phi_0}(\phi)$, with $h'_{\phi_0}(\phi_0/2) = 0$. The function $h_{\phi_0}(\phi)$ attains its minimum value for $\phi = \phi_0/2$. An equivalent condition to determine $g_3(\phi_0)$ is thus $\mathcal{P}'(\phi_0/2; g_2 = \frac{4}{3}, g_3(\phi_0)) = 0$. It is useful to recall that

$$\Omega(g_2, g_3) = \int_{e_1}^{+\infty} \frac{dt}{\sqrt{4t^3 - g_2t - g_3}} \quad (549)$$

where $t = e_1$ is the largest positive root of $4t^3 - g_2t - g_3 = 0$.

We already know the exact solution in one case, $\phi_0 = \pi$. Indeed then $\tilde{u}(r, \phi) = -6/y^2$. This corresponds to

$$h_{\pi}(\phi) = -\frac{1}{3} + \frac{1}{\sin^2 \phi} \quad (550)$$

which, as we can check, indeed satisfies the equation (545). We can use the other property of the Weierstrass function, $g_3 = 4\mathcal{P}(z)^3 - \mathcal{P}'(z)^2 - g_2\mathcal{P}(z) = 4h(\phi)^3 - h'(\phi)^2 - \frac{4}{3}h(\phi)$, to find the value of g_3 corresponding to that case, and one finds $g_3(\pi) = \frac{8}{27}$. The roots are $e_1 = \frac{2}{3}$ and double roots $e_{2,3} = -\frac{1}{3}$ and in that case the period is $\phi_0 = 2\Omega(g_2 = \frac{4}{3}, \frac{8}{27}) = \pi$.

Let us reexamine the bound (543). From (450) in $d = 2$ it implies that for all $\phi \in]0, \phi_0[$ one must have

$$h_{\phi_0}(\phi) > \frac{1}{3} \quad (551)$$

A necessary condition is thus

$$\mathcal{P}(\Omega; \frac{2}{3}, g_3) = e_1 > \frac{1}{3} \quad (552)$$

which is equivalent to $g_3 > -\frac{8}{27}$. One can check that the point $g_3 = -\frac{8}{27}$ corresponds to the point where the period diverges and the solution there is $h_{-8/27}(\phi) = \frac{1}{3} + \frac{1}{\sinh^2(\phi)}$. Hence the interval of variation of g_3 is included in $]-\frac{8}{27}, +\infty[$. In fact, as we see below g_3 varies in $]g_3^c, +\infty[$, where g_3^c is slightly larger than $-\frac{8}{27}$.

Let us start with the limit of a small opening angle $\phi_0 \ll 1$. One easily sees that it corresponds to large positive g_3 . In the large g_3 limit one can neglect g_2 (i.e. set it to zero in a first approximation) and one is back to our well studied function $h_{\phi_0}(\phi) \simeq \mathcal{P}_0(\phi)$. Hence we obtain

$$\phi_0 \simeq \left(\frac{g_3^0}{g_3}\right)^{1/6} \quad , \quad g_3 \simeq g_3^0 / \phi_0^6 \quad (553)$$

where we recall $g_3^0 = \frac{\Gamma(1/3)^{18}}{(2\pi)^6}$. In this regime the cone acts as two almost parallel boundaries, and the results are very similar to the $d = 1$ problem studied above.

As the angle ϕ_0 is increased from this limit the value of g_3 decreases. For some standard cases, we have solved numerically the condition (547) and we find

$$\phi_0 = \frac{\pi}{2} \quad , \quad \Omega = \frac{\pi}{4} \quad , \quad g_3 \approx 52.665 \quad , \quad h_{\phi_0}\left(\frac{\phi_0}{2}\right) = 2.40836 \quad (554)$$

$$\phi_0 = \frac{2\pi}{3} \quad , \quad \Omega = \frac{\pi}{3} \quad , \quad g_3 \approx 8.59156 \quad , \quad h_{\phi_0}\left(\frac{\phi_0}{2}\right) = 1.37624 \quad (555)$$

$$\phi_0 = \frac{3\pi}{2} \quad , \quad \Omega = \frac{3\pi}{4} \quad , \quad g_3 \approx -0.2751955 \quad , \quad h_{\phi_0}\left(\frac{\phi_0}{2}\right) = 0.403541 \quad (556)$$

We also find that the case $g_3 = 0$ corresponds exactly to

$$\frac{\phi_0}{2} = \Omega\left(\frac{4}{3}, 0\right) = \sqrt[4]{3}K(-1) = \frac{\sqrt[4]{3}\Gamma\left(\frac{1}{4}\right)^2}{4\sqrt{2\pi}} \quad , \quad h_{\phi_0}\left(\frac{\phi_0}{2}\right) = \frac{1}{\sqrt{3}} \quad (557)$$

that is $\frac{\phi_0}{\pi} = 1.098430697$. Note that there may be spurious roots for g_3 which are not obtained continuously from this solution, hence can be eliminated.

Finally, the interesting case $\phi_0 = 2\pi$ corresponds to the value $g_3 = g_3^c$ which we find numerically as $g_3^c \approx -0.295402 = -\frac{8}{27} + .0008941$. It corresponds to the constraint that the avalanche does not intersect the positive axis. The solutions for $-\frac{8}{27} < g_3 < g_3^c$ do not seem to correspond to physical cases, since ϕ_0 cannot be larger than 2π . The extreme case $g_3 = -\frac{8}{27}$ in a loose sense corresponds to the weaker constraint of not visiting $x = 0$ studied previously. Indeed, it has infinite period and upon some rescaling by this infinite period, one can eliminate the term $1/\sinh^2(\phi)$, recovering $h(\phi) \simeq \frac{2}{3}$ and thus the solution $\tilde{u}(x) = -\frac{4}{r^2}$ valid in this case (for $d = 2$).

Once the solution for the wedge ϕ_0 is obtained one can easily obtain the solution for the "angular extensions", φ_1, φ_2 which are the angular analogs of ℓ_1, ℓ_2 . We can define, for a seed at $x_s = (r, \phi_s = 0)$

$$\varphi_2 = \max_{x=(r,\phi)\in\Omega} \phi \quad , \quad \varphi_1 = - \min_{x=(r,\phi)\in\Omega} \phi \quad (558)$$

Then the CDF of (φ_1, φ_2) is given by

$$\text{Prob}(\varphi_1 < \phi_1, \varphi_2 < \phi_2) = \exp\left(-\frac{6}{r^2}\left(\frac{1}{3} + h_{\phi_1+\phi_2}(\phi_1)\right)\right) \quad (559)$$

Taking derivatives one obtains the PDF, the density, and the PDF of the total angular extension $\varphi = \varphi_1 + \varphi_2$, analogous to ℓ .

Acknowledgments

I thank C. Le Priol, A. Rosso, T. Thiery for collaborations on related topics. This work was supported initially by PSL grant ANR-10-IDEX-0001-02-PSL, then by ANR grant ANR-17-CE30-0027-01 RaMaTraF.

Appendix A: Weierstrass and Elliptic functions

Here we recall some properties of Weierstrass's elliptic function \mathcal{P} (source is Ref.²⁸ chapter 18, and Wolfram Mathworld). It appears in complex analysis as the only doubly periodic function on the complex plane with a double pole $1/z^2$ at zero³⁷. Denoting ω_1, ω_2 the two (a priori complex) primitive half-periods, every point of the lattice $\Lambda = \{2m\omega_1 + 2n\omega_2 | (n, m) \in \mathbb{Z}^2\}$ is a pole of order 2 for \mathcal{P} . It can be constructed for $z \in \mathbb{C} - \Lambda$ as

$$\mathcal{P}(z|\omega_1, \omega_2) := \frac{1}{z^2} + \sum_{m,n \neq (0,0)} \frac{1}{(z - 2m\omega_1 - 2n\omega_2)^2} - \frac{1}{(2m\omega_1 + 2n\omega_2)^2} \quad (\text{A1})$$

It is an even function of the complex variable z , with $\mathcal{P}(z) = \mathcal{P}(-z)$. Note that the choice of primitive vectors $(2\omega_1, 2\omega_2)$ is not unique, since one can alternatively choose any linear combination. The conventional choice of roots g_2 and g_3 is defined from its expansion around $z = 0$,

$$\mathcal{P}(z|\omega_1, \omega_2) = \frac{1}{z^2} + \frac{g_2}{20}z^2 + \frac{g_3}{28}z^4 + \mathcal{O}(z^6). \quad (\text{A2})$$

The function \mathcal{P} is alternatively denoted $\mathcal{P}(z|\omega_1, \omega_2) = \mathcal{P}(z; g_2, g_3)$, the notation used here, and defined in Mathematica as WeierstrassP[$z, \{g_2, g_3\}$]. The parameters g_2, g_3 are expressed from the half-periods

$$g_2 = 60 \sum_{m,n \neq (0,0)} \frac{1}{(2m\omega_1 + 2n\omega_2)^4}, \quad g_3 = 140 \sum_{m,n \neq (0,0)} \frac{1}{(2m\omega_1 + 2n\omega_2)^6}. \quad (\text{A3})$$

The Weierstrass elliptic function verifies the homogeneity property,

$$\mathcal{P}(\lambda z; \lambda^{-4}g_2, \lambda^{-6}g_3) = \lambda^{-2}\mathcal{P}(z; g_2, g_3), \quad (\text{A4})$$

and the non-linear differential equation

$$\mathcal{P}'(z)^2 = 4\mathcal{P}(z)^3 - g_2\mathcal{P}(z) - g_3. \quad (\text{A5})$$

It is thus linked to elliptic integrals. Restricting now to $g_2, g_3 \in \mathbb{R}$ and focusing on $z \in \mathbb{R}$ one can choose one half-period to be real, which we denote Ω ³⁸. The function $\mathcal{P}(z)$ is then periodic in \mathbb{R} of period 2Ω and diverges at all points $2m\Omega, m \in \mathbb{Z}$. It is defined in the fundamental interval $]0, 2\Omega[$, repeated by periodicity. In this interval it satisfies the symmetry $\mathcal{P}(2\Omega - z; g_2, g_3) = \mathcal{P}(z; g_2, g_3)$. Its values in the first half-interval, i.e. for $z \in [0, \Omega]$ are such that (with $y \in [e_1, \infty)$)

$$z = \int_y^\infty \frac{dt}{\sqrt{4t^3 - g_2t - g_3}} \Leftrightarrow y = \mathcal{P}(z; g_2, g_3) \quad (\text{A6})$$

where e_1 is the largest real root of the polynomial in t

$$4t^3 - g_2t - g_3 = 4(t - e_1)(t - e_2)(t - e_3). \quad (\text{A7})$$

The roots e_i are all real if $\Delta = g_2^3 - 27g_3^2 > 0$ and only one, namely e_1 , is real if $\Delta < 0$. Hence the period is given by

$$\Omega = \int_{e_1}^\infty \frac{dt}{\sqrt{4t^3 - g_2t - g_3}}, \quad \mathcal{P}(\Omega) = e_1, \quad \mathcal{P}'(\Omega) = 0. \quad (\text{A8})$$

It is always finite, except when e_1 is a double root, in which case $\Delta = 0$ and the period is infinite $\Omega = \infty$.

For $g_2 = 0$ the integral (A8) can be calculated explicitly using

$$\begin{aligned} \int_1^\infty \frac{du}{\sqrt{u^3 - 1}} &= \frac{\Gamma(1/3)^3}{4^{2/3}\pi} = \frac{-\sqrt{\pi}\Gamma(1/6)}{\Gamma(-1/3)}, \\ \int_{-1}^\infty \frac{du}{\sqrt{u^3 + 1}} &= \sqrt{\pi} \frac{\Gamma(1/3)}{\Gamma(5/6)}. \end{aligned} \quad (\text{A9})$$

The half-periods are

$$\Omega = \begin{cases} \frac{1}{4\pi} \Gamma(1/3)^3 g_3^{-1/6} & \text{when } g_3 > 0 \\ \sqrt{\pi} \frac{\Gamma(1/3)}{4^{1/3} \Gamma(5/6)} |g_3|^{-1/6} & \text{when } g_3 < 0 \end{cases}, \quad (\text{A10})$$

and the other period can be chosen as $\frac{1}{2}\Omega(1 + i\sqrt{3})$. Finally, taking another derivative of (A5) we see that the Weierstrass function also satisfies

$$\mathcal{P}''(z) = 6\mathcal{P}(z)^2 - \frac{g_2}{2}, \quad (\text{A11})$$

and $\mathcal{P}(z; g_2, g_3)$ is the only solution of this differential equation which diverges at $z = 0$ as in (A2). The Weierstrass function allows to find solutions to the 1D instanton equation in a region with no source

$$\tilde{u}''(x) - A\tilde{u}(x) + \tilde{u}(x)^2 = 0, \quad (\text{A12})$$

where $A = 1$ is the massive case and $A = 0$ the massless case. Comparing with Eq. (A11) we see that a family of solutions are

$$\tilde{u}(x) = \frac{A}{2} - 6b^2\mathcal{P}\left(c + bx; \frac{A^2}{12b^4}, g_3\right). \quad (\text{A13})$$

Because of the homogeneity relation (A4), this is a two-parameter family. These solutions are periodic. In the massless case $A = 0$, the period of (A13) is Ω/b where Ω is given by (A10).

Derivatives w.r.t. g_2, g_3 . There are formula for derivatives w.r.t. g_2 and g_3 (Mathematica). They simplify for $g_2 = 0$ and become

$$\partial_{g_3}\mathcal{P} = \frac{2\mathcal{P} + z\mathcal{P}'}{6g_3}, \quad \partial_{g_3}\mathcal{P}' = \frac{\mathcal{P}' + 2z\mathcal{P}^2}{2g_3} \quad (\text{A14})$$

Note that the first equation, $2\mathcal{P} + z\mathcal{P}' - 6g_3\partial_{g_3}\mathcal{P} = 0$, simply expresses the scale invariance.

Expansion in series of g_3 . Let us again specify to $g_2 = 0$. Using the definition (A6) and expanding the integrand in series of g_3 and integrating over t , one recognizes an hypergeometric series and one can rewrite

$$z = \frac{{}_2F_1\left(\frac{1}{6}, \frac{1}{2}; \frac{7}{6}; \frac{g_3}{4y^3}\right)}{\sqrt{y}} \quad (\text{A15})$$

Inverting this series we obtain the series expansion of \mathcal{P} in powers of g_3 as

$$\mathcal{P}(z, g_2 = 0, g_3) = \frac{1}{z^2} + \frac{g_3 z^4}{28} + \frac{g_3^2 z^{10}}{10192} + \frac{g_3^3 z^{16}}{5422144} + \frac{3g_3^4 z^{22}}{9868302080} + O(z^{26}) \quad (\text{A16})$$

Note that it is the same as the expansion in powers of z . More generally it can be written as

$$\mathcal{P}(z, g_2 = 0, g_3) = \sum_{p=0}^{\infty} c_p g_3^p z^{6p-2} \quad (\text{A17})$$

where c_p satisfies the recursion

$$c_p = \frac{1}{(p-1)(6p+1)} \sum_{k=1}^{p-1} c_k c_{p-k} \quad (\text{A18})$$

with initial condition $c_0 = 1$ and $c_1 = 1/28$.

Appendix B: Levy stable laws and some inverse Laplace transforms

One sided Levy stable function $\mathcal{L}_\alpha(x)$, defined for $0 < \alpha < 1$ and $x > 0$, are such that

$$\text{LT}_{x \rightarrow p} \mathcal{L}_\alpha(x) = e^{-p^\alpha} \Leftrightarrow \mathcal{L}_\alpha(x) = \text{LT}_{p \rightarrow x}^{-1} e^{-p^\alpha} \quad (\text{B1})$$

They satisfy the property that they are stable under convolution, up to a rescaling

$$[\mathcal{L}_\alpha \star \mathcal{L}_\alpha](x) = 2^{-1/\alpha} \mathcal{L}_\alpha(2^{-1/\alpha} x) \quad (\text{B2})$$

which means that the (scaled) sum of two random variables $2^{-1/\alpha}(X + X')$ distributed with \mathcal{L}_α is also distributed with \mathcal{L}_α , i.e. it is infinitely divisible and attractor of all i.i.d. sums of positive random variables which distribution decays as $1/X^{1+\alpha}$ at large X .

Let us recall that a PDF is infinitely divisible if it can be expressed as the PDF of a sum of an arbitrary number of i.i.d random variables. Every infinitely divisible probability distribution corresponds in a natural way to a Levy process (i.e. a process with stationary independent increments), and their characteristic function are parameterized by the Levy-Kintchine formula. Stable laws are particular cases.

Their large x asymptotics can be written as a series representation³³

$$\mathcal{L}_\alpha(x) = \frac{1}{\pi} \sum_{j=1}^{\infty} \frac{(-1)^{j+1}}{j! x^{1+\alpha j}} \Gamma(1 + \alpha j) \sin(\pi \alpha j) \quad (\text{B3})$$

and the small x asymptotics is obtained from the saddle-point method as

$$\mathcal{L}_\alpha(x) \sim_{x \rightarrow 0^+} x^{\frac{-2+\alpha}{2(1-\alpha)}} \exp\left(- (1-\alpha) \left(\frac{\alpha}{x}\right)^{\frac{1-\alpha}{1-\alpha}}\right) \quad (\text{B4})$$

Its Fourier transform has the form

$$\int dz e^{ikx} \mathcal{L}_\alpha(x) = \exp(-|k|^\alpha e^{-i \frac{k}{|k|} \frac{\pi \alpha}{2}}) \quad (\text{B5})$$

There is a general expression of $g_\alpha(x)$ for generic rational values $\alpha = \ell/k$, $\ell < k \in \mathbb{N}$, in terms of either (i) a Meijer G function (ii) a sum of $k - 1$ generalized hypergeometric functions, see formula (2) and (3-4) in³⁰.

Let us recall some simplest and useful ones

$$\mathcal{L}_{1/2}(x) = \frac{1}{2\sqrt{\pi} x^{3/2}} e^{-1/(4x)} \quad (\text{B6})$$

known as the Levy-Smirnov function, then (see e.g.³¹)

$$\mathcal{L}_{1/3}(x) = \frac{1}{3\pi x^{3/2}} K_{1/3}\left(\frac{2}{\sqrt{27x}}\right) = \frac{\text{Ai}\left(\frac{1}{(3x)^{1/3}}\right)}{3^{1/3} x^{4/3}} \quad (\text{B7})$$

in terms of the modified Bessel function of the second kind, then

$$\mathcal{L}_{2/3}(x) = \frac{\sqrt{3}}{x\sqrt{\pi}} e^{-\frac{2}{27x^2}} W_{1/2,1/6}\left(\frac{4}{27x^2}\right) \quad (\text{B8})$$

in terms of the Whittaker W function, then

$$\mathcal{L}_{1/4}(x) = \frac{\Gamma\left(\frac{1}{4}\right) {}_0F_2\left(\frac{1}{4}; \frac{3}{2}, \frac{5}{4}; -\frac{1}{256x}\right)}{4\sqrt{2\pi} x^{5/4}} + \frac{\Gamma\left(-\frac{1}{4}\right) \Gamma\left(\frac{1}{4}\right) {}_0F_2\left(\frac{3}{4}, \frac{5}{4}; -\frac{1}{256x}\right)}{16\sqrt{2\pi} x^{3/2} x^{3/2}} - \frac{\Gamma\left(-\frac{1}{4}\right) {}_0F_2\left(\frac{5}{4}, \frac{3}{2}; -\frac{1}{256x}\right)}{32\sqrt{2\pi} x^{7/4}} \quad (\text{B9})$$

and finally

$$\mathcal{L}_{3/4}(x) = \frac{{}_3F_2\left(\frac{5}{6}, \frac{7}{6}, \frac{3}{4}, \frac{5}{4}; -\frac{27}{256x^3}\right)}{8\sqrt{\pi} x^{5/2}} + \frac{\Gamma\left(\frac{7}{4}\right) {}_2F_2\left(\frac{7}{12}, \frac{11}{12}, \frac{1}{2}, \frac{3}{4}; -\frac{27}{256x^3}\right)}{\sqrt{2\pi} x^{7/4}} + \frac{\Gamma\left(\frac{13}{4}\right) {}_2F_2\left(\frac{13}{12}, \frac{17}{12}, \frac{5}{4}, \frac{3}{2}; -\frac{27}{256x^3}\right)}{6\sqrt{2\pi} x^{13/4}} \quad (\text{B10})$$

which we have rechecked carefully. Note that the formula given in³² for $\alpha = 3/4$ contains misprints.

Note that the paper Ref.³⁴ contains some further useful ILT formula. For instance it shows that if one knows $f(x) = LT_{p \rightarrow x}^{-1} F(p)$ then one can write

$$LT_{p \rightarrow x}^{-1} F(p^\alpha) = \int dt f(t) \frac{1}{t^{1/\alpha}} g_\alpha(x/t^{1/\alpha}) \quad , \quad LT_{p \rightarrow x}^{-1} p^{\alpha-1} F(p^\alpha) = \frac{x}{\alpha} \int dt f(t) \frac{1}{t^{1+1/\alpha}} g_\alpha(x/t^{1/\alpha}) \quad (\text{B11})$$

and a few more identities from which one can deduce some ILT formula (for instance the one of $p^{-1/4} e^{-p^{1/4}}$ and so on).

Appendix C: Density of local sizes, details for the massive case

We give here some details of derivation for the massive case results of Section IV B.

For a general driving kick $w(x)$ the general (formal) formula for the PDF of local size at $x = 0$ is

$$P_{\{w(x)\}}(S_0) = LT_{-\lambda=-3z(1-z^2) \rightarrow S_0}^{-1} \exp\left(\int dx w(x) \frac{6(1-z^2)e^{-|x|}}{(1+z+(1-z)e^{-|x|})^2}\right) \quad (C1)$$

Let us sketch first the two (known) easier cases.

Uniform kick. We have $\int dx \tilde{u}^\lambda(x) = 6(1-z)$. Hence

$$S_0 P_w(S_0) = \int_C \frac{d\lambda}{2i\pi} e^{-\lambda S_0} \partial_\lambda e^{6w(1-z\lambda)} = \int_C \frac{dz}{2i\pi} e^{-3z(1-z^2)S_0} \partial_z e^{6w(1-z)} \quad (C2)$$

$$= -6w \int_C \frac{dz}{2i\pi} e^{-3z(1-z^2)S_0 + 6w(1-z)} = -6w \Phi(a, b, c)|_{a=9S_0, b=0, c=-3S_0-6w} \quad (C3)$$

leading to formula (122) in the text.

Local kick at $x = 0$. We have $\tilde{u}^\lambda(0) = \frac{3}{2}(1-z^2)$. Hence

$$S_0 P_w(S_0) = \int_C \frac{d\lambda}{2i\pi} e^{-\lambda S_0} \partial_\lambda e^{w \frac{3}{2}(1-z^2)} = \int_C \frac{dz}{2i\pi} e^{-3z(1-z^2)S_0} \partial_z e^{w \frac{3}{2}(1-z^2)} \quad (C4)$$

$$= 3w \int_C \frac{dz}{2i\pi} e^{-3z(1-z^2)S_0} z e^{w \frac{3}{2}(1-z^2)} = 3w e^{\frac{3}{2}w} \partial_c \Phi(a, b, c)|_{a=9S_0, b=-\frac{3}{2}w, c=-3S_0} \quad (C5)$$

leading to formula (123) in the text.

We now use the formula for the avalanche density associated to a local kick at x_s . It satisfies:

$$\int_0^\infty dS_0 (e^{\lambda S_0} - 1) \rho_{x_s}(S_0) = u^\lambda(x_s) \quad (C6)$$

We thus search for the inverse Laplace transform of $S_0 \rho_x(S_0)$ as the contour integral:

$$\begin{aligned} S_0 \rho_x(S_0) &= \int \frac{d\lambda}{2i\pi} \partial_\lambda u^\lambda(x) e^{-\lambda S_0} = - \int \frac{d\lambda}{2i\pi} u^\lambda(x) \partial_\lambda e^{-\lambda S_0} = \int \frac{dz}{2i\pi} \frac{6(1-z^2)e^{-|x|}}{(1+z+(1-z)e^{-|x|})^2} \partial_z e^{-3z(1-z^2)S_0} \\ &= 3S_0 \int \frac{dz}{2i\pi} \frac{6(1-z^2)e^{-|x|}}{(1+z+(1-z)e^{-|x|})^2} (3z^2 - 1) e^{-3z(1-z^2)S_0} \end{aligned}$$

We now exponentiate the denominator:

$$\rho_x(S_0) = \int_0^\infty dt f(t) \quad , \quad f(t) = -18te^{-|x|} \int \frac{dz}{2i\pi} (1-z^2)(1-3z^2) e^{-t(1+z+(1-z)e^{-|x|})-3z(1-z^2)S_0}$$

The contour integral is an Airy type integral. It can be written as:

$$f(t) = -18te^{-|x|-t(1+e^{-|x|})} (1-\partial_b)(1-3\partial_b) \Phi(a, b, c)|_{a=9S_0, b=0, c=-3S_0-t(1-e^{-|x|})}$$

we obtain after a rescaling of t , $t \rightarrow t3^{2/3}s_0^{1/3}/(1-e^{-|x|})$

$$\rho_x(S_0) = -12 \frac{e^{-|x|}}{(1-e^{-|x|})^2} \frac{1}{S_0} \int_0^\infty dt t e^{-t3^{2/3}s_0^{1/3} \frac{1+e^{-|x|}}{1-e^{-|x|}}} \left[\frac{1}{2} t(t - 2 \times 3^{1/3} S_0^{2/3}) \text{Ai} \left(t + 3^{1/3} S_0^{2/3} \right) + \text{Ai}' \left(t + 3^{1/3} S_0^{2/3} \right) \right] \quad (C7)$$

which takes the scaling form (125) with

$$\phi(s, s_0) = -12s^{2/3} \int_0^{+\infty} dt t e^{-2 \times 3^{2/3} t s^{1/3}} \left(\frac{t(t-2s_0)}{2} \text{Ai}(t+s_0) + \text{Ai}'(t+s_0) \right) \quad (C8)$$

$$= -12s^{2/3} \int_0^{+\infty} dt e^{-2 \times 3^{2/3} t s^{1/3}} \left[\frac{d}{dt} \left(\frac{t^2}{2} \text{Ai}'(t+s_0) \right) - \frac{3}{2} s_0 t^2 \text{Ai}(t+s_0) \right] \quad (C9)$$

transformed into (126) after integration by parts.

To verify (127) we first integrate (C7) over x using that $\frac{d}{dx} \frac{1+e^{-x}}{2(1-e^{-x})} = -\frac{e^{-x}}{(1-e^{-x})^2}$ and then we check the identity

$$-\frac{1}{S_0^{4/3}} 4\sqrt{3} \int_0^{+\infty} dt e^{-3^{2/3} \sqrt[3]{S_0} t} \left(\frac{1}{2} t \left(t - 2\sqrt[3]{3} S_0^{2/3} \right) \text{Ai} \left(t + \sqrt[3]{3} S_0^{2/3} \right) + \text{Ai}' \left(t + \sqrt[3]{3} S_0^{2/3} \right) \right) \quad (\text{C10})$$

$$= \frac{2 \times 3^{1/3}}{S_0^{4/3}} \text{Ai}(3^{1/3} S_0^{2/3}) \quad (\text{C11})$$

Appendix D: Expansion in λ , more details

We give some more details for the expansion in λ of Section V A 4. We start from (169), with $z = r - x_0$, and substitute (168) to obtain λ as a series in g_3 (at fixed z). Then we invert the series and we find g_3 as a series in λ as

$$g_3 = -\frac{2\lambda}{3z^3} - \frac{\lambda^2}{252} - \frac{\lambda^3 z^3}{22932} - \frac{5\lambda^4 z^6}{7842744} - \frac{4379\lambda^5 z^9}{399666234240} - \frac{199\lambda^6 z^{12}}{953050250880} - \frac{256124087\lambda^7 z^{15}}{59920808579914044672} \quad (\text{D1})$$

$$- \frac{3501234283\lambda^8 z^{18}}{37970870279061320939520} - \frac{10873895503273\lambda^9 z^{21}}{5252130776999761912354406400} + O(\lambda^{10})$$

We then use that $\rho = x_0 + 1/\sqrt{\mathcal{P}(z, g_3)}$ where we can insert the above series and obtain

$$\rho = r + \frac{\lambda z^4}{84} + \frac{\lambda^2 z^7}{3822} + \frac{53\lambda^3 z^{10}}{8133216} + \frac{1223\lambda^4 z^{13}}{7136897040} + \frac{3223267\lambda^5 z^{16}}{693820582640640} + \frac{407163391\lambda^6 z^{19}}{3170413152376404480} \quad (\text{D2})$$

$$+ \frac{346172136673\lambda^7 z^{22}}{96192871373622013046784} + \frac{857301071467\lambda^8 z^{25}}{8416876245191926141593600} + \frac{1352811921954613\lambda^9 z^{28}}{465688928893978889562090700800} + O(\lambda^{10})$$

From this we obtain both branches of the instanton solution to higher orders than in (172), for $x_0 > 0$

$$\tilde{u}_r^\lambda(0) = -\frac{6}{\rho^2} = -\frac{6}{r^2} + \frac{\lambda z^4}{7r^3} + \frac{\lambda^2 (16rz^7 - 13z^8)}{5096r^4} + \frac{\lambda^3 (477r^2 z^{10} - 684rz^{11} + 247z^{12})}{6099912r^5} \quad (\text{D3})$$

$$+ \frac{\lambda^4 (273952r^3 z^{13} - 536220r^2 z^{14} + 355680r z^{15} - 80275z^{16})}{133222078080r^6} + O(\lambda^5) \quad (\text{D4})$$

and for $x_0 < 0$

$$\tilde{u}_r^\lambda(0) = -6\mathcal{P}(r, 0, g_3) = -\frac{6}{r^2} + \frac{\lambda r^4}{7z^3} + \lambda^2 \left(\frac{r^4}{1176} - \frac{r^{10}}{3822z^6} \right) + \frac{\lambda^3 (2r^{16} - 19r^{10}z^6 + 57r^4z^{12})}{6099912z^9} \quad (\text{D5})$$

$$+ \frac{\lambda^4 (-48r^{22} + 780r^{16}z^6 - 5795r^{10}z^{12} + 18200r^4z^{18})}{133222078080z^{12}} + O(\lambda^5) \quad (\text{D6})$$

Appendix E: Expectation values conditioned to avalanche extensions

Let us give some relations used in the text to calculate from the solution of the instanton equation some expectation values conditioned to avalanche (one sided) extensions ℓ_1 and ℓ_2

Single boundary. Consider an observable $S_\phi = \int dx \phi(x) S(x)$ and $u_r^\lambda(x)$ the solution of the instanton equation with $\lambda\phi(x)$ as a source and a boundary at r . For a kick at $x = 0$, we start from

$$\int dS_\phi P(\ell_2 < r, S_\phi) e^{\lambda S_\phi} = e^{f u_r^\lambda(0)} \quad , \quad P(\ell_2 < r) = e^{f u_r^0(0)} \quad (\text{E1})$$

This leads to the formula for the conditional average

$$\langle e^{\lambda S_\phi} \rangle_{\ell_2 < r} = \frac{\int dS_\phi P(\ell_2 < r, S_\phi) e^{\lambda S_\phi}}{P(\ell_2 < r)} = e^{f(u_r^\lambda(0) - u_r^0(0))} \quad (\text{E2})$$

One can also write, taking a derivative of (E1) w.r.t. r

$$\int dS_\phi P(\ell_2, S_\phi) e^{\lambda S_\phi} = f \partial_r u_r^\lambda(0) e^{f u_r^\lambda(0)} \Big|_{r=\ell_2} \quad , \quad P(\ell_2) = f \partial_r u_r^0(0) e^{f u_r^0(0)} \Big|_{r=\ell_2} \quad , \quad \rho(\ell_2) = \partial_r u_r^0(0) \Big|_{r=\ell_2} \quad (\text{E3})$$

leading to the conditional average

$$\langle e^{\lambda S_\phi} \rangle_{\ell_2=r} = \frac{\int dS_\phi P(\ell_2, S_\phi) e^{\lambda S_\phi}}{P(\ell_2)} \Big|_{\ell_2=r} = \frac{\partial_r u_r^\lambda(0)}{\partial_r u_r^0(0)} \langle e^{\lambda S_\phi} \rangle_{\ell_2 < r} \quad (\text{E4})$$

Expanding to first order in λ , denoting $u_r^{(1)} = \partial_\lambda u_r^\lambda|_{\lambda=0}$, one obtains

$$\langle S_\phi \rangle_{\ell_2 < r} = f u_r^{(1)}(0) \quad (\text{E5})$$

$$\langle S_\phi \rangle_{\ell_2=r} = \frac{\partial_r u_r^\lambda(0)}{\partial_r u_r^0(0)} e^{f(u_r^\lambda(0) - u_r^0(0))} = \frac{\partial_r u_r^{(1)}(0)}{\partial_r u_r^0(0)} + f u_r^{(1)}(0) = \frac{\partial_r u_r^{(1)}(0)}{\partial_r u_r^0(0)} + \langle S_\phi \rangle_{\ell_2 < r} \quad (\text{E6})$$

Two boundaries. Now we start from

$$\int dS_\phi P(\ell_1 < -r_1, \ell_2 < r_2, S_\phi) e^{\lambda S_\phi} = e^{f u_{r_1, r_2}^\lambda(0)} \quad , \quad P(\ell_1 < -r_1, \ell_2 < r_2) = e^{f u_{r_1, r_2}^0(0)} \quad (\text{E7})$$

This leads to the formula for the conditional average

$$\langle e^{\lambda S_\phi} \rangle_{\ell_1 < -r_1, \ell_2 < r_2} = \frac{\int dS_\phi P(\ell_1 < -r_1, \ell_2 < r_2, S_\phi) e^{\lambda S_\phi}}{P(\ell_1 < -r_1, \ell_2 < r_2)} = e^{f(u_{r_1, r_2}^\lambda(0) - u_{r_1, r_2}^0(0))} \quad (\text{E8})$$

One can also write, taking two derivatives

$$\int dS_\phi P(\ell_1, \ell_2, S_\phi) e^{\lambda S_\phi} = -(f \partial_{r_1} \partial_{r_2} u_{r_1, r_2}^\lambda(0) + f^2 \partial_{r_1} u_{r_1, r_2}^\lambda(0) \partial_{r_2} u_{r_1, r_2}^\lambda(0)) e^{f u_{r_1, r_2}^\lambda(0)} \Big|_{r_1=-\ell_1, r_2=\ell_2} \quad (\text{E9})$$

from which one gets $P(\ell_1, \ell_2)$ setting $\lambda = 0$ and taking a derivative w.r.t f at $f = 0^+$ the density

$$\rho(\ell_1, \ell_2) = -\partial_{r_1} \partial_{r_2} u_{r_1, r_2}^0(0) \Big|_{r_1=-\ell_1, r_2=\ell_2} \quad (\text{E10})$$

Since Eq. (E9) is a complicated formula we will only study its small f behavior. In the limit $f = 0^+$ one finds

$$\langle e^{\lambda S_\phi} \rangle_{\ell_1, \ell_2} = \frac{\int dS_\phi P(\ell_1, \ell_2, S_\phi) e^{\lambda S_\phi}}{P(\ell_1, \ell_2)} = \frac{\partial_{r_1} \partial_{r_2} u_{r_1, r_2}^\lambda(0)}{\partial_{r_1} \partial_{r_2} u_{r_1, r_2}^0(0)} \Big|_{r_1=-\ell_1, r_2=\ell_2} \quad (\text{E11})$$

Appendix F: expansion around λ^*

Here we push the expansion around λ^* in (198) to higher orders. The WeierstrassP function near a zero has a simpler expansion in g_3

$$\begin{aligned} \mathcal{P}(1; 0, g_3) &= \frac{gX}{6} - \frac{g^2 X}{72} + \frac{g^3 X}{1296} + \frac{g^4 X(12X + 65)}{31104} - \frac{g^5(X(96X + 529))}{186624} + \frac{7g^6 X(516X + 2845)}{6718464} + O(g^7) \\ g &= \frac{g_3 - g_3^*}{g_3^*} \quad , \quad X = \mathcal{P}(1; 0, g_3^*) = -\sqrt{-g_3^*} \end{aligned} \quad (\text{F1})$$

From this we can solve order by order in $\lambda^* - \lambda$ the equation (183) (here we denote $\tilde{\lambda} \rightarrow \lambda$ for notational simplicity). We find

$$A(\lambda) = \frac{(\lambda^* - \lambda)^{1/2}}{3\sqrt{2}} - \frac{1}{54}(\lambda^* - \lambda) + \frac{(5\lambda^* - 54)(\lambda^* - \lambda)^{3/2}}{972\sqrt{2}\lambda^*} + \left(\frac{1}{54\lambda^*} - \frac{2}{2187} \right) (\lambda^* - \lambda)^2 + O((\lambda^* - \lambda)^{5/2}) \quad (\text{F2})$$

which gives

$$f(\lambda) = \frac{9\lambda^*}{\sqrt{2}\sqrt{\lambda^* - \lambda}^3} + \frac{\lambda^* - 54}{12\sqrt{2}\sqrt{\lambda^* - \lambda}} + \left(1 - \frac{2\lambda^*}{81} \right) + \frac{(\lambda^*(35\lambda^* - 1188) - 1620)\sqrt{\lambda^* - \lambda}}{2592\sqrt{2}\lambda^*} + O(\sqrt{\lambda^* - \lambda}^2) \quad (\text{F3})$$

This leads to a series expansion for $p(\sigma)$, not displayed here.

Appendix G: Bessel functions

We use in the text the explicit form of the half-integer modified Bessel functions

$$I_{7/2}(x) = \frac{\left(-\frac{30}{x^3} - \frac{12}{x}\right) \sinh(x) + \left(\frac{30}{x^2} + 2\right) \cosh(x)}{\sqrt{2\pi}\sqrt{x}} \quad , \quad I_{5/2}(x) = \frac{\left(\frac{6}{x^2} + 2\right) \sinh(x) - \frac{6 \cosh(x)}{x}}{\sqrt{2\pi}\sqrt{x}} \quad (\text{G1})$$

Appendix H: Shape with two boundaries, expansions in powers of λ

Here we obtain (278), (280) by a direct expansion of (265) and (266) in powers of λ . We define

$$H(z) = \partial_{g_3}|_{g_3=g_3^0} \mathcal{P}(z; g_3) = \frac{2\mathcal{P}_0(z) + z\mathcal{P}'_0(z)}{6g_3^0} \quad , \quad H'(z) = \partial_{g_3}|_{g_3=g_3^0} \mathcal{P}'(z; g_3) = \frac{\mathcal{P}'_0(z) + 2z\mathcal{P}_0(z)^2}{2g_3^0} \quad (\text{H1})$$

Note that $H(z)$ satisfies the differential equation $H''(z) = 12\mathcal{P}_0(z)H(z)$. Using the symmetries $\mathcal{P}_0(z_0) = \mathcal{P}_0(1 - z_0)$ and $\mathcal{P}'_0(z_0) = -\mathcal{P}'_0(1 - z_0)$ one also shows the "Wronskian"-type identity

$$H'(1 - z_0)H(z_0) + H'(z_0)H(1 - z_0) = \frac{1}{12(g_3^0)^2} (4\mathcal{P}_0(z_0)^3 - \mathcal{P}'_0(z_0)^2) = \frac{1}{12g_3^0} \quad (\text{H2})$$

which we use below. Let us now expand to first order in λ . We denote $\delta g_3^\pm = g_3^\pm - g_3^0$, hence from (266) we have to first order

$$H(z_0)\delta g_3^- = H(1 - z_0)\delta g_3^+ \quad , \quad H'(z_0)\delta g_3^- + H'(1 - z_0)\delta g_3^+ = -\hat{\lambda} \quad (\text{H3})$$

Solving for δg_3^\pm , we can insert the solution in the expansion of the instanton solution (265) to first order in λ . For $x_0 > 0$ we find

$$\tilde{u}_{r_1, r_2}^{\lambda, x_0}(0) = \frac{-6}{(r_1 - r_2)^2} \mathcal{P}(1 - p, g_2 = 0, g_3^-) \quad , \quad 1 - p = -\frac{r_1}{r_2 - r_1} \quad (\text{H4})$$

$$= \frac{-6}{(r_1 - r_2)^2} \left(\mathcal{P}_0(1 - p) - \frac{\lambda}{6} (r_2 - r_1)^3 \frac{H(1 - z_0)H(1 - p)}{H'(1 - z_0)H(z_0) + H'(z_0)H(1 - z_0)} \right) \quad (\text{H5})$$

$$= \frac{-6}{(r_1 - r_2)^2} \left(\mathcal{P}_0(1 - p) - 2g_3^0 \lambda (r_2 - r_1)^3 H(1 - z_0)H(1 - p) \right) \quad (\text{H6})$$

where we have used (H2). Similarly for $x_0 < 0$ we obtain

$$\tilde{u}_{r_1, r_2}^{\lambda, x_0}(0) = \frac{-6}{(r_1 - r_2)^2} \left(\mathcal{P}_0(p) - 2g_3^0 \lambda (r_2 - r_1)^3 H(z_0)H(p) \right) \quad , \quad p = \frac{r_2}{r_2 - r_1} \quad , \quad x_0 < 0 \quad (\text{H7})$$

Now we see, using $H(z) = \psi_1(z_0)/(6g_3^0)$, that these equations lead to (278), (280).

Appendix I: Higher conditional moments of the total size

Here we give the second moment $\langle S^2 \rangle_{\ell_1 < -r_1, \ell_2 < r_2}$. Performing the expansion as explained in the text we find, in the small f limit, with $p = r_2/(r_2 - r_1)$ the aspect ratio

$$\langle S^2 \rangle_{\ell_1 < -r_1, \ell_2 < r_2} = f \partial_\mu^2 |_{\mu=0} \tilde{u}_{r_1, r_2}^\mu(0) = 2f(r_2 - r_1)^6 g_2(p) \quad (\text{I1})$$

$$g_2(p) = g_2(1 - p) = \frac{8\pi^6}{81\Gamma\left(\frac{1}{3}\right)^{36}} \times \left(9\Gamma\left(\frac{1}{3}\right)^{18} + 256\pi^6 \left(P_0(p)^2 \left(-12\pi^2 p^2 - 9\zeta_0(p)^2 + 4\sqrt{3}\pi(3p\zeta_0(p) - 2) \right) \right) \right) \quad (\text{I2})$$

$$+ P_0(p) \left(\left(6\sqrt{3}\pi p - 9\zeta_0(p) \right) P'_0(p) + 28\pi^2 \right) + 4\pi \left(2\pi p - \sqrt{3}\zeta_0(p) \right) P'_0(p) - 9P_0(p)^3 \quad (\text{I3})$$

$$= \frac{32\pi^8 p^4}{63\Gamma\left(\frac{1}{3}\right)^{18}} - \frac{p^6}{1800} + \frac{\pi p^8}{1540\sqrt{3}} - \frac{\pi^2 p^{10}}{22932} + O(p^{11}) \quad (\text{I4})$$

This extends the result (306) in the text to the second moment. Similar manipulations as in the text allow to obtain from it $\langle S^2 \rangle_{\ell, p}$ and $\langle S^2 \rangle_\ell$.

Appendix J: Driving at the tip, local jumps $P_w(S_0)$, massive case.

Set $\mu = 0$, i.e. $\beta = 1$ in (331), (332), in the massive case $A = 1$. One obtains

$$S_0 P_w(S_0) = \int \frac{d\lambda_0}{2i\pi} e^{-\lambda_0 S_0} \partial_{\lambda_0} e^{wZ} \quad (\text{J1})$$

where $Z = \frac{3}{2}m_0^2(1-z^2)$ and $\lambda_0 - Z = 3z(1-z^2)$. Hence we can trade the variable λ_0 for the variable z and write

$$S_0 P_w(S_0) = \int \frac{dz}{2i\pi} e^{-S_0[\frac{3}{2}m_0^2(1-z^2)+3z(1-z^2)]} \partial_z e^{\frac{3}{2}wm_0^2(1-z^2)} \quad (\text{J2})$$

$$= 3wm_0^2 e^{m_0^2 \frac{3}{2}(w-S_0)} \int \frac{dz}{2i\pi} z e^{-3z(1-z^2)S_0 + m_0^2(S_0-w)\frac{3}{2}z^2} \quad (\text{J3})$$

$$= 3wm_0^2 e^{m_0^2 \frac{3}{2}(w-S_0)} \partial_c \Phi(a, b, c) \Big|_{a=9S_0, b=\frac{3}{2}m_0^2(S_0-w), c=-3S_0} \quad (\text{J4})$$

This leads to

$$P_w(S_0) = \frac{wm_0^2}{3^{1/3}S_0^{5/3}} e^{\frac{m_0^6(S_0-w)^3}{36S_0^2} + m_0^2(w-S_0)} (-y \text{Ai}(y^2 + 3^{1/3}S_0^{2/3}) - \text{Ai}'(y^2 + 3^{1/3}S_0^{2/3})) \quad , \quad y = \frac{m_0^2(S_0-w)}{2 \times 3^{1/3}S_0^{2/3}} \quad (\text{J5})$$

which is the analog of (349) for the massive case. We have checked that it recovers the moments given in Section VII B 1. Note that in the limit $m_0 \rightarrow +\infty$ the PDF (J5) becomes a delta-function around $S_0 = w$.

Appendix K: Mean shape $d > 1$ in the massive case and the Green function of the $1/r^2$ potential

In Section VIII C we studied the mean shape $\langle S(x) \rangle_{S(x_0)=0}$ around a point such that $S(x_0) = 0$ for the massless case. To study the massive case we must solve (464) with an additional mass term $-m^2 \tilde{u}_1$ on the l.h.s. The equation (466) is still correct with the replacement $G_{\ell+\frac{d-2}{2}}(r, r') \rightarrow G_{\ell+\frac{d-2}{2}}(r, r', E)$ where, instead of (467), we need the Green function at finite energy E , solution of

$$\left(\frac{d^2}{dr^2} + E - \frac{\alpha + (\ell + \frac{d-2}{2})^2 - \frac{1}{4}}{r^2} \right) G_{\ell+\frac{d-2}{2}}(r, r', E) = -\delta(r-r') \quad (\text{K1})$$

where we parametrize $E = -q^2 \leq 0$, with here $q = m$, and $\alpha = 4(4-d) > 0$. The solution is

$$G_{\ell+\frac{d-2}{2}}(r, r', E = -q^2) = \sqrt{rr'} (I_{s_\ell}(qr) K_{s_\ell}(qr') \theta(r' - r) + K_{s_\ell}(qr) I_{s_\ell}(qr') \theta(r - r')) \quad (\text{K2})$$

$$s_\ell = \sqrt{\alpha + \left(\ell + \frac{d-2}{2}\right)^2}$$

which has the right derivative discontinuity at $r = r'$. Note that for $d = 1$ one has $s_0 = s_1 = 7/2$, and one finds the Bessel with index $7/2$ again. One then obtain the mean shape in the massive case from from $\langle S(r, \phi) \rangle_{S(0)=0} = fu_1(r_s, \phi_s, r, \phi)$ and inserting (K2) into (466).

¹ P. Le Doussal and K.J. Wiese, *First-principle derivation of static avalanche-size distribution*, Phys. Rev. E 85 (2011) 061102, arXiv:1111.3172.

² P. Le Doussal and K.J. Wiese, *Distribution of velocities in an avalanche*, EPL 97 (2012) 46004, arXiv:1104.2629.

³ P. Le Doussal and K.J. Wiese, *Avalanche dynamics*

of elastic interfaces, Phys. Rev. E 88 (2013) 022106, arXiv:1302.4316.

⁴ A. Dobrinevski, P. Le Doussal and K.J. Wiese, *Avalanche shape and exponents beyond mean-field theory*, EPL 108 (2014) 66002, arXiv:1407.7353.

⁵ T. Thiery and P. Le Doussal, *Universality in the mean*

- spatial shape of avalanches*, EPL 114 (2016) 36003, arXiv:1601.00174.
- ⁶ A. Dobrinevski, PhD thesis, *Field theory of disordered systems – avalanches of an elastic interface in a random medium*, arXiv:1312.7156 (2013).
- ⁷ T. Thiery, PhD thesis, *Analytical Methods and Field Theory for Disordered Systems*, arXiv:1705.07457 (2017).
- ⁸ A. Dobrinevski, P. Le Doussal and K.J. Wiese, *Non-stationary dynamics of the Alessandro-Beatrice-Bertotti-Montorsi model*, Phys. Rev. E 85 (2012) 031105, arXiv:1112.6307.
- ⁹ T. Thiery, P. Le Doussal and K.J. Wiese, *Spatial shape of avalanches in the Brownian force model*, J. Stat. Mech. 2015 (2015) P08019, arXiv:1504.05342.
- ¹⁰ M. Delorme, P. Le Doussal and K.J. Wiese, *Distribution of joint local and total size and of extension for avalanches in the Brownian force model*, Phys. Rev. E 93 (2016) 052142, arXiv:1601.04940.
- ¹¹ R. Garcia-Garcia, *On dissipation in crackling noise systems*, EPL 121, 26001 (2018), arXiv:1712.07254.
- ¹² B. Alessandro, C. Beatrice, G. Bertotti and A. Montorsi, *Domain-wall dynamics and Barkhausen effect in metallic ferromagnetic materials. I. Theory*, J. Appl. Phys. 68 (1990) 2901.
- ¹³ B. Alessandro, C. Beatrice, G. Bertotti and A. Montorsi, *Domain-wall dynamics and Barkhausen effect in metallic ferromagnetic materials. II. Experiments*, Journal of Applied Physics 68 (1990) 2908.
- ¹⁴ F. Colaiori, *Exactly solvable model of avalanches dynamics for barkhausen crackling noise*, Advances in Physics 57 (2008) 287, arXiv:0902.3173.
- ¹⁵ S. Zapperi, P. Cizeau, G. Durin and H.E. Stanley, *Dynamics of a ferromagnetic domain wall: Avalanches, depinning transition, and the Barkhausen effect*, Phys. Rev. B 58 (1998) 6353.
- ¹⁶ P. Le Doussal, K. J. Wiese, *Driven particle in a random landscape: disorder correlator, avalanche distribution and extreme value statistics of records*, Phys. Rev. E 79 (2009) 051105, arXiv:0808.3217.
- ¹⁷ A.A. Middleton, *Asymptotic uniqueness of the sliding state for charge-density waves*, Phys. Rev. Lett. 68 (1992) 670.
- ¹⁸ C. Baesens and R. S. MacKay, *Gradient dynamics of tilted Frenkel-Kontorova models*, Nonlinearity, 11:949, (1998), M. W. Hirsch. *Systems of Differential Equations that are Competitive or Cooperative II: Convergence Almost Everywhere*. SIAM J. Math. Anal., 16(3):423, (1985).
- ¹⁹ A. Rosso, *Depiégeage de variétés élastiques en milieu aléatoire*, PhD thesis (2002), <https://tel.archives-ouvertes.fr/tel-00002097/file/tel-00002097.pdf>.
- ²⁰ P. Le Doussal, T. Thiery, *Correlations between avalanches in the depinning dynamics of elastic interfaces*, Phys. Rev. E 101, 032108 (2020), arXiv:1904.12136.
- ²¹ T. Thiery, P. Le Doussal, and K. J. Wiese, *Universal correlations between shocks in the ground state of elastic interfaces in disordered media*, Physical Review E 94.1 (2016): 012110.
- ²² L. E. Aragon, A. B. Kolton, P. Le Doussal, K. J. Wiese, E. A. Jagla, *Avalanches in Tip-Driven Interfaces in Random Media*, arXiv:1510.06795, EPL 113 (2016) 10002.
- ²³ P. Le Doussal, *Equivalence of the mean-field avalanches and branching diffusions: from the Brownian force model to the super-Brownian motion*, arXiv:2203.10512 (2022).
- ²⁴ Z. Zhu, K.J. Wiese, *Spatial shape of avalanches*, Phys. Rev. E, 96(6), 062116 (2017).
- ²⁵ O. Narayan and D.S. Fisher, *Threshold critical dynamics of driven interfaces in random media*, Phys. Rev. B 48 (1993) 7030.
- ²⁶ P. Le Doussal and K.J. Wiese, *Size distributions of shocks and static avalanches from the functional renormalization group*, Phys. Rev. E 79 (2009) 051106, arXiv:0812.1893.
- ²⁷ H.E. Camblong, C. R. Ordon, *Regularized Green's function for the inverse square potential*, Modern Physics Letters A 17 (13) (2002) 817, arXiv:hep-th/0110278.
- ²⁸ M. Abramowitz and A. Stegun, *Pocketbook of Mathematical Functions*, Harri-Deutsch-Verlag, 1984.
- ²⁹ W. Duke, O. Imamoglu, *the zeros of the Weierstrass P-function and hypergeometric series*, Mathematische Annalen, 340, 4, 897 (2008).
- ³⁰ K. A. Penson and K. Gorska, *Exact and explicit probability densities for one-sided Lévy stable distributions*, Phys. Rev. Lett. 105, 210604 (2010), arXiv:1007.0193.
- ³¹ E. Barkai, *Fractional Fokker-Planck equation, solution, and application*, Phys. Rev. E 63, 046118 (2001).
- ³² H. Scher and E. W. Montroll, *Anomalous transit-time dispersion in amorphous solids*, Phys. Rev. B 12, 2455 (1975).
- ³³ P. Humbert, Bull. Soc. Math. Fr. 69, 121 (1945).
- ³⁴ K. A. Penson and K. Gorska, *On the properties of Laplace transform originating from one-sided Levy stable laws*, Journal of Physics A: Mathematical and Theoretical, 49(6), p.065201 (2016), arXiv:1406.3802,
- ³⁵ Note that in the BFM, even a small uniform kick f always produces many very small avalanches of order $O(f^2)$, so the meaning of "single avalanche regime" depends on the scale, and here we focus on avalanches which are $O(1)$ as $f \rightarrow 0^+$.
- ³⁶ It can be constructed as the rightmost metastable state of the Hamiltonian $\mathcal{H}[u, w] = \int d^d x [\frac{1}{2}(\nabla_x u)^2 + V(u(x), x) + \frac{m^2}{2}(u(x) - w(x))^2]$, where $F(u, x) = -\partial_u V(u, x)$, which leads to the equation of motion (1), setting $w(x) = w_0(x)$.
- ³⁷ It also appears as the second derivative of the Green function of the free field on a torus.
- ³⁸ The conventions are such that if $\Delta < 0$, $\Omega = \omega_1$ is real and ω_2 imaginary (for $g_3 > 0$ and the reverse for $g_3 < 0$), and if $\Delta < 0$, $\Omega = \omega_1 \pm \omega_2$.